ARTIFICIAL NEURAL NETWORK APPROACH TO TRANSMISSION LINE RELAYING

FATHIMA ZAHRA

INFORMATION TO USERS

This manuscript has been reproduced from the microfilm master. UMI films the text directly from the original or copy submitted. Thus, some thesis and dissertation copies are in typewriter face, while others may be from any type of computer printer.

The quality of this reproduction is dependent upon the quality of the copy submitted. Broken or indistinct print, colored or poor quality illustrations and photographs, print bleedthrough, substandard margins, and improper alignment can adversely affect reproduction.

In the unlikely event that the author did not send UMI a complete manuscript and there are missing pages, these will be noted. Also, if unauthorized copyright material had to be removed, a note will indicate the deletion.

Oversize materials (e.g., maps, drawings, charts) are reproduced by sectioning the original, beginning at the upper left-hand corner and continuing from left to right in equal sections with small overlaps.

Photographs included in the original manuscript have been reproduced xerographically in this copy. Higher quality 6" x 9" black and white photographic prints are available for any photographs or illustrations appearing in this copy for an additional charge. Contact UMI directly to order.

Bell & Howell Information and Learning
300 North Zeeb Road, Ann Arbor, MI 48106-1346 USA

UMI®
800-521-0600

ARTIFICIAL NEURAL NETWORK APPROACH TO TRANSMISSION LINE RELAYING

by

© Fathima Zahra, B. ENG., M. SC (ENG)

A thesis submitted to the School of Graduate

Studies in partial fulfillment of the

requirements for the degree of

Master of Engineering

Faculty of Engineering and Applied Science

Memorial University of Newfoundland

September 1998

St. John's Newfoundland Canada

Abstract

This thesis deals with the design of an Artificial Neural Network (ANN) based relay for transmission line protection. A novel feedforward neural network that indicates whether a fault is within or outside the protection zone (fault indication) of a transmission line is presented. This method has been extended to locate the distance of the fault (fault location). The proposed scheme utilizes the frequency components of the voltages and currents to make a decision.

The first part of the work employed frequency components of one cycle of post-fault data as the inputs to the ANN. The results obtained were promising, thus forming the basis to improve the speed of the relaying decision. This is achieved by using the frequency components of half cycle of pre-fault and half-cycle post-fault data as the inputs to the ANN.

The neural network employed is small in size, fast and robust. Data obtained from the Electromagnetic Transients Program (EMTP) for single-line-to-ground faults and three-phase faults have been used for testing and the results are found to be accurate. The performance of the trained neural network is good and the proposed ANN has the potential for implementation in a digital relay for transmission line protection. The results of the proposed ANN methodology are found to be accurate under the conditions of different fault location, fault inception angle and fault resistance.

Acknowledgments

I would like to thank and express my indebtedness and heartiest gratitude to my supervisors Dr. B. Jeyasurya and Dr. J. E. Quaicoe for their constant advice, encouragement and guidance during all stages of this research.

I take this opportunity to express my profound gratitude to my parents and my two brothers for their constant support and encouragement during my study in Canada.

Thanks are due to the staff at CCAE, faculty and friends for all the useful discussions and suggestions.

Finally, I would like to express my thanks to Memorial University of Newfoundland for the financial support, which made this research possible.

Contents

List of Figures

List of Tables

List of Abbreviations and Symbols

ANN : Artificial Neural Network

EMTP : Electromagnetic Transients Program

F : Fault

θ : Impedance angle

ADC : Analog to Digital Converters

p.u : Per unit

PF : Pre-fault loading

φ : Fault inception angle (Fault occurrence)

R_f : Fault resistance

DFT : Discrete Fourier Transform

MLP : Multilayer Perceptron

FFT : Fast Fourier Transform

THD : Total Harmonic Distortion

Chapter 1

Introduction

1.1 Protective Relaying of Power Systems

Electric energy is one of the most fundamental requirements of the modern industrial society. The power system is made up of interconnected equipment, broadly classified into three main groups namely, the power equipment, protection equipment and the control equipment. The power equipment generates, transforms and distributes the electric power to the loads. The control equipment maintains the power system at its normal voltage and frequency, and maintains optimum economy and security in the interconnected network. The protection equipment protects the power system.

The power system is subject to constant disturbances created by random load changes, natural causes, and equipment or operator error. Faults may result from insulation, electrical, mechanical or thermal failure [1]. The major types and causes of failures are listed in Table 1.1.

Protective relays are installed in different parts of the power system. The protective relay detects abnormal power system conditions, and initiates corrective action as quickly

as possible to restore the power system to its normal state. The purpose of protective relays is to ensure normal operation of the power system. Protective relay systems must perform correctly under adverse system and environmental conditions.

Table 1.1: Major types and causes of failure in power systems [1]

Type	Causes
Insulation	Design defects, aging insulation, improper manufacture, improper installation, contamination
Electrical	Lightning surges, switching surges, overvoltages
Thermal	Coolant failure, overcurrent, overvoltage, increase in the surrounding temperatures
Mechanical	Snow or ice, earthquake, overcurrent forces

Protective relays must meet these general requirements: *correct diagnosis of trouble, quickness of response and minimum disturbance to the power system* [2]. For a well-designed and efficient protective system, the following design criteria are necessary [3, 4].

- Reliability

It is the measure of the degree of certainty that the relay will perform correctly. System reliability consists of two main elements: dependability and security. Dependability ensures the correct operation in response to system trouble, while security signifies the ability of the relay to avoid mal-operation from all system disturbances [2].

- Speed

Speed is required to obtain minimum fault clearing time, thus protecting the equipment. A high speed, instantaneous relay is preferred. High speed indicates that the time taken to locate the fault should not exceed certain pre-defined time limit (usually 3 cycles at 60 Hz), and instantaneous indicates that there is no delay in the operation of the relay.

- Selectivity

Selectivity is the interrelated performance of the relay with other protective devices. Complete selectivity is obtained when a minimum amount of equipment is removed from service for the isolation of a fault.

- Economics

The concern is to obtain the maximum protection at minimum cost. Relays having a clearly defined zone of protection provide better selectivity, but generally cost more. A compromise is made between the high performance and the cost, and consequently both low speed and high speed relays are used to protect the power systems.

- Simplicity

A protective relay system should be kept as simple and straightforward as possible, while still accomplishing its intended goals. A simple design is needed for easy implementation and maintenance.

Transmission lines are the connecting links between the generating stations and the distribution systems, and lead to other power system networks over interconnections. Transmission lines physically integrate the output of generating plants and requirements

of customers by providing pathways for the flow of electric power. Transmission line protection forms an important topic of research, as they are the vital elements of the network, and are subjected to a majority of faults occurring in the power system. The range of the possible fault current, the effect of load, the direction of the fault as seen from the relay, the impact of system configuration, all have to be considered in the design of transmission line protection schemes.

The focus of the research presented in this thesis is on transmission line protection. Distance relays are normally used to protect high voltage transmission lines. Conventional distance relays measure the impedance of the transmission lines from the relay location to the point of fault. Under ideal conditions, impedance is directly proportional to fault distance. If the fault is located within the relay's protection zone, the relay generates a trip signal. Over the years, distance relays for transmission line protection have undergone changes from electromechanical relays to static relays and to digital relays [5-7]. Digital relays also provide communication capability [7]. High-speed processing and communication capabilities of modern microprocessors are leading to research work using adaptive relaying and Artificial Neural Networks (ANN) for improved protection [8-12].

When a fault occurs on the transmission line, it is very important to find the fault location and make necessary repairs, in order to prevent the fault from spreading and thus restoring the power system to its normal state. Hence, accurate fault location is essential. Different types of fault locators are available [13, 14]. Recently, ANN based fault locators have been proposed [15, 16].

1.2 Aim of the Thesis

Fast and accurate location of faults in an electrical power transmission line is vital for the secure and economic operation of power systems. This is more so in view of the fact that due to an increase in transmission requirements and environmental pressures, utilities are being forced to maximize the transmission capabilities of the existing transmission lines. This effectively means that in order to maintain system security and stability, there is a demand for minimizing damage by restoring the faulted line as quickly as possible.

Power system engineers are always investigating innovative and challenging ways to enhance the performance of the power system and related protective devices. Recently, there has been considerable interest in the application of ANN to power system protection [8-12, 15, 16]. The response of a trained ANN to the inputs is extremely fast. However, to the author's best knowledge, the time required for making a trip decision of an ANN based algorithm is found to be at least one cycle of the power system frequency. Also, the time taken to train the network is found to be quite long, in terms of hours and even days [8, 10, 11, 15]. This drawback is present both in the case of distance protection and fault location schemes. Also, the work reported considers only the single-line-to-ground fault case.

This work explores the application of an ANN based methodology for transmission line relaying. A novel feedforward neural network, which indicates whether a fault is within or outside the protection zone of a transmission line, is presented. The neural network scheme is extended to locate the distance of the fault location. It is

proposed to design an ANN based algorithm to perform the functions of distance protection and fault location. The proposed scheme utilizes the frequency spectrum of the voltages and currents to make a trip decision. The emphasis of this work is to:

- minimize the time required for reaching the decision
- provide an accurate relaying decision

Single-line-to-ground fault and three-phase fault cases are considered. The performance of the trained neural network is evaluated by testing the ANN based algorithm with data obtained from the simulation of a transmission line model, using Electromagnetic Transients Program (EMTP). The obtained results are compared with a simulated Fourier-based algorithm in terms of speed and accuracy. The results are found to be accurate in the presence of different fault conditions, such as fault location, fault resistance and fault inception angle. The decision of the ANN output is obtained in about half-cycle after the fault inception.

1.3 Organization of the Thesis

Chapter 2 of this thesis focuses on the zones of protection, principle of operation of distance relays, equations governing the three-phase distance relays for the various fault types, the effect of fault resistance, the different types of relays and operation of fault locators used in transmission line protection.

Chapter 3 discusses the computer relay architecture. The transmission line model used in the simulation is described. The procedure used to obtain the data of the

transmission line model using EMTP is explained. The simulation results obtained using a Fourier-based algorithm are presented.

A brief discussion on ANN is presented in Chapter 4. Applications of ANN for distance protection and fault location in a transmission line are discussed. The proposed ANN based methodology for transmission line relaying is described in this chapter.

The structure and design of the ANN based relaying for transmission line protection is presented in Chapter 5. The concept of using the frequency components of voltage and current as inputs for the ANN is explained. The work is divided into two main parts; in the first part, the ANN based methodology uses the post-fault information and in the second part, both pre-fault and post-fault information are used. The ANN based relaying is considered for single-line-to-ground faults and three-phase faults.

Chapter 6 is devoted to the simulation results of the ANN based relay. The proposed ANN based methodology for transmission line relaying shows promise and has potential for implementation in a digital relay. The proposed scheme for transmission line relaying is also compared with the Fourier-based algorithm. Some of the advantages of the proposed scheme for ANN based transmission line protection are highlighted. A possible on-line configuration of the proposed scheme is presented.

In Chapter 7, the summary of the thesis highlighting the contribution of the research and suggestions for future work are outlined.

Chapter 2

Transmission Line Protection

2.1 Introduction

Transmission lines form a major component of the power system. Transmission line protection is a challenging area in power system protection. The extent of exposure in miles of transmission lines to weather conditions, different system configurations, and the compromises to be made between dependability and security make transmission line protection challenging. A complete transmission line protection scheme would include distance protection (fault indication) and fault location. A relay used in distance protection indicates whether a fault is inside or outside the protection zone, whereas a fault locator indicates the exact location of the fault.

The following chapter discusses the zones of protection in a transmission line. The need for the distance relay and the basic principle of distance protection of transmission lines is explained. A fault occurring in a transmission line can be analyzed by its sequence network. The equations governing these sequence networks are presented. The effect of fault resistance on a transmission line is also discussed. The improvement in the types of

relay is described. When a fault occurs in a transmission line, it is necessary to determine the location of the fault in order to isolate the fault section from the power system. Fault location in a transmission line is briefly discussed.

2.2 Zones of Protection

The common parameters that reflect the presence of a fault are the voltages and currents at the terminals of the protected apparatus. Every fault in the neighbourhood of a relay will disturb its input voltages and currents. However, the relay should disregard those voltage and current conditions produced by faults that are not within the responsibility of the relay. This responsibility for protecting a portion of the power system is defined by a term known as zone of protection. Zone of protection is a region defined by an imaginary boundary line on the power system one-line diagram. A fault in a protective zone initiates the operation of the relay, and the fault is called internal. A fault outside the protective zone does not initiate operation of the relay, and therefore it is called an external or through fault [17, 18]. The zone of protection should meet the following requirements [3]:

- There must be at least one zone of protection for all the power system elements.
- The zones of protection must always overlap to ensure that no portion of the power system is left without protection.

The region of overlap must be such that the likelihood of a fault occurring inside the region of overlap is minimized. This overlapping of adjacent zones is illustrated in Fig. 2.1. Each element of the power system is defined by a protection zone and these zones

overlap. In Fig. 2.1 the zones of protection, for the bus connected to the transmission line (AB) are designated as bus protective zone and the line protective zone respectively. The circuit breakers, represented by the numbers 1, 2 and 3 are located between the two adjacent elements. A bus is an integral part of the power system, with incoming and outgoing lines terminated on it with appropriate circuit breakers. Usually, the line protective zone is set between 85% and 90% of the line length. In this case, the bus protective zone covers for the fault occurring near terminal A of the transmission line. A fault **F** in the protective zone causes the tripping of circuit breakers 1 and 3. Eventually, circuit breaker 2 will trip after certain delay, as it is located within the line protective zone. This ensures correct removal of the fault element.

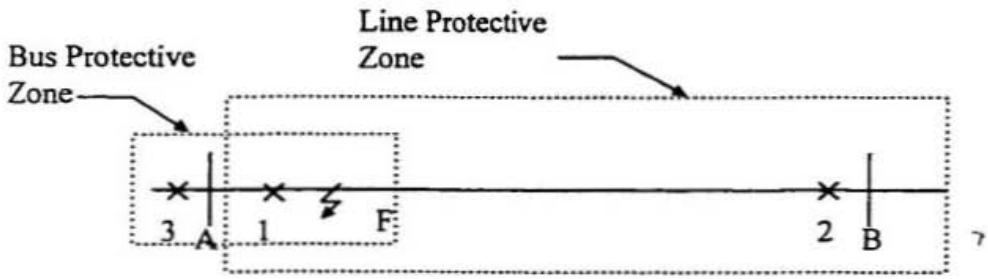

Figure 2.1: Overlapping of protective zones around circuit breaker.

2.3 Distance Protection of Transmission Lines

As mentioned in chapter 1, the function of protective relaying is to promptly remove from service any element that starts to operate in an abnormal condition. The relays prevent further damage to equipment, reduce stress on other equipment, and remove the faulted equipment from the power system as quickly as possible, so that the

integrity and stability of the remaining system is maintained. There are several protective techniques used for transmission line protection [5] such as:

- Overcurrent relaying - These relays respond to the change in the current magnitude.
- Differential relaying – These relays respond to the phase angle between two ac inputs. These relays are suitable for a small extent of protection.
- Directional relaying – These relays respond to the magnitude of the algebraic sum of two or more inputs and are usually used in double-end-feed lines.
- Distance relaying – These relays respond to the distance to a fault.

Among these, distance relays are commonly used to protect high voltage transmission line circuits. The impedance of the transmission line is fairly constant and these relays respond to the distance to a fault on the transmission line. The major advantage of distance relays lies in the fact that they have a fixed reach, *i.e.*, the relay's zone of protection is a function of only the protected line impedance, which is a fixed constant, and it is relatively independent of the current and voltage magnitudes. Distance relays also have the ability to operate for fault currents near or less than maximum load current. They have a greater instantaneous trip coverage compared to an overcurrent relay.

2.3.1 Basic Principle of Distance Protection

In the single-phase system represented by Fig. 2.2, a short circuit at location **F** is considered. The distance relay under consideration is located at line terminal **A**. AB represents the transmission line and **S** denotes the sending end. Z_s represents the equivalent impedance of the transformer, R_{ab} and R_{ba} represent the relays. The voltage

and current at the relay location are related by equations (2.1) and (2.2). Equation (2.3) relates the primary and secondary impedance.

$$Z_{f,P} = E_P/I_P \quad (2.1)$$

$$Z_{f,S} = E_s/I_s \quad (2.2)$$

$$Z_{f,S} = Z_{f,P} * (n_i/n_e) \quad (2.3)$$

where E is the voltage, I is the current, Z is the impedance, subscript p and s denote the primary and secondary quantities respectively.

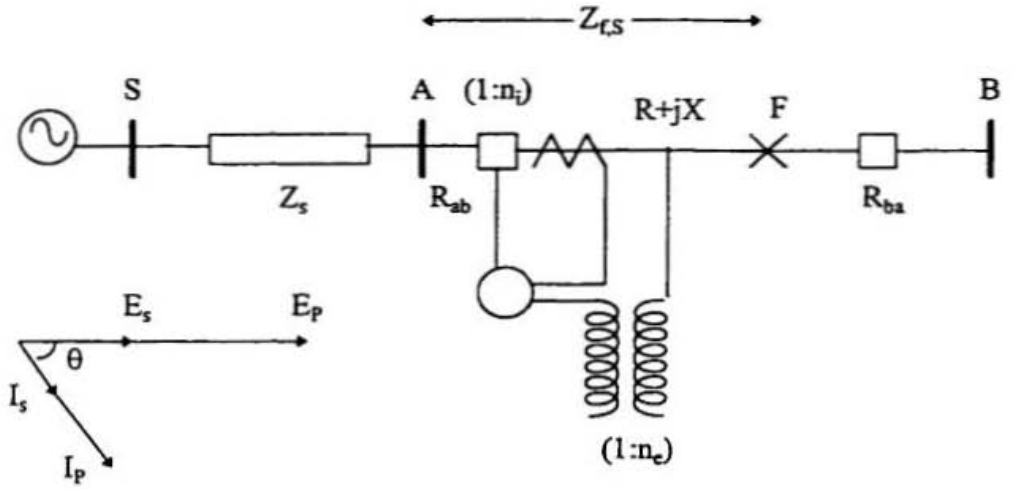

Figure 2.2: Voltage, current and impedance as seen by the relay

In equation (2.3) n_i and n_e represent the current transformer and voltage transformer turns ratio. The ratio E/I is known as the apparent impedance seen by the relay. This impedance is represented by the point **Z**, when plotted in the complex R-X plane, as shown in Fig. 2.3. The R-X diagram is commonly used to analyze the relay response [1].

Most of the relays for distance protection of transmission line use the mho characteristics. If the load current is of constant magnitude, and the sending end voltage at

the relay location is constant, then the corresponding voltage phasor and hence the impedance will be a circle in the R-X plane. The point **Z** in Fig. 2.3 corresponds to the fault at a certain portion of the transmission line. As the location of the fault is moved along the transmission line, the point **Z** moves along the straight line AB in Fig. 2.3. The line AB makes an angle θ with the R-axis, where θ is the impedance angle of the transmission line. For an overhead transmission line, θ lies between 70° and 88°, depending upon the system voltage [2]. Whenever the ratio of the system voltage and current falls within the circle, the relay operates. Knowing the inaccuracies and fault resistance that can be allowed, a more accurate zone shape can be defined so as to occupy a minimum area of the complex R-X plane.

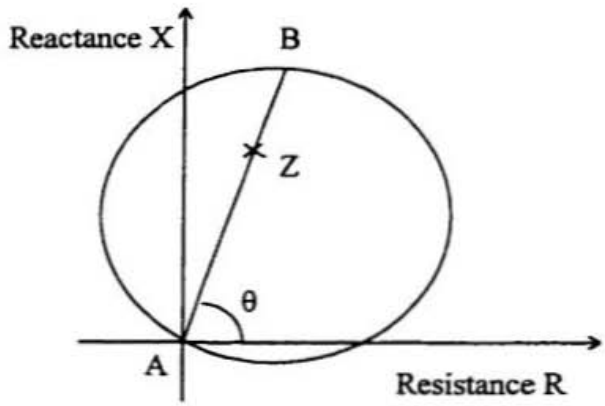

Figure 2.3: Typical R - X diagram to illustrate the relay characteristics

(θ = Impedance angle, AB = Length of the transmission line)

The distance relay is energized by voltage and current supplied by voltage and current transformers respectively. The purpose of the current and voltage transformers is to reduce voltages and currents to levels manageable by the relays and to physically isolate the relays from high voltage [4, 17]. According to the principle of operation explained earlier, the relay detects the fault condition and issues a trip signal to the circuit breaker. The circuit breaker disconnects the faulted transmission line, so as to avoid further damage to the system.

2.3.2 Distance Relay Characteristics

There are four types of distance relays based on the shape of their operating characteristics namely, impedance relays, admittance or mho relays, reactance relays and quadrilateral relays. As mentioned earlier, the R-X diagram is commonly used to represent the characteristics of the relay.

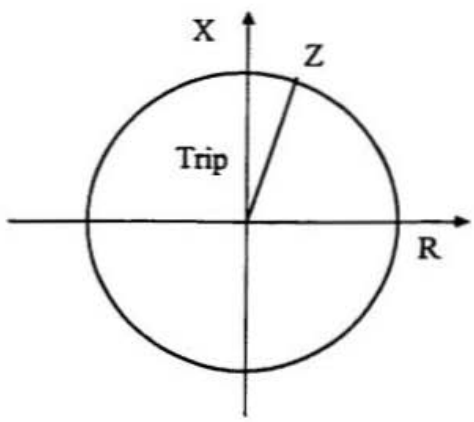

Figure 2.4(a): Impedance relay characteristics

An impedance relay compares the system current and voltage in amplitude, and the calibration of this relay is in terms of the ratio of the two, thus indicating impedance. Fig. 2.4(a) illustrates the impedance relay characteristics. The characteristics plot as a circle with suitable radius, called the setting Z. The center of the circle coincides with the origin of the R-X diagram.

A mho relay takes into account, the phase angle between the voltage and the current, producing a more complex response characteristics. The mho relay characteristics, shown in Fig. 2.4(b) are also described as a circle, but the periphery passes through the origin in the R-X diagram. In Fig. 2.4(b), the line OA has magnitude Z, called the setting at the impedance angle θ.

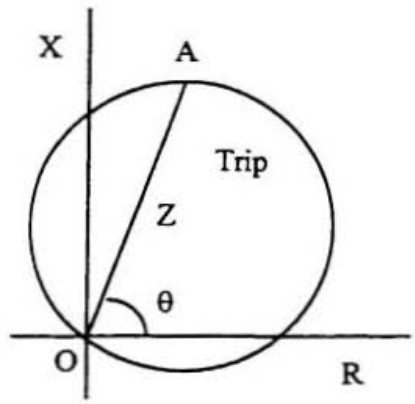

Figure 2.4(b): Mho relay characteristics

A reactance relay illustrated in Fig. 2.4(c), is non-directional, and hence not preferred. The reactance relay has a straight-line characteristic, parallel to the R-axis and offset by the setting X, along the axis represented by the reactance. The reactance relay characteristics have a tripping region below the setting X.

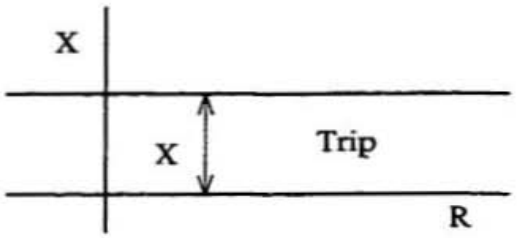

Figure 2.4(c): Reactance relay characteristics

Figure 2.4(d) represents the quadrilateral relay characteristics. The quadrilateral relay characteristics are made use of in solid state or computer relays. In computer relays, the characteristics of a quadrilateral relay are defined in the software of the relay, such that the effect of fault resistance and overreach can be accommodated [17]. If the impedance of the faulted transmission line falls inside the quadrilateral characteristic, the relay indicates a trip output.

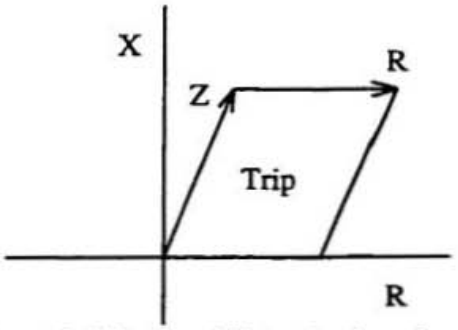

Figure 2.4(d): Quadrilateral relay characteristics

2.4 Three Phase Distance Relay

There are basically ten types of faults on a three phase power system, for which a relay should operate (phases are referred to as *a*, *b*, *c* and ground is referred to as *g*):

- Phase-to-ground (*a-g, b-g, c-g*)
- Phase-to-phase (*a-b, b-c, c-a*)
- Two-phase-to-ground (*a-b-g, b-c-g, c-a-g*)
- Three-phase (*a-b-c*)

Single-line-to-ground fault is the most common type of fault and a three-phase fault is the most severe one compared to the other types of faults [1]. The equations that govern the relationship between the voltages and currents at the relay location are different for each of the ten distinct types of faults. Regardless of the type of fault involved, the voltage and the current used to energize the appropriate relay unit are such that the relay will measure the positive-sequence impedance to the fault [3, 4]. The computation of the fault current and voltage is greatly simplified by the use of the sequence networks. When a fault occurs, an unbalance is created in the system. The three unbalanced phasors of a three-phase system can be resolved into three balanced system of phasors, namely the positive sequence, negative sequence and the zero sequence components. The sequence networks represent the equivalent circuit of the sequence impedances and shows all the paths for the flow of the sequence currents.

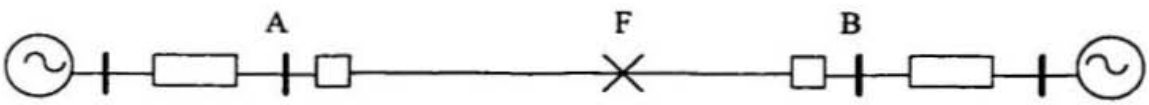

Figure 2.5: Single-line diagram of the transmission line model

(AB = Length of the transmission line, F = fault)

The behaviour of these sequence networks to the various types of faults is explained below. The one-line diagram of the transmission line model, shown in Fig. 2.5 is used to determine the appropriate voltage and current inputs to be used for the distance relays for the different faults. AB represents the transmission line, with a fault **F** at certain portion of it.

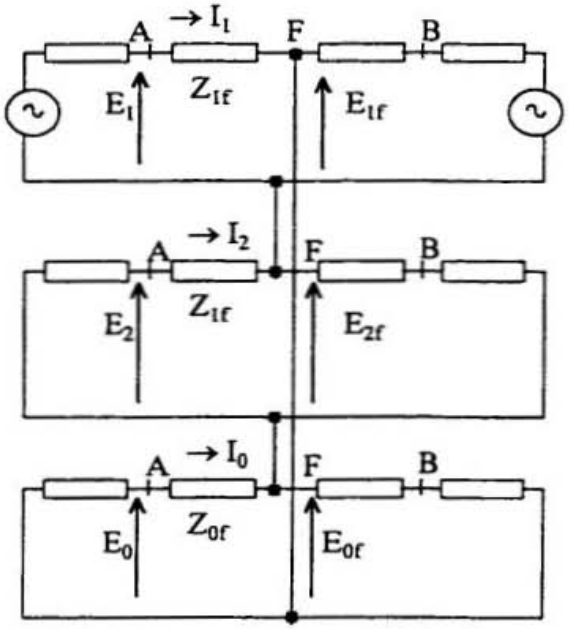

Figure 2.6: Sequence network connection for phase *a*-ground fault

For a fault between phase *a* and ground of the transmission line considered, the sequence networks will be interconnected as in Fig. 2.6. The positive sequence, negative sequence and zero sequence components of voltage at the relay location are represented by equations (2.4), (2.5) and (2.6) respectively [2].

$$E_{1f} = E_1 - Z_{1f} I_1 \tag{2.4}$$

$$E_{2f} = E_2 - Z_{2f} I_2 \tag{2.5}$$

$$E_{0f} = E_0 - Z_{0f} I_0 \tag{2.6}$$

where E_1, E_2, E_0, I_1, I_2, and I_0 are the positive sequence, negative sequence and the zero sequence components of voltage and current respectively. The voltage at the fault point can be set equal to zero and is given by equation (2.8).

$$E_{af} = E_{1f} + E_{2f} + E_{0f} \tag{2.7}$$

$$i.e., E_{af} = E_a - Z_{1f} I_a - (Z_{0f} - Z_{1f}) I_0 = 0 \tag{2.8}$$

$$I_a = (I_1 + I_2 + I_0)/3 \tag{2.9}$$

where E_a is the total voltage at phase a, I_a is the current at phase a and E_{af} is the voltage at the point of fault. From equation (2.8),

$$E_a = Z_{1f}\left[I_a + \left(\frac{Z_{0f} - Z_{1f}}{Z_{1f}} \right) I_0 \right] \tag{2.10}$$

$$E_a = Z_{1f}[I_a + mI_0] \tag{2.11}$$

$$m = \frac{Z_{0f} - Z_{1f}}{Z_{1f}} = \frac{Z_0 - Z_1}{Z_1} \tag{2.12}$$

The factor m in equation (2.11) is known as the compensation factor, and this compensates the phase current for the mutual coupling between the faulted phase and the other two unfaulted phases.

$$E_a = Z_{1f} I_a^{'} \tag{2.13}$$

where $I_a^{'}$ is the compensated phase a current. Thus, for phase a to ground fault, the fault impedance is as illustrated by equation (2.14).

$$Z_{1f} = \frac{E_a}{I_a^{'}} = \frac{E_a}{I_a + mI_0} \tag{2.14}$$

This indicates that the distance relay measures the positive sequence impedance to the fault, when energized with the phase *a* voltage and the compensated phase *a* current.

For the case of a fault between phases *b* and *c* of a three-phase transmission line, the positive sequence and the negative sequence voltages at the fault are equal, and are represented as $E_{1f} = E_{2f}$ and $E_{1f} = E_1 - Z_{1f} I_1$

Thus the fault impedance is given by

$$Z_{1f} = \frac{E_1 - E_2}{I_1 - I_2} \tag{2.15}$$

The phase *b* and *c* voltage quantities, at the relay location are given by equations (2.16) and (2.17).

$$E_b = E_0 + \alpha^2 E_1 + \alpha E_2 \tag{2.16}$$

$$E_c = E_0 + \alpha E_1 + \alpha^2 E_2 \tag{2.17}$$

where $\alpha = 1\angle 120^\circ$. Hence,

$$(E_b - E_c) = (\alpha^2 - \alpha)(E_1 - E_2) \tag{2.18}$$

$$(I_b - I_c) = (\alpha^2 - \alpha)(I_1 - I_2) \tag{2.19}$$

$$Z_{1f} = \frac{E_b - E_c}{I_b - I_c} = \frac{E_1 - E_2}{I_1 - I_2} \tag{2.20}$$

Equation (2.20) indicates that when a fault occurs between phases *b* and *c*, the distance relay will measure the positive sequence impedance. Similarly, for the faults between phase *a-b* and *c-a* faults, the corresponding relay will measure the positive sequence impedance to the fault.

For faults occurring between phase-to-phase-to-ground, the performance equations for the sequence networks are exactly similar to equations (2.15) to (2.20) of the phase-to-phase fault.

The sequence network for a three-phase fault is indicated in Fig. 2.7 [2]. A three-phase fault causes maximum abnormal short-circuit current and hence is the most dangerous fault [17]. For a three-phase fault, the sequence quantities are represented by equations (2.21) and (2.22). The respective phase voltages are given by equations (2.23), (2.24) and (2.25).

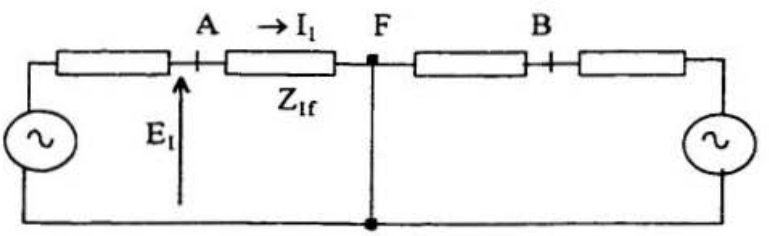

Figure 2.7: Sequence network connection for a three-phase fault

$$E_1 = E_a = Z_{1f} I_1 = Z_{1f} I_a \quad (2.21)$$

$$E_2 = E_0 = 0 \quad (2.22)$$

$$E_a = E_1 \quad (2.23)$$

$$E_b = \alpha^2 E_1 \quad (2.24)$$

$$E_c = \alpha E_1 \quad (2.25)$$

where $\alpha = 1\angle 120°$. Hence for a three-phase fault, fault impedance Z_{1f} is represented as in equation (2.26).

$$Z_{1f} = \frac{E_a - E_b}{I_a - I_b} = \frac{E_b - E_c}{I_b - I_c} = \frac{E_c - E_a}{I_c - I_a} = \frac{E_a}{I_a} = \frac{E_b}{I_b} = \frac{E_c}{I_c} \qquad (2.26)$$

The fault impedance for the different types of fault is illustrated in Table 2.1, with the nomenclature as explained above. For the faults at other phases, the corresponding phase voltages/currents are used to calculate the fault impedance.

Table 2.1: Summary of the fault impedance for different types of fault

Type of fault	Fault impedance
Single-line-to-ground (at phase a)	$\frac{E_a}{I_a + \frac{Z_0 - Z_1}{Z_1} I_0}$
Phase-phase (between phase b and c)	$\frac{E_b - E_c}{I_b - I_c}$
Phase-phase-to-ground (between phase b - c and ground)	$\frac{E_b - E_c}{I_b - I_c}$
Three-phase	$\frac{E_a}{I_a}$

2.5 Effect of Fault Resistance

All the above equations have been derived assuming that the fault is a metallic short circuit. If the fault involves an arc or a path through the ground, non-linear impedances are introduced which tend to introduce harmonics into the current or voltage [2]. As a result, an error is introduced in the fault distance estimate, and hence may lead to an unreliable operation of the distance relay. To accommodate the fault resistance, the trip

zone of the distance relay is selected such that the region surrounding the apparent impedance is included inside the zone [2, 5, 18].

In the single-line diagram of Fig. 2.8, R_f represents the fault resistance. The contribution to the fault from the remote end is I_r and hence the fault current is given by:

$$I_f = I + I_r \tag{2.27}$$

The voltage at the relay location is given by equation (2.89).

$$E = Z_f I + R_f (I + I_r) \tag{2.28}$$

Z_f is the impedance when the fault resistance is zero. The apparent impedance Z_a seen by the relay is:

$$Z_a = \frac{E}{I} = Z_f + R_f \{\frac{I_r}{I} + 1\} \tag{2.29}$$

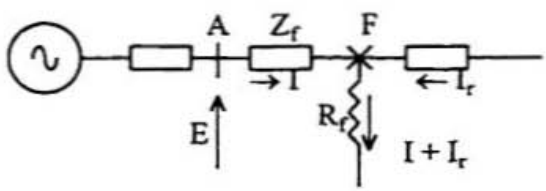

Figure 2.8: Fault path resistance

The voltage drop in the fault from the remote source magnifies the fault resistance as seen at the local bus and shifts the apparent impedance to the right in the R-X plane. The total voltage drop in the fault will not be in phase with the local fault current and the fault resistance thus becomes more reactive. This leads to possible overreach and underreach errors. In an overreach error condition, the fault will be outside the zone, but is seen by the relay as being inside the zone. Underreach error condition occurs when the

fault occurs inside the protection zone, but the relay is not able to identify it. This type of condition creates serious problem when heavy load flow and heavy fault resistance are encountered.

2.6 Types of Relay

Distance relays are commonly used for transmission line protection, due to their insensitivity to variations in fault current and their virtual immunity from operating on normal load current. Over the years, distance relays have undergone changes leading to improved relay performance. The earliest relays used for transmission line protection were the electromechanical relays. They were later replaced by the solid-state relays. With the advent of the digital technology, the solid state relays gave way to the relays based on the computer relaying algorithms. The recent trend is to use Artificial Neural Network (ANN) based relays.

2.6.1 Electromechanical and Solid-state Relays

These relays utilize the actuating forces produced by electromagnetic interaction between a combination of the input signals and the stored energy in the springs. In an electromechanical relay, the measurement is derived from a balance of magnetic or mechanical forces within the relay by the operation of the electrical contacts. The most common electromechanical relays are the magnetic attraction, magnetic induction, D' Arsonval and the thermal units.

In general, electromechanical relays respond to one or more of the conventional torque producing input quantities: (a) voltage, (b) current, (c) product of voltage, current, and the angle between them, and (d) a physical or design force such as a control spring. When the current or voltage applied to the magnetic attraction unit exceeds the pick up value, the operating coil will provide a force to overcome the restraint, causing the contacts to change position. The magnetic induction units operate by torque derived from the interaction of fluxes produced by an electromagnet with those from induced currents in the plane of a rotatable aluminium disc. In the D'Arsonval unit, a moving coil is energized by direct current, which reacts with the air gap flux to create rotational torque. In a thermal unit, as the temperature changes, the different coefficients of thermal expansion of the bimetallic strips cause the free end of the coil to move. A contact attached to the free end will then operate based on the temperature change [1]. The advantages of an electromechanical relay are the simplicity involved and low cost.

The solid-state relays use combinations of solid-state components which are designed using dc voltage signals to perform the logic functions. In solid-state relays, fault sensing and data processing logic circuits use power system inputs to determine if any intolerable system conditions exist within the relay's zone of protection. In this case, the measurement of electrical quantities is performed by the static network. The output signal operates a tripping device when the threshold condition is exceeded. Compared to the electromechanical relays, the performance of the solid-state relays is superior, it has reduced size and is faster in operation. It has a longer life and offers high resistance to shock and vibration [5]. Due to the absence of mechanical inertia, a high resetting value

can be obtained. Some of the disadvantages associated with the solid-state relay are the low short-time overload capacity and voltage withstand capability.

2.6.2 Digital Relays

A digital relay has the remarkable capability of sampling voltages and currents at very high speed, retaining fault information and performing self-checking functions. A major requirement of a digital relay is to estimate precisely and quickly the electrical distance to the fault. Some of the features provided by digital relays are good communication capability, automatic self-testing, fault locating, metering and load-encroachment logic [7]. Many algorithms for digital distance protection have been proposed [6, 19, 20] with the aim of improving the speed of the relaying decision. Among them, the most common ones are the Fourier algorithm, Kalman filtering algorithm and the Walsh algorithm. The performance of these algorithms depends upon the accuracy of estimating the fundamental frequency components of voltages and currents from a few samples. Most of the existing algorithms in use for digital relaying are based on the waveform itself, *i.e.*, the voltage or the current. The fundamental frequency voltage and current phasors are used for the impedance relaying. A distance relay filter must save the fundamental frequency components and reject the noise signals. The relay response to the noise signals depends on the filtering process.

Usually, any non-fundamental frequency signal constitutes an error [6, 21]. The relay voltage and current are full of harmonics and dc offset. The digital relays are capable of filtering this noise by suitable algorithms without producing secondary

transients. The filtering extracts the fundamental frequency components and the magnitude and angle of the impedance is calculated. Based on these fundamental frequency values, a tripping or no-tripping decision is made.

In addition to the Fourier, Walsh and Harr filters, it is found that a sine-cosine filter exhibits good response when dc offset is present in the current signal and the voltage is contaminated with high frequency damped oscillations [19]. Algorithms based on a variable sampling frequency will be able to extract the fundamental frequency components of the fault signals correctly, and at the same time, the burden of computation is greatly reduced [20].

The disadvantage of the microprocessor relays is that they cannot adapt dynamically to the system operating conditions. If presented with a noisy signal, there is a possibility of an incorrect operation. A digital distance relay based on Fourier algorithm was simulated, the results of which will be presented in chapter 3 of the thesis.

2.6.3 Recent Trends

Recently there has been considerable interest in ANN based protection relays [8-12, 15, 16]. ANNs have the capability of learning and self-organization [22]. ANNs are being used for problem solving applications in fields related to power engineering. An inherent advantage of using ANN based algorithm for protective relaying is the possibility of shorter trip decisions and robustness to changing system conditions.

The motivation of using ANN based algorithms for transmission line relaying stem from the fact that ANNs possess excellent noise immunity, robustness, fault-

tolerance and generalization capability. ANN applications in transmission line relaying are related to improvements in distance relaying. Conventional algorithms try to determine the fault area corresponding to the relay by the estimation of impedance or distance using current and voltage measurements. Algorithms based on ANN make use of the pattern recognition capability. A detail review of some of the applications of ANN for transmission line relaying will be presented in chapter 4.

2.7 Transmission Line Fault Locator

When a fault occurs on the transmission line, it is very important to find the location of the fault, in order to clear the fault. Locating faults on transmission lines with high accuracy accelerates the maintenance operation and saves time and effort. The degree of accuracy required in clearing the faults is ever increasing. The fault location is determined by the measurement of the impedance between the relaying location and the fault.

Considerable work has been done in developing digital techniques for locating faults on transmission lines. Fault location techniques that use fundamental frequency voltages and currents have been proposed [13, 14]. However, the effect of fault resistance is not taken into account. Also, the algorithms fail to estimate the fault location during the changes in the system configuration such as different fault resistance and loading condition. ANN based protection schemes have showed encouraging results. To improve the accuracy of fault locators, ANN based fault locators are recently proposed in [15, 16].

Applications of ANN for fault location in transmission line will be presented more in detail in chapter 4.

2.8 Summary

This chapter has explained the general operating principle of distance protection of transmission lines. An overview of the three-phase distance relays and the performance equations governing the sequence networks have been provided. Due to the presence of the fault resistance, the impedance measured by a distance relay is different from the actual impedance, leading to overreach or underreach conditions. The fault resistance has to be accounted for while designing an algorithm for transmission line protection. Distance relays for transmission line protection have evolved from electromechanical relays to solid-state relays followed by microprocessor based (digital) relays. The recent trend in the area of transmission line protection is ANN based-relay. Relays based on ANN algorithm show promising results. A review of the ANN applications for transmission line relaying and the motivation for investigating an ANN based relay in this research will be discussed in chapter 4.

Chapter 3

Digital Distance Relays for Protection of Transmission Lines

3.1 Introduction

The availability of high speed, low cost microprocessors has led to the development of digital protective relays for transmission line protection. A digital relay, by its very nature, makes a measurement of power system quantities of interest (*i.e.*, voltages and currents) and then makes a relaying decision based on these measurements. This is in contrast to conventional relays, where the operating characteristic is inherent in the relay design. Digital relays provide large setting ranges, high-speed operation, programmability and are low in cost. Digital relays also provide communication capability. Due to these advantages, digital relays find wide application in electric power utilities.

In this chapter, the block diagram of a typical computer relay architecture will be described. As long as there is no fault, the voltage and current waveforms are purely sinusoidal. When there is a fault, the post-fault voltage and current waveforms are

distorted. Many algorithms are proposed to extract the fundamental frequency component of voltage and current waveforms. A full cycle Fourier algorithm used in the digital relay is presented in this chapter. The transmission line model used in the simulation will be described in detail, followed by the EMTP procedure used to obtain the data for simulation. The simulation results obtained for the transmission line model considered, using Fourier algorithm will be presented.

3.2 Computer Relay Architecture

The basic tasks of a computer relay is accepting the inputs, processing the inputs, giving an output representing a system quantity and making a decision. The inputs to the relay are voltages and currents. To obtain a digital representation of these quantities, the analog signals are sampled using suitable data acquisition systems.

Fig. 3.1 represents a configuration for a digital relay [2]. The current and voltage signals obtained from current and voltage transformer must be scaled down. The current and voltage signals are processed by the surge filters to suppress or remove the surge present in them. Surges are usually created by faults and switching operations on the power system. The high frequency transients are removed by the anti-aliasing filters that have a low cut-off frequency. The Analog to Digital Converter (ADC) converts the analog signals to digital form. The sample-and-hold circuit is used to obtain simultaneous sampling of all signals. The sampling clock provides pulses at the sampling frequency. The core of the digital relay is the algorithm used. The processor executes the relay programs, maintains the various timing functions and communicates with the peripheral environment.

The relaying algorithm processes the sampled data to produce a digital output. This output will be used to give trip signals to circuit breakers, which will isolate the faulted transmission line.

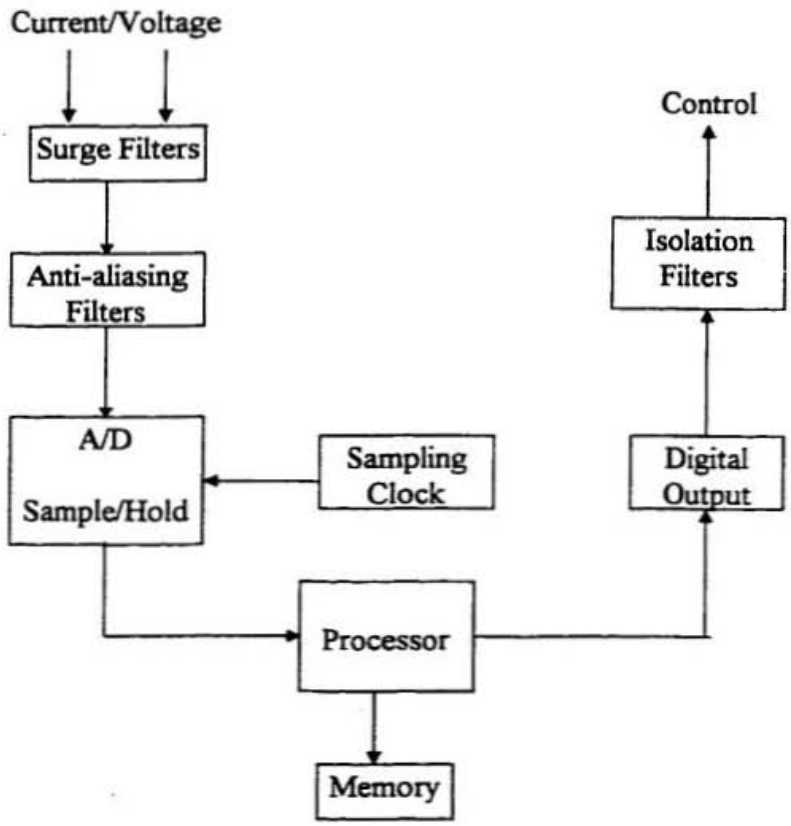

Figure 3.1: Block diagram of a computer relay

3.3 Fourier Algorithm

A fault in a transmission line increases current magnitude and decreases voltage magnitude and changes the phase shift between them. The fault also causes transients or noise, such as dc offset and harmonics. Transients may lead to relay malfunction, where the relay is assumed to be fed only with sinusoidal quantities. Thus, any event or fault generated noise needs to be removed or filtered from the relaying voltages or currents and then fed to the relay.

Full-cycle Fourier algorithm is one of the commonly used algorithms for filtering out the transients present in the post fault voltage and current waveforms [19, 20]. This algorithm uses consecutive sampled values of voltage and current and evaluates the fundamental frequency component of the voltage and current. These components are then used to determine the apparent impedance. Apparent impedance is the loop impedance using the voltages and currents that the relay receives [1]. A digital relay based on full-cycle Fourier algorithm was simulated as an initial part of the work. Full-cycle Fourier algorithm is chosen for this study because of its good frequency response [21].

In the simplest form, a Fourier algorithm extracts the fundamental phasor from samples of a periodic signal taken at equal intervals over a full period of the signal. Taken over a full period, the Fourier calculation rejects harmonics of the fundamental frequency. Any periodic waveform can be represented by a fundamental and series of harmonic frequencies [1, 17]. The n^{th} harmonic component of the signal is represented by the Fourier series, given by equation (3.1).

$$f_n(t) = a_n \cos(\omega_n t) + b_n \sin(\omega_n t) \tag{3.1}$$

where

$$a_n = \frac{2}{T_o} \int_{-T_o/2}^{T_o/2} f(t) \cos(n\omega t) dt \tag{3.2}$$

$$b_n = \frac{2}{T_o} \int_{-T_o/2}^{T_o/2} f(t) \sin(n\omega t) dt \tag{3.3}$$

and $f(t)$ = the original function

T_o = the period of the waveform

n = the order of the harmonic

The sum of the product of the function and the sine of the frequency that is to be extracted, taken over the period of the fundamental, produces a total that contains only the desired frequency. This is the fundamental premise of Fourier analysis. The comparable digital process involves the multiplication of individual samples by stored values from a reference sinewave as represented by equations (3.4) and (3.6) and summing the products over a full cycle.

$$A_C = \sum_{K=0}^{N-1} f_K(t) C_{AK} \tag{3.4}$$

$$C_{AK} = \frac{2}{N} \cos\left(2\pi \frac{K}{N}\right) \tag{3.5}$$

$$A_S = \sum_{K=0}^{N-1} f_K(t) C_{BK} \tag{3.6}$$

$$C_{BK} = \frac{2}{N} \sin\left(2\pi \frac{K}{N}\right) \tag{3.7}$$

K = number of samples

N = samples per cycle

Only the fundamental frequency is required for line protection using the impedance concept. Frequency response of the full-cycle Fourier algorithm is presented in Fig. 3.2, which shows that the full-cycle Fourier algorithm filters out the dc offset and the non-fundamental frequency components, upto half the sampling rate. The anti-aliasing filter needs to filter out harmonics above N/2. The frequency response of the Fourier algorithm is summarized in Table 3.1. For a pure sinusoidal waveform, only the fundamental frequency component is present, as seen from Table 3.1.

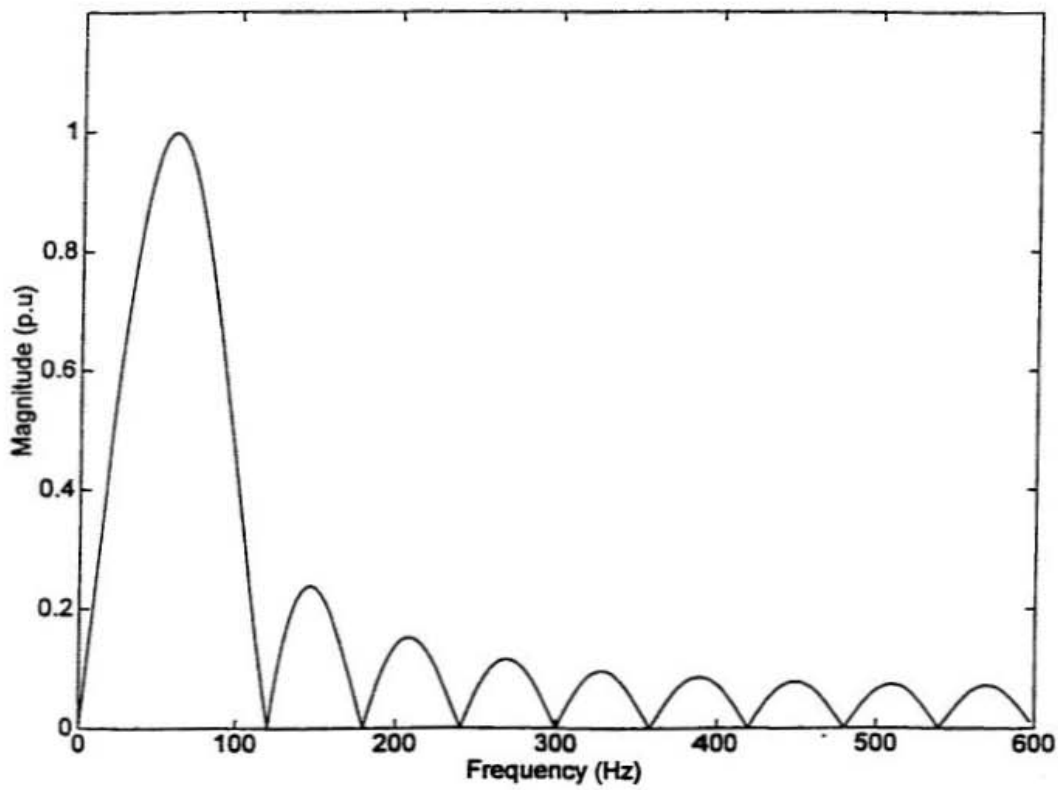

Figure 3.2: Frequency response of full cycle Fourier algorithm

Table 3.1: Frequency components of Fourier algorithm [17]

DC	Fundamental	2nd	3rd	4th	5th	6th	7th	8th	Harmonics
0	100%	0	0	0	0	0	0	0	

3.4 Description of the Transmission Line Model

A 345 kV, 160 mile transmission line was simulated using Electromagnetic Transients Program (EMTP), for various fault cases [23]. The purpose of this simulation is to obtain the data needed for the design of the full-cycle Fourier algorithm. The single-line diagram of the transmission line model is shown in Fig. 3.3 [24]. A generator is connected through a step-up transformer to a 345 kV transmission line. A distance relay R is assumed to be at this substation. The transmission line is 160 miles long and is connected to a 400 MVA generating station at the sending end and an equivalent of a large interconnected system at the receiving end. AB represents the transmission line, and F is the fault point. It is customary to set zone 1 of protection between 85% and 90% of the line length [2]. The zone of protection is selected to be 90% of the line. The details of the transmission line parameters are given in appendix A.

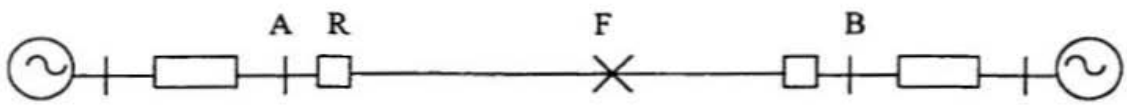

Figure 3.3: Single line diagram of the transmission line model

(Voltage at substation **A** = 1.02 p.u, Voltage at substation **B** = 0.97 p.u)

(AB = length of transmission line, R = relay, F = fault)

Four types of faults namely, single-line-to-ground fault (between phase *a* - ground), phase-to-phase fault (between phases *a* - *b*), two-phase-to-ground fault (between phases *a* - *b* - ground) and three phase fault (between phases *a* - *b* - *c*) are simulated using the EMTP program. The sampling rate is chosen to be 16 samples/cycle. For a sampling rate of 16 samples per full-cycle window of the input signal, the sampling instants will be for every 360°/16 = 22.5°. For each cycle, there will be 32 multiplications and the number of additions/subtractions will be 32.

The location of the fault point is selected at 40%, 60%, 80% and 95% of the transmission line. The data for various fault types is generated for a fault resistance R_f of 0 Ω and 10 Ω in the fault path. The instant of fault occurrence φ is chosen to be at an angle of 0° and 90°. The fault switch is suddenly closed when the voltage waveform just crosses the time axis scale, to represent the fault occurring at 0° and the fault switch is closed when the voltage waveform has reached its peak to represent the fault occurring at 90° case. Five cycles of data are obtained, with 2 cycles of pre-fault condition and 3 cycles of post-fault condition.

3.5 General Procedure for EMTP Simulation

EMTP software is used to simulate the transmission line model shown in Fig. 3.3, to obtain the voltages and currents. EMTP is a computer program for simulating electromagnetic, electromechanical and control system transients on multiphase electric power systems. The EMTP was developed in the late 1960's by Dr. Hermann Dommel, as a digital computer counterpart to the analog Transient Network Analyzer (TNA) [23].

Distributed parameter model of the high voltage transmission line is considered for this study. This EMTP code is written in FORTRAN language, with every node represented by a name and the component values indicated between these node names. EMTP provides provision to change the time step accordingly, so as to obtain the desired sampling rate. To simulate the condition of faults occurring at different lengths of transmission line, the corresponding impedance is selected and the desired fault resistance is inserted at that point. For the simulation of faults occurring at a particular angle, the angle is converted to the corresponding time and the fault switch is closed at that instant of time.

The voltage data of a faulted phase, as attained from the transmission line model, for an *a* phase to ground fault at 80% of the transmission line from the relay location, with fault resistance of 0 Ω and the fault inception angle φ at 0° is shown in Fig. 3.4. As seen from Fig. 3.4, the post-fault voltage has decreased in magnitude and is highly distorted. The post-fault current has increased in magnitude and contains a dc-offset. The voltage and current waveforms obtained from the EMTP are exported to an Excel file and later converted into a text file. This text file contains the voltage and current data at the required sampling rate.

For obtaining the data to design the ANN based algorithm, many cases of fault are simulated and the details will be presented in chapter 5.

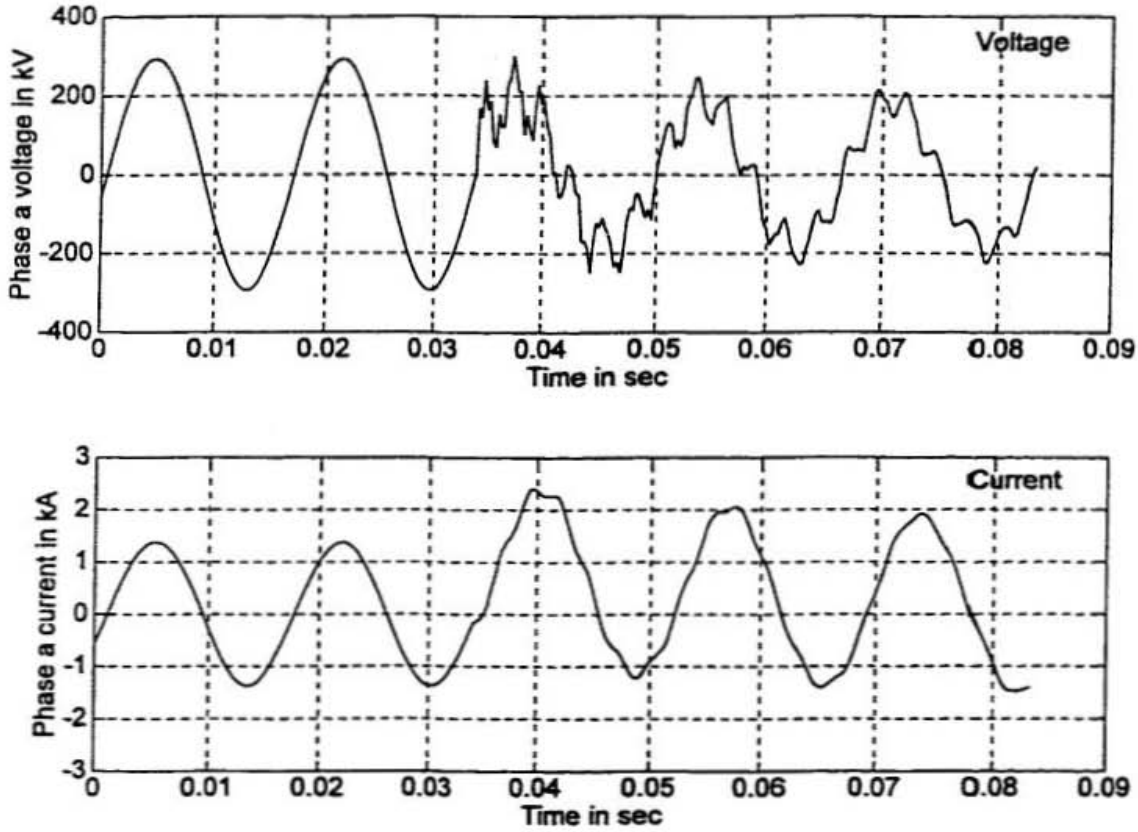

Figure 3.4: Voltage and current of the faulted phase

(Phase *a* to ground fault at 80% of the line, $R_f = 0\ \Omega$, $\varphi = 0°$)

3.6 Simulation Results

A digital relay based on full-cycle Fourier algorithm is simulated. The aim is to extract the fundamental frequency components from the fault signals and then to evaluate the impedance. Few typical fault cases were considered, and the response of the Fourier algorithm for the faults was obtained using MATLAB [25].

The performance of this algorithm for the single-line-to-ground fault at phase *a* at 40%, 60%, 80% and 95% of the transmission line and with fault resistance R_f of 0 Ω and fault inception angle φ of 0°, is plotted in the impedance trajectory, as shown in Fig. 3.5. In Fig. 3.5, AC represents 90% of the line, which is taken as the zone of protection, and PF represents the pre-fault loading condition. The line AC is drawn at an angle of 75°, which is taken as the standard impedance angle, to the x-axis represented by the resistance [2]. Since the sampling rate is taken as 16 samples/cycle, the first 16 points are concentrated at a point (represented by PF in Fig. 3.5) corresponding to the pre-fault impedance. The trajectory moves from the point corresponding to the pre-fault loading to a point inside the relay operating characteristics. The time taken to reach this point is around 24 points, which corresponds to about 1½ cycles. As seen from Fig. 3.5, for the case of fault occurring at 95% of the line, the trajectory never reaches a point inside the circle. A trip signal is issued for faults occurring at 40%, 60% and 80% of the transmission line, whereas for the case of fault occurring at 95% of the transmission line, no trip signal is given.

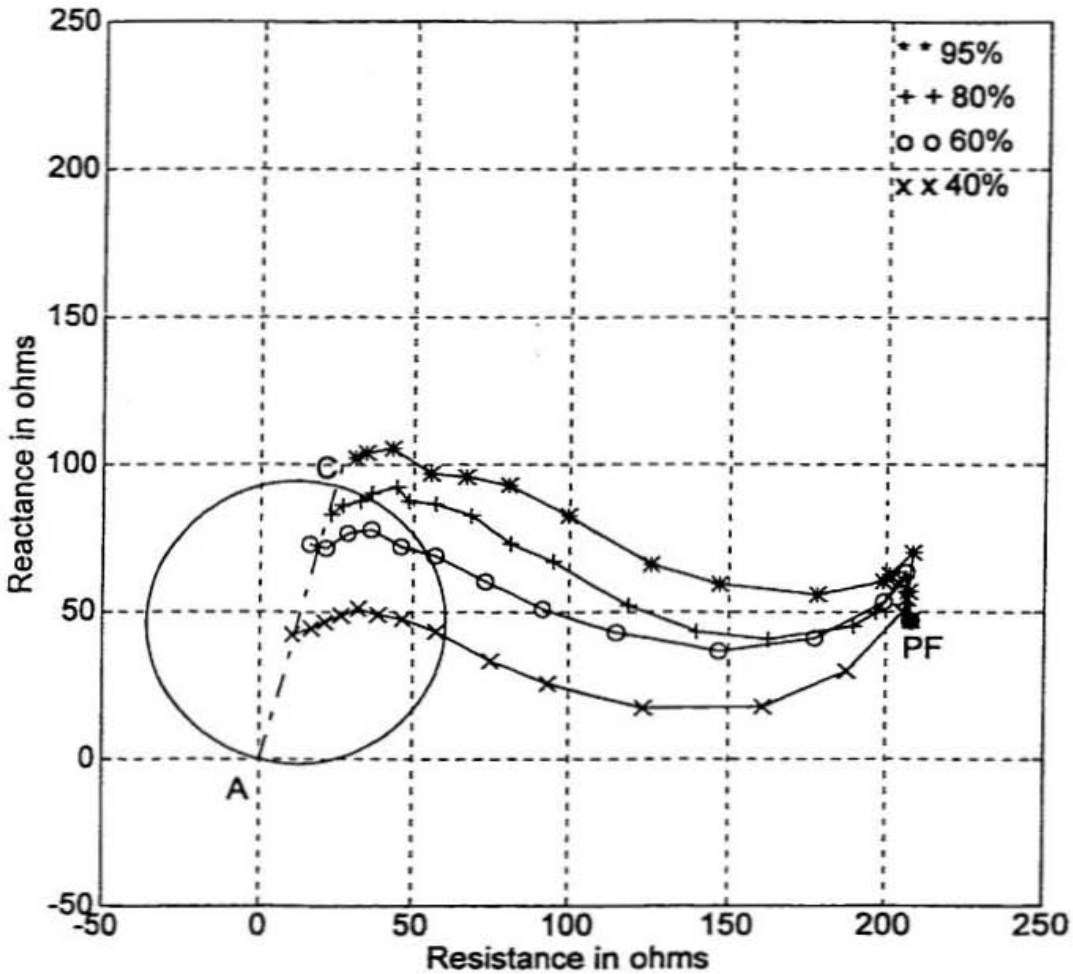

Figure 3.5: Distance relay trajectory for phase *a* to ground fault, $R_f = 0\ \Omega$

(Fault at 40%, 60%, 80% and 95% of the transmission line, $\varphi = 0°$)

AC → 90% of the line, PF → Pre-fault loading condition

Figure 3.6 represents the impedance trajectory for the single-line-to-ground fault at phase *a* with fault resistance R_f of 10 Ω and φ of 0°. Line AC in Fig. 3.6 represents 90% of the line and line AD represents 80% of the line. As seen in Fig. 3.6, for the case of fault occurring at 95% of the line, the trajectory has moved inside the circle, which should not have been the case. As discussed in chapter 2, the effect of fault resistance present at the fault location is generally to reduce the effective reach of the measuring element. Hence for the fault occurring at 95% of the line, which is outside the zone of protection, the Fourier algorithm fails to identify it correctly. Also, though the trajectory reaches the zone of protection described by the circle, it fails to reach the exact operating line AC. In order to accommodate the effect of fault resistance, the trip zone is shaped in the form of a circle so that for faults occurring within the zone of protection, the impedance trajectory falls inside the circle.

In case the zone of protection is selected to be 80% of the line from the relay location, then for the case of fault occurring at 95%, the Fourier algorithm will be able to identify it clearly as fault occurring outside the trip zone, as seen from Fig. 3.6. The smaller circle in Fig. 3.6 is for the case when the zone of protection is considered as 80% of the line. The results have been verified for faults occurring at different lengths of the transmission line. Thus, for the Fourier algorithm to work accurately, the zone of protection will be limited. Error compensation techniques are available to overcome the possible overreach condition and thus provide accurate relaying [26].

Figure 3.7 represents the impedance trajectory for the single-line-to-ground fault at phase *a* with fault resistance R_f of 0 Ω and fault inception angle of 90°. For this case,

the Fourier algorithm identifies the faults correctly. The response is similar to the one obtained in Fig. 3.5.

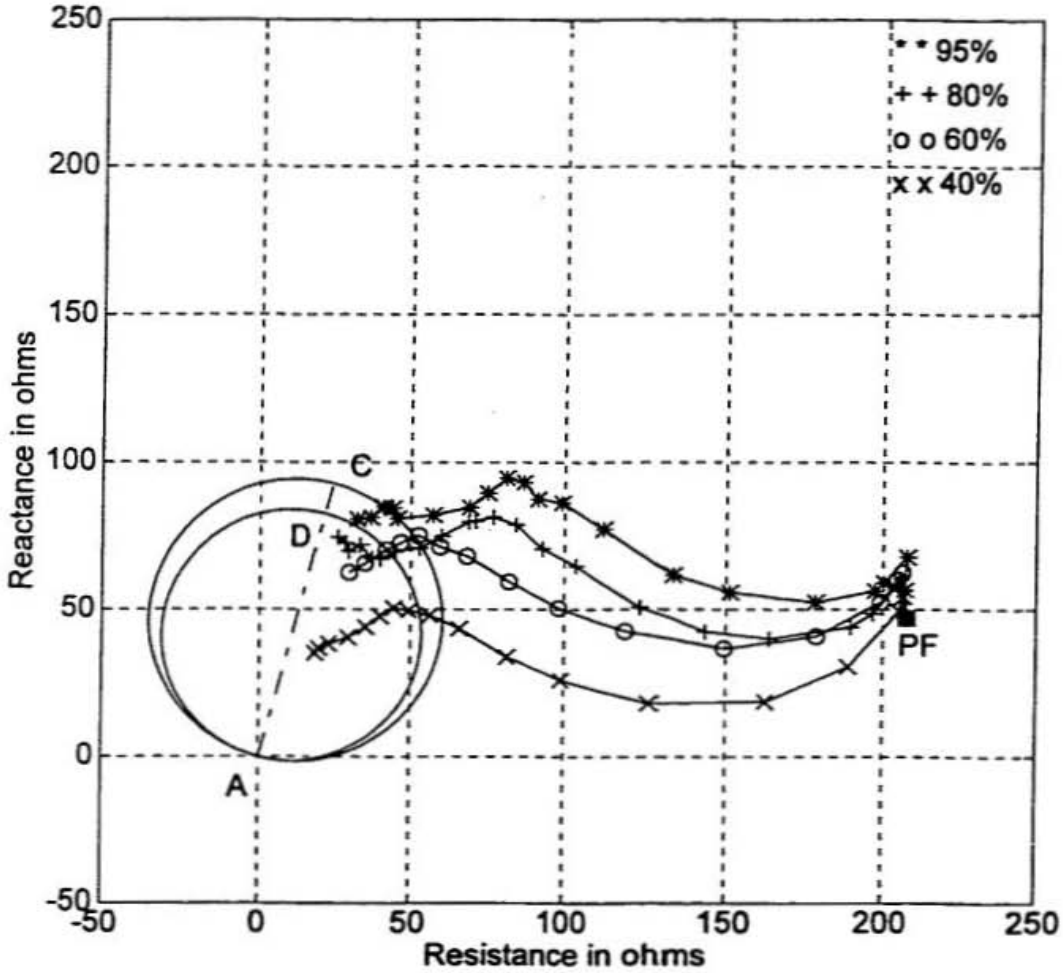

Figure 3.6: Distance relay trajectory for phase a to ground fault, $R_f = 10\ \Omega$

(Fault at 40%, 60%, 80% and 95% of the transmission line, $\varphi = 0°$)

AC → 90% of the line, AD → 80% of the line, PF → Pre-fault loading condition

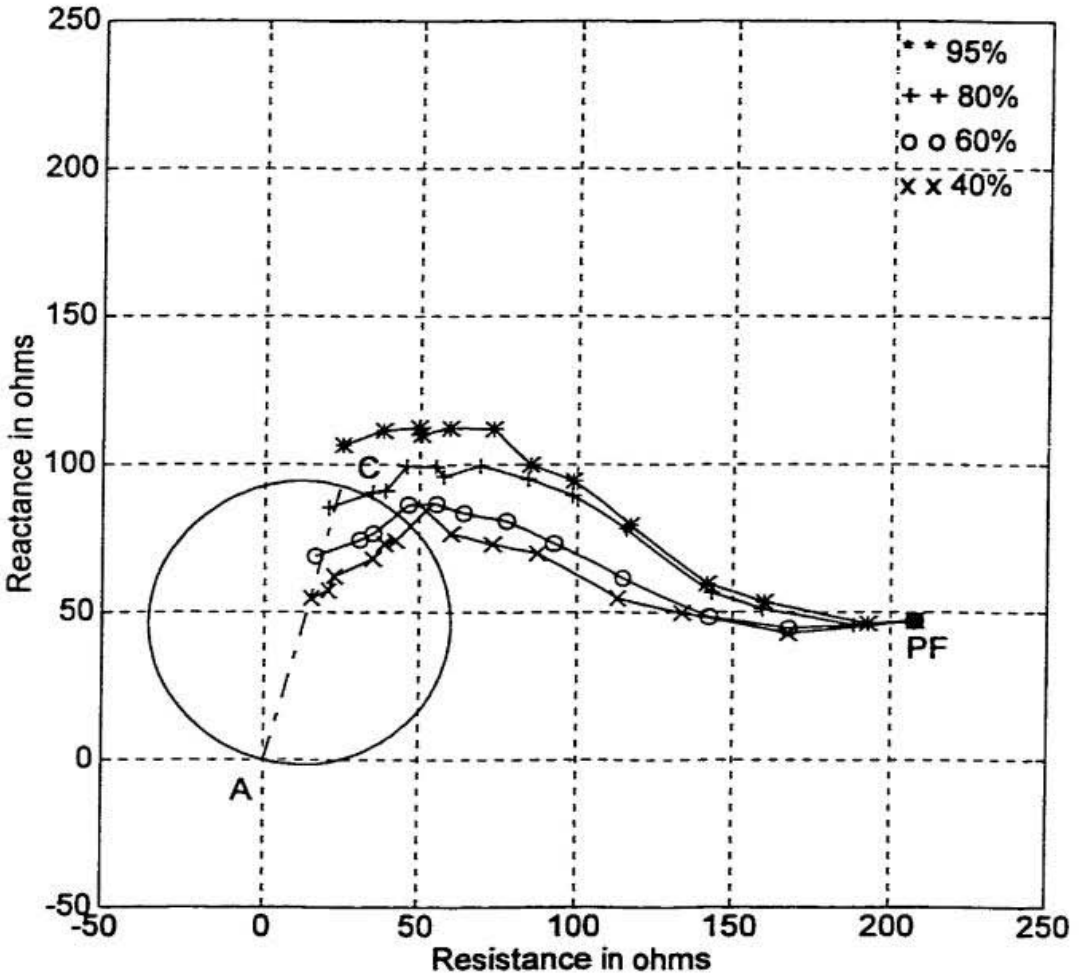

Figure 3.7: Distance relay trajectory for phase *a* to ground fault, $R_f = 0\ \Omega$

(Fault at 40%, 60%, 80% and 95% of the transmission line, $\varphi = 90°$)

AC → 90% of the line, PF → Pre-fault loading condition

The distance relay trajectory for the three phase fault (*a-b-c*) at 40%, 60%, 80% and 95% from the relay end of the transmission line is as shown in Fig. 3.8. The fault resistance R_f is 0 Ω and fault inception angle φ is 0°. As in the case of phase *a* - ground fault, the Fourier algorithm accurately classifies the faults occurring within the trip region (faults at 40%, 60%, 80% of the line) and outside it (fault at 95% of the line).

The response of the Fourier algorithm for the three phase fault (*a-b-c*) at 40%, 60%, 80% and 95% of the transmission line and with R_f of 10 Ω and φ at 0° is shown in Fig. 3.9. Since a fault resistance of 10 Ω is included in the fault path, an overreach condition as explained in chapter 2 is encountered and the Fourier algorithm fails to identify the fault case at 95% of the line to be outside the trip region. The circle with diameter AD represents the case of 80% zone of protection. As explained above, the Fourier algorithm identifies all the fault cases accurately for a smaller zone of protection.

For the case when the fault occurs at R_f of 0 Ω and φ of 90°, the distance relay trajectory is as shown in Fig. 3.10. As seen from the figure, a trip decision is given after around 24-25 points corresponding to about 1½ cycles for faults occurring at 40%, 60% and 80% of the line. For the fault occurring at 95% of the line, no trip signal is given.

Similar results are obtained for the phase-to-phase fault and two-phase-to-ground faults. Since the performance equations of the sequence networks for two-phase-to-ground fault are similar to that for phase-to-phase fault, the impedance trajectories for these two cases resemble each other.

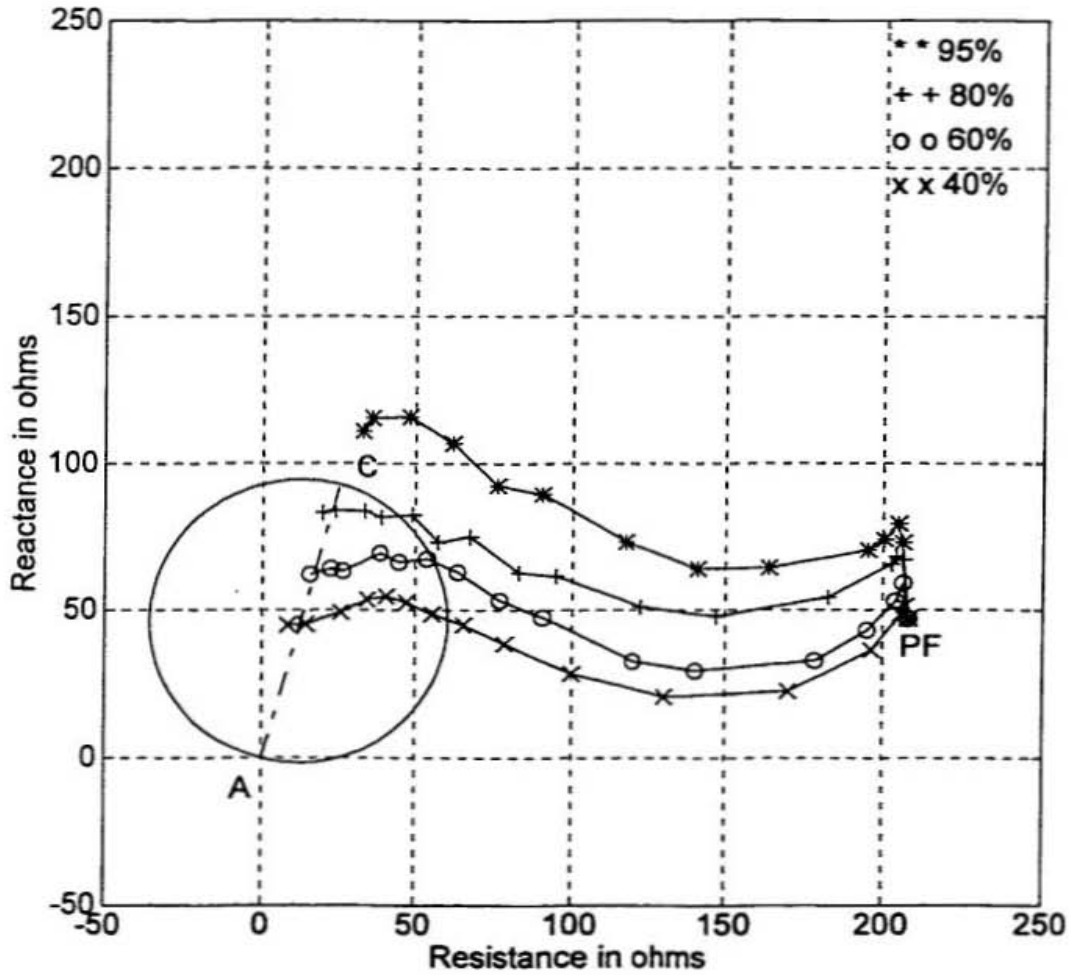

Figure 3.8: Distance relay trajectory for phase *a* - *b* - *c* fault, $R_f = 0\ \Omega$

(Fault at 40%, 60%, 80% and 95% of the transmission line, $\varphi = 0°$)

AC → 90% of the line, PF → Pre-fault loading condition

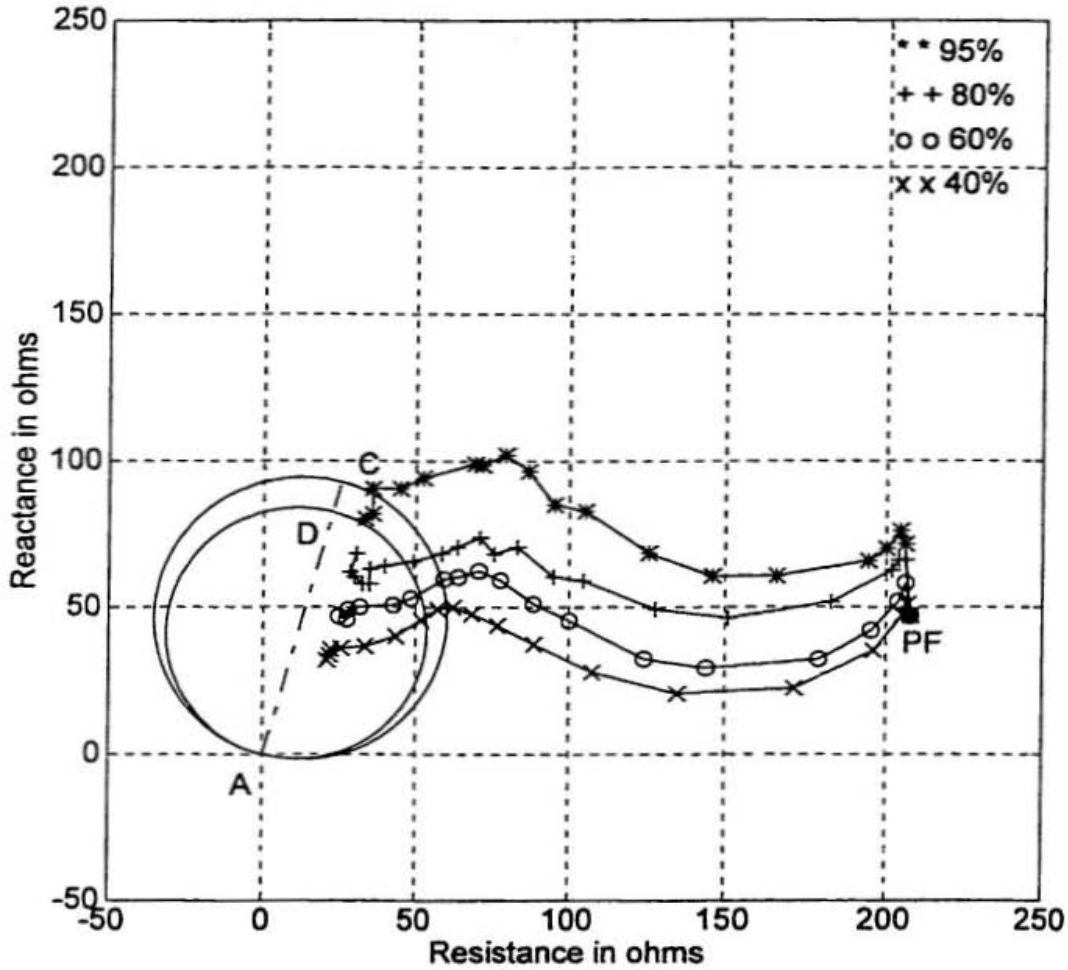

Figure 3.9: Distance relay trajectory for phase *a* - *b* - *c* fault, $R_f = 10\ \Omega$

(Fault at 40%, 60%, 80% and 95% of the transmission line, $\varphi = 0°$)

AC → 90% of the line, AD → 80% of the line, PF → Pre-fault loading condition

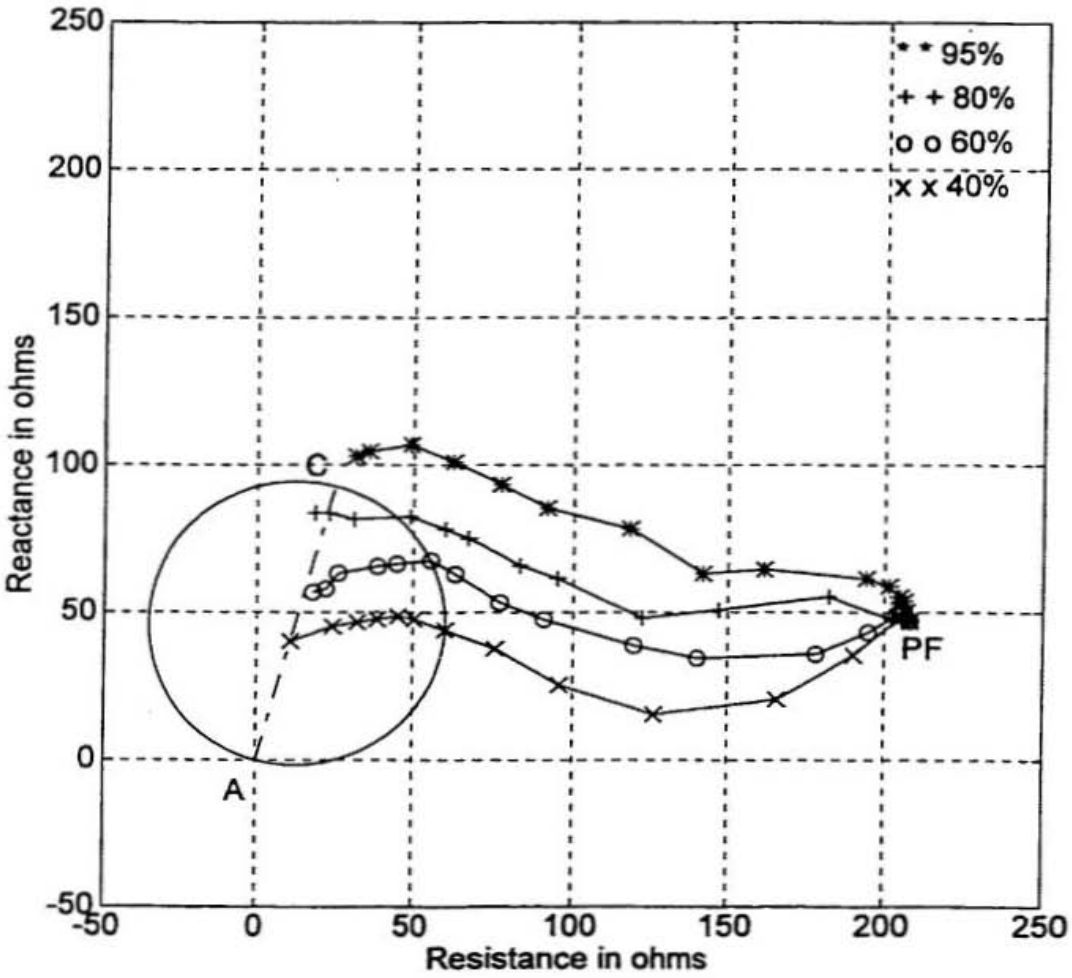

Figure 3.10: Distance relay trajectory for phase *a* - *b* - *c* fault, $R_f = 0\ \Omega$

(Fault at 40%, 60%, 80% and 95% of the transmission line, $\varphi = 90°$)

AC → 90% of the line, PF → Pre-fault loading condition

The simulation results indicate that the Fourier algorithm is quite accurate when the fault resistance is zero. In the presence of a fault resistance, the Fourier algorithm will be able to classify the faults clearly into trip/no trip region when the zone of protection is limited to a smaller portion of the line. A smaller zone of protection compromises in speed. The reliability and the speed of the Fourier algorithm depends on the efficiency and accuracy of extracting the power frequency components. This algorithm does not have the ability to adapt dynamically to the system operating conditions. Many other algorithms are available which can give a faster trip decision [6, 19, 20].

3.7 Summary

This chapter has described typical digital distance relays for transmission line protection. EMTP was used to simulate the transmission line model used in this study. A digital relay based on Fourier algorithm was simulated. This algorithm used the consecutive sampled values of voltage and current and evaluated the fundamental frequency components. These components were then used to determine the apparent impedance. The digital relay based on Fourier algorithm is found to be accurate for shorter zones of protection. The results obtained using Fourier algorithm will be compared with that obtained using the proposed ANN based algorithm in chapter 6.

Chapter 4

Artificial Neural Network for Transmission Line Relaying

4.1 Introduction

The potentials of Artificial Neural Networks (ANNs) have attracted researchers to solve problems related to various fields such as control systems, robotics, and recently in power systems engineering. ANNs are powerful in pattern recognition and classification, and possess generalization capabilities. The application of ANN to power systems became well established in the late eighties and have been tried as well as implemented in the areas of power system monitoring, control and protection. This chapter presents the basic concepts of ANNs and their application to transmission line protection. A review of the existing literature on ANN approach to distance protection and fault location in a transmission line indicates that the results are encouraging. The proposed ANN based algorithm for transmission line relaying will be presented in this chapter.

4.2 Artificial Neural Networks

A neural network is a massively parallel distributed processor that has a natural propensity for storing experiential knowledge and making it available for use at a later stage [22]. It is an information processing system that extracts information from the input and produces an output corresponding to the extracted information. ANNs are inspired by the biological brain in hopes of achieving human-like performance in solving certain difficult problems. An ANN consists of a large number of processing units analogous to neurons, joined to each other by some form of linkage analogous to the synapses from the biological counterpart. The presence of high degree of connectivity between neurons gives neural networks an enormous parallel structure with significant fault tolerance. Artificial neural networks provide the method of mapping a set of input and output variables by learning the weights associated with the interconnections of the neurons and the thresholds which activate the neuron [22].

4.2.1 Neuron Model

A neuron is an information processing unit that is fundamental to the operation of a neural network. The inputs to a neuron include its bias b and the sum of its weighted inputs. The output of a neuron depends on the neuron's inputs and on its transfer function. A single neuron with x_p inputs is shown in Fig. 4.1. Each input is weighted with a weight w. The sum of the weighted inputs and the bias forms the input to the transfer function φ. In mathematical terms, the output y of a neuron k is described by equation (4.1).

$$y_k = \psi\,(u_k + b_k) \tag{4.1}$$

where

$$u_k = \sum_{j=1}^{p} w_{kj} x_j \qquad (4.2)$$

$x_1, x_2, \ldots\ldots\ldots x_P$ are the input signals,

$w_{k1}, w_{k2}, \ldots\ldots\ldots w_{kP}$ are the synaptic weights of neuron k,

u_k is the linear combiner output, b_k is the bias, ψ is the activation function and y_k is the output signal of the neuron.

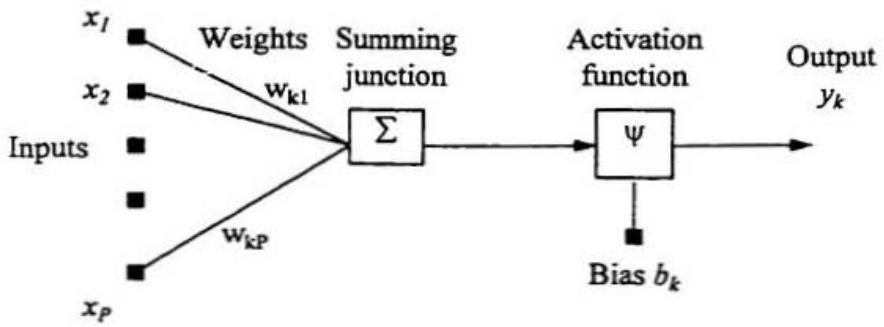

Figure 4.1: General Neuron Model

The activation function defines the output of a neuron in terms of the activity level at its input. The commonly used activation or transfer functions are:

1. Hard limit transfer function
2. Linear transfer function
3. Sigmoid transfer function

The hard limit transfer function depicted in Fig. 4.2(a) limits the output of the neuron to either 0 or 1. The hard limit transfer function is mathematically represented as:

$$\psi(v) = \begin{cases} 1 \ if \ v \geq 0 \\ 0 \quad v < 0 \end{cases}$$

where $v = u_k + b_k$

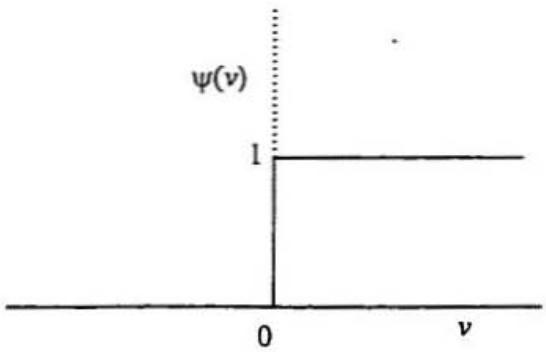

Figure 4.2(a): Hard limit transfer function

The linear transfer function represented by Fig. 4.2(b) takes linear values between 0 and 1. The linear transfer function can be mathematically expressed as:

$$\psi(v) = \begin{cases} 1 & if \quad v \geq 0.5 \\ 0.5 + v & 0.5 > v > -0.5 \\ 0 & v \leq -0.5 \end{cases}$$

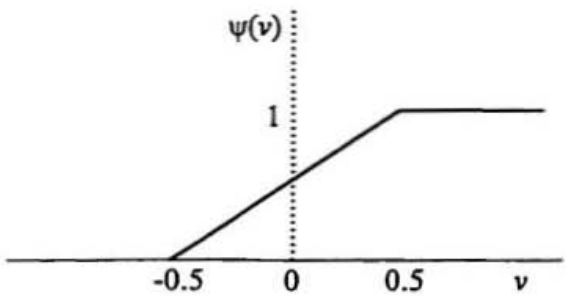

Figure 4.2(b): Linear transfer function

The sigmoid transfer function is differentiable. The sigmoid function can be either log-sigmoid or tan-sigmoid. The log-sigmoid function assumes a continuous range of values from 0 to 1, while a tan-sigmoid function assumes a continuous range of values from -1 to +1. The log-sigmoid and tan-sigmoid transfer function are mathematically represented as:

$$\psi(v) = \log sig(v) = \frac{1}{1+e^{-nv}} \tag{4.3}$$

$$\psi(v) = \tan sig(v) = \frac{1-e^{-2v}}{1+e^{-2v}} \tag{4.4}$$

The log-sigmoid transfer function is shown in Fig. 4.2(c). The slope parameter n can be varied to obtain different shapes of the log-sigmoid transfer function. A proper decision has to be made while selecting the transfer functions for the neural network structure. If the output of the ANN is to be limited between 0 and 1, log-sigmoidal transfer function should be chosen and if the ANN output is a continuos range of values between +1 and -1, tan-sigmoidal transfer function should be selected.

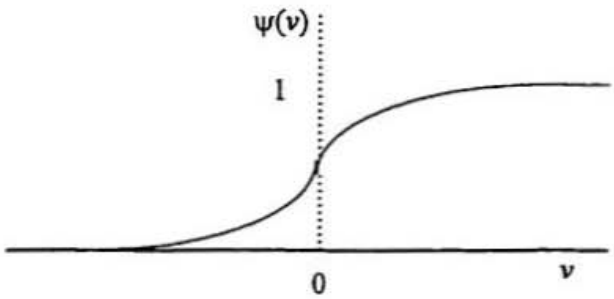

Figure 4.2(c): Log-sigmoid transfer function

4.2.2 Network Architecture

The most important class of neural networks is the feedfoward neural networks. In a feedforward neural network, the input signal propagates through the network in a forward direction, on a layer-by-layer basis. A layered neural network is a network of neurons organized in the form of layers. In its simplest form, a single-layer feedforward network consists of an input layer of source nodes that projects onto an output layer of neurons. Figure 4.3 illustrates the structure of a simple two layer network.

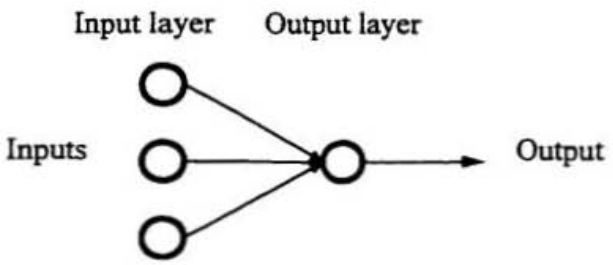

Figure 4.3: Feedforward network with two layers

Multilayer feedforward neural networks (FFNN) are widely used in power system applications [8-12, 15, 16]. Multilayer feedforward neural networks have one or more hidden layers, whose computation nodes are correspondingly called hidden neurons or hidden units. Figure 4.4 shows a three layer fully connected feedforward neural network in which each node represents a single neuron. Neurons in a given layer receive inputs from neurons in the layer immediately below it and send their outputs to neurons in the layer immediately above it. The function of hidden neurons is to intervene between the

external input and the network output. By adding one or more hidden layers, the network is able to extract higher order statistics, for the network acquires a global perspective despite its local connectivity by virtue of the extra synaptic connections and the extra dimension of neural interactions.

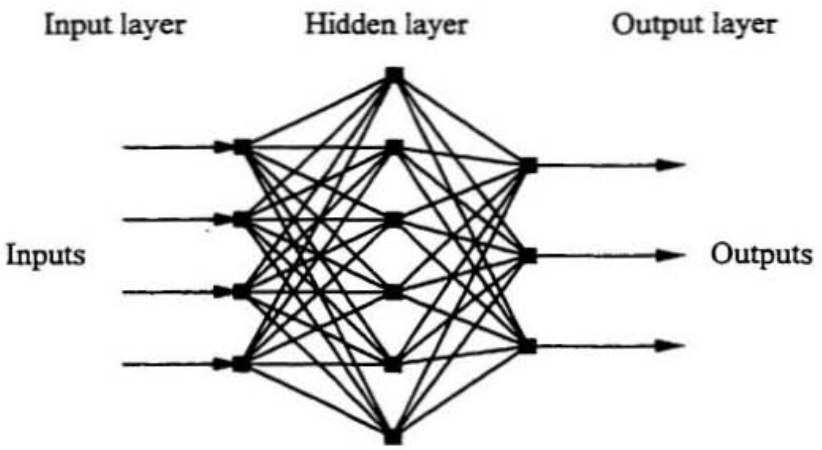

Figure 4.4: Structure of a three layer feedforward network

4.2.3 Backpropagation Algorithm

The most popular method of training a layered perceptron neural network is through error backpropagation [8-12, 15, 16]. These networks learn from examples by constructing an input-output mapping for the problem at hand. Backpropagation is an example of supervised learning where, in order to learn, the network requires a set of examples consisting of the input values and target output values. These target output values are then used as a basis for correction of weights and biases. The sigmoid transfer

function is commonly used in backpropagation networks [8-12]. The backpropagation algorithm consists of several forward and backward passes through the different layers of the network:

- Forward pass: In this, the input vector is applied to the nodes of the network and its effect propagates through the network layers in the forward direction until it reaches the output layer. Finally, a set of outputs is produced as the actual response of the network. During this pass, there is no change in the weight and the bias.
- Backward pass: During this pass, the weights are all adjusted in accordance with the error correction rule. An error is the difference between the target and actual response. The target is known as it is specified before training the ANN and the actual response is obtained through the forward pass. The error signal is propagated backward through the network. The weights and biases are adjusted so as to make the actual response of the network closer to the desired response.

4.2.4 Training Issues in Applying Backpropagation Algorithm

Trained backpropagation networks tend to give reasonable answers when presented with inputs that they have never seen [22, 27]. But, backpropagation algorithm depends upon a number of training issues, some of which are training functions, initialization, stopping criteria, number of hidden neurons used and so on. To make use of the MATLAB neural network toolbox, a program is simulated that includes the input data, the corresponding target outputs and the associated training functions. The training process is a means by which the network adapts itself to the desired output and thus

organizes the information within itself. The neural network toolbox of MATLAB provides provision to change the training parameters on which the backpropagation algorithm depends, so that a good neural network can be designed [27].

4.2.4.1 Training Functions

The MATLAB neural network toolbox is used for training and testing the network. Some of the training functions available in the MATLAB neural network toolbox, for the design of the network are *trainbpx*, *trainbpm* and *trainlm* [27].

Trainbpx

Simple backpropagation (*trainbp*) is very slow because it requires small learning rates for stable learning. *Trainbpx* uses techniques called momentum and an adaptive learning rate to increase the speed and reliability of backpropagation. *Trainbpx* is much better than *trainbp* in terms of speed as well as reliability. Backpropagation as implemented in *trainbpx* is based on gradient descent, in which the parameters such as weights and biases, are moved in the opposite direction to the error gradient. After each step, the gradient results in smaller errors until an error minimum is reached.

Trainbpm

The function *trainbpm* is similar to *trainbpx*, but has more training parameters. It is used so that the network would not get stuck in a shallow minimum. It acts like a low pass filter and allows the network to ignore small features in the error surface.

TrainIm

The function *trainlm* gives better performance since it uses an approximation of Newton's method called Levenberg-Marquardt. This optimization technique is more powerful than gradient descent, but requires more memory.

4.2.4.2 Initialization

Every multilayer feedforward network is associated with a set of weights and biases. Weights and biases should be initialized to small, random values, usually between ±0.5 [22, 27]. A good choice of initial values for the weights and biases will lead to a successful network design. The wrong choice of initialization values can lead to a condition called premature saturation, where the instantaneous sum of squared errors remains almost constant for some period of time during the learning process. There is a choice for initializing the weights and biases using one of these three functions available in the neural network toolbox:

(a) nwlog → This function uses the Nguyen-Widrow random generator for *logsig* neurons.

(b) nwtan → This function uses the Nguyen-Widrow random generator for *tansig* neurons.

(c) rands → This function is used in the generation of symmetric random numbers.

4.2.4.3 Stopping Criteria

The backpropagation algorithm is considered to have converged when the absolute rate of change in the average squared error per epoch is sufficiently small. Each epoch or training iteration represents the presentation of the set of training vectors to a network and the calculation of new weights and biases. The error goal to be achieved is pre-defined in the code for designing the neural network. In a well designed network, with increasing epochs, the error starts decreasing.

4.2.4.4 Hidden Neurons

Networks are quite sensitive to the number of neurons in their hidden layers. If too few neurons are selected, the network will not be able to learn all of the patterns correctly. Too many neurons will result in the network tending to memorize the patterns instead of learning to detect the global features of the pattern.

4.3 Applications of ANN to Transmission Line Protection

ANN based algorithms have given encouraging results in the area of transmission line protection [8-12, 15, 16]. Most of the reported literature using ANN are aimed at improvements in the following areas of transmission line protection.

- Distance Relaying
- Fault Classification
- Fault Location
- Fault Direction

The present area of work focuses on distance relaying and fault location. A review of the earlier work using ANN in these areas is presented in the following sections.

4.3.1 ANN Approach to Distance Protection

Distance relays are widely applied to protect transmission lines. ANNs, being a relatively new branch of artificial intelligence with promising results, are being adopted in the relays for distance protection of transmission lines.

ANN based distance relay is found to keep the reach accuracy, even with the changes in the network configuration [8]. The overreach trend of the half-cycle Discrete Fourier Transform (DFT) is canceled out by the proposed scheme. The study concentrated on phase *a* to earth faults with backpropagation algorithm used for the training. The magnitudes of the voltage and current phasors corresponding to the post-fault fundamental frequency formed the inputs. The learning process converged in about 80,000 cycles and took 2 hours of computing time. The algorithm is found to be reliable and about 95% of the test cases estimated the expected answer for the ANN distance relay.

ANN can also remove dc-offset from the corrupted voltage and current signals and provide a quick operating decision [10, 11]. The proposed ANN based algorithm is trained with the input patterns of distorted signals within a quarter cycle data window and with the target patterns of real or imaginary values of power frequency components of the signals. Four artificial neural networks having the same structure with different weights are used in the distance relaying algorithm. Two of them are for the real and imaginary values of the current phasors and the other two for voltage phasors respectively. Each input pattern

consists of eight samples of a quarter cycle of the power frequency. The first hidden layer has 20 units and the second has 4 units. The error backpropagation method is used to train the algorithm. Each current neural network required about 200 hours of training time and about 6 hours for each voltage network. The impedance locus is found to have good convergence characteristics for various settings.

An ANN based distance relay shows good performance in detecting a single-line-to-ground fault with nonlinear arcing resistance along the whole transmission line [12]. A mathematical nonlinear arc resistance model is used in the study. A three layered neural network with back-propagation learning algorithm is used, with 5 units in the hidden layer. The input signals to the network are the measured impedance of the faulted transmission line, the apparent impedance angle of the transmission line and the system equivalent reactance. The ANN relay adapted to source impedance changes and responded correctly.

A neural network fault area estimator that determines the fault area directly is found to give reliable results indicating whether a fault is inside or outside the protection area [9]. A feed-forward multilayer perceptron using backpropagation method is used, with 3-phase voltages and currents as the input. The time needed to train the network is about 12 hours. A comparison of conventional algorithms and the ANN based approach using different fault data showed that the ANN classification is faster and has better classification qualities compared to the conventional algorithms. The obtained results indicate that noise and harmonics do not impair the classification quality, but the

classification is not perfectly clear for fault location at the boundary of the zone of protection for the transmission line.

In the preliminary case study of the application of ANN in transmission line protection, single-phase-to-ground faults are examined [28]. The input of the ANN of the Multilayer Perceptron (MLP) type consists of the criterion signals positive sequence impedance components (R, X) seen from the relaying point and the zero-sequence current amplitude calculated by a measurement processor. The ANN decided whether the input data indicates an internal fault or not, after 10 ms from fault inception.

An adaptive digital distance relay that maintains the reach accuracy of the transmission line is proposed [29]. An ideal trip region is selected for a given fixed system conditions. Four feedforward neural networks are designed for trip region identification. The measured values of resistance and impedance as seen by the relay forms the inputs. The output accurately identifies whether the fault is inside or outside the protection zone. However, when there is a change in the power flow or source capacities, the relay operating region has to be updated.

4.3.2 ANN Approach to Fault Location

Accurate estimates of the fault location are desirable for inspection, maintenance and repair of the actual fault. Locating faults on transmission lines with high accuracy accelerates the maintenance operation and saves time and effort. Fault location also enables fast restoration of the transmission to service.

A feedforward neural network that estimates the fault location in a series compensated line, has provided encouraging results [15]. The network consists of three layers, the input layer with 10 inputs and the hidden layer with 9 neurons. The algorithm is found to provide accurate results, half cycle after fault inception. The initial data window after the fault contains pre-fault data only. It is justified that in practice, a transient fault detector would start the data window after fault inception with the trajectories not crossing the operating zone for the faults outside the zone.

A fault locator proposed in [16] using backpropagation algorithm and learning vector quantization has been able to locate faults with reasonable accuracy. The fault locator consists of two networks, a main network and an auxiliary network. The output of the main network indicates the fault location in per unit (p.u) of the length of the line. The output of the auxiliary networks representing the time reference points of the input wave forms the inputs to the main network. The auxiliary network consists of 400 input nodes, 18 nodes in the hidden layer and 18 output nodes. The results indicate that ANNs could be used as a pattern recognition tool to estimate the fault location.

A fault locator for series compensated lines has been investigated [30] and the results demonstrates the feasibility of the proposed approach. This scheme employed 8 samples of instantaneous voltage and current as the inputs. The feedforward neural network has 16 input neurons in the input layer, 12 neurons in the hidden layer and 2 output neurons indicating the fault and its location. Fault points are identified through directly analyzing the type of fault [31]. Post-fault voltage and current are used as inputs, and both supervised and non-supervised methods of training are adopted. It is found that

when a fault occurs at any node of the power system, the current patterns of the transmission line connected to that fault are similar. The fault at that node is determined by referring to its voltage pattern.

An accurate fault locator based on the integrated approach of fuzzy logic and neural networks has been proposed in [32]. The neural network is used in the input-output mapping to extract the rules and to learn the membership functions. This learning is employed in the fuzzification of the network. The input to the ANN is the frequency components of the voltages and currents. The test results shows high accuracy and robustness under a vast majority of different system and fault conditions.

4.4 Proposed ANN-based Algorithm for Transmission Line Relaying

An overview of the earlier work demonstrates the use of ANN based algorithms in the area of distance protection and fault location. The main aim of the work reported was to improve the relaying algorithms used in transmission line protection. In some cases, it was found that the time taken to give a trip decision corresponds to half cycle of the power system frequency [15]. The reported work in the application of ANN for transmission line relaying concentrated either on distance protection or on fault location, but not on both. The work has been reported only for the case of single-line-to-ground faults. Other fault cases are not considered. Some of the other drawbacks are that the network structure is big in size and the training time is too long. In case of a big network

structure, the hardware implementation will be more complicated. Longer training times will become an obstacle when the network has to be re-trained for certain critical conditions such as reversal of load flow.

Taking into account the above concerns, a novel feedforward neural network for distance protection of transmission lines is proposed. The technique has been extended to locate the distance of the fault location. The aim of the work is to develop an ANN based algorithm for the distance protection and fault location in transmission lines that is reliable, fast, accurate and small in size. The ANN based algorithm is designed for single-line-to-ground fault and three-phase fault cases. The single-line-to-ground fault is chosen as it is the most common type of fault. The three-phase fault is found to be the most severe type of fault. Four neural networks, one each for single-line-to-ground fault indication (to indicate whether the fault is inside or outside the protection zone), single-line-to-ground fault location (for exact location of the fault), three-phase fault indication and three-phase fault location are designed.

In the proposed scheme, the frequency spectrum of voltages and currents is utilized to make a decision. The data is obtained from the Electromagnetic Transients Program (EMTP) simulation. The main work is undertaken in two parts. In the first part, one-cycle of post-fault information is used as the input to the ANN based methodology for transmission line relaying. To improve the speed of the relaying decision, half-cycle pre-fault and half-cycle post-fault information of the voltage and current signals are used in the proposed ANN based relay. This forms the second part of the work. The specific

design details of the neural network and the simulation results of the proposed ANN based relay will be presented in Chapters 5 and 6 respectively.

4.5 Summary

This chapter has reviewed the applications of ANN in the area of distance protection of transmission lines and fault location. In most of the cases, multilayer feedforward network is used. ANN based algorithms have given encouraging results in the area of transmission line protection, but have some limitations in the design and in the application aspects. Some of the drawbacks of the proposed ANN based relays are highlighted. The motivation for undertaking the present research work has been described.

Chapter 5

Design of a Novel Artificial Neural Network Based Relay for Transmission Line Protection

5.1 Introduction

This thesis has discussed the principle of transmission line protection and the algorithms used for the protective relaying of transmission lines in digital relays. The application of Artificial Neural Network (ANN) based algorithms has also been successful in the areas of distance protection and fault location. Most of these applications in transmission line protection use voltage and current samples as inputs. A new approach for transmission line protection using the frequency spectrum of the voltage and current signals and training an ANN is investigated in this thesis.

An ANN based methodology for transmission line relaying is presented in this chapter. Two neural networks are designed: one to indicate whether the fault is inside or outside the protection zone (fault indication) and another neural network to precisely indicate the location of the fault (fault location) from the relay location. The reasons for selecting the frequency components of the voltage and current as the inputs to the ANN,

and the simulation procedure to obtain these frequency components are explained. The ANN algorithm for single-line-to-ground faults and three-phase faults are discussed. The simulation results based on the proposed method will be presented in chapter 6.

5.2 Choice of the Inputs to the ANN-based Relay

A number of neural network structures have been suggested in the literature and each structure is specifically suited for solving a particular type of problem. Most of the transmission line relaying methods based on neural networks use multilayered perceptron. In this research, a feedforward neural network for transmission line protection is designed. Any design process for a feedforward ANN based transmission line relaying consists of the following steps [33].

(i) Preparing suitable training data

(ii) Proper selection of the ANN structure

(iii) Training of the ANN

(iv) Evaluating the trained network

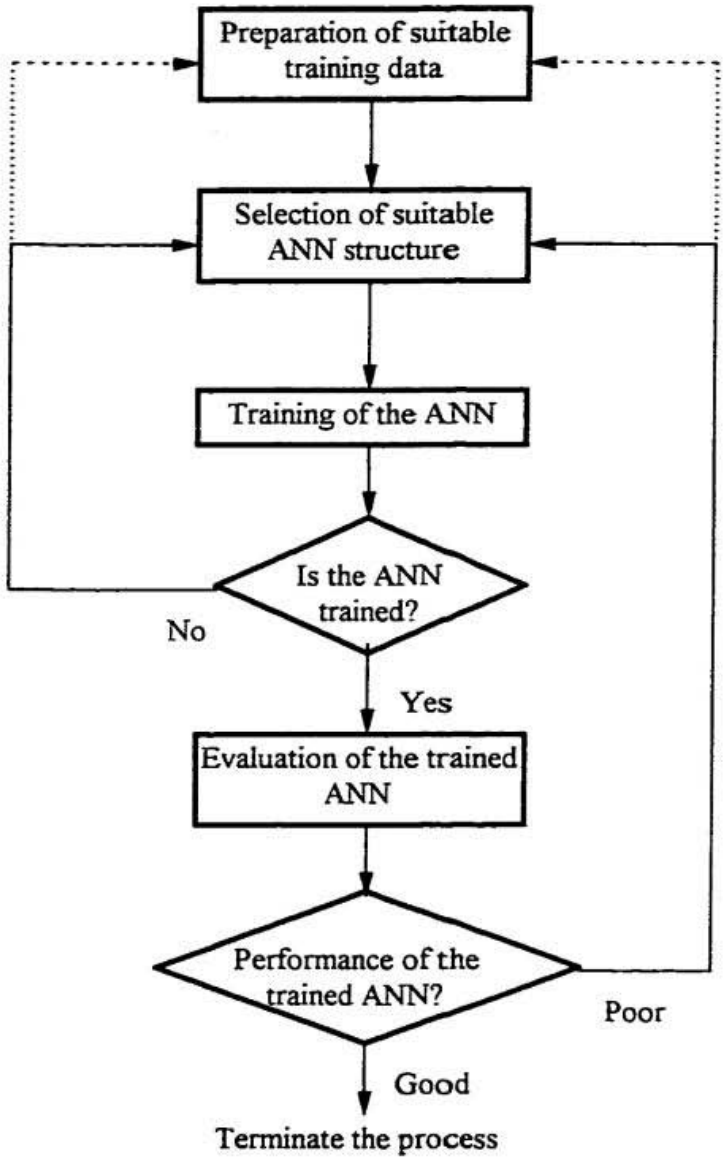

Figure 5.1: Design process for a typical ANN structure

The design process is iterative as illustrated in Fig. 5.1. The first step of the design process is to select suitable and meaningful data for training. It is important to give meaningful training patterns, which contain all the necessary information to generalize the

problem. Special care must be taken to include boundary patterns. It is possible that a particular ANN structure with the given training data may not train properly, *i.e.*, the training process takes too long. The structure and/or parameters must be changed and the network retrained. Also, a trained network might not perform satisfactorily because of inadequate training data, or due to the structure of the network. In that case, the structure of the network should be re-designed and the process should be repeated. Structural differences arise on account of the number and type of inputs, number and type of outputs and complexity of the application, which would govern the number of layers and the number of neurons in different layers. These parameters of the network are decided by experimentation, which involves training and testing a number of network configurations. The process is terminated when a suitable network with satisfactory performance is established. The process of the neural network training must be quite efficient and straightforward [33, 34].

Many of the algorithms on transmission line protection are based on the instantaneous values of the current and voltage waveform [12, 28]. These algorithms use a pre-processor to obtain resistance and reactance, which are given as inputs to the ANN. Another approach is to use the magnitude of the voltages and currents [8]. Inputs with consecutive samples of voltage and current data, is yet another approach to design the ANN [9]. As mentioned in chapter 4, though these algorithms are found to be reliable and accurate, one of the drawbacks is that the training times are quite long.

Prior to using the frequency components as the inputs to the ANN, three cases of possible inputs to the neural network are considered, namely:

1. Instantaneous values of voltages and currents without removing the noise
2. Magnitude of voltages and currents
3. Instantaneous values of voltages and currents after filtering the noise

Using instantaneous values of voltages and currents as the inputs proved to be a wrong decision, as it leads to long hours of training times. The instantaneous values of voltage and current contain lot of harmonics, as is observed in Fig. 3.4. The ANN is not able to extract any meaningful information from these patterns. Similarly, providing the magnitude (RMS value over one cycle) of the voltage and current components as the inputs to the ANN results in the same setback. The magnitudes of the voltage and current are represented by points which are very close to each other and hence the ANN is not able to learn when provided with these type of inputs. Considering the third case, the instantaneous values of the voltage and current after filtering away the noise resemble a sinusoidal wave; no matter at what point the fault has occurred. There is no significant variation in these patterns, except an increase in voltage with increasing distance of fault location. This can be clearly seen from Fig. 5.2 which illustrates the filtered phase *a* voltage for a single-line-to-ground fault occurring at 20%, 50%, 90% and 95% of the line from substation **A**. The ANN takes a long training time. Even after long training times, there is every possibility that the ANN algorithm would fail, as it might lead to memorization of the patterns rather than learning [27, 33].

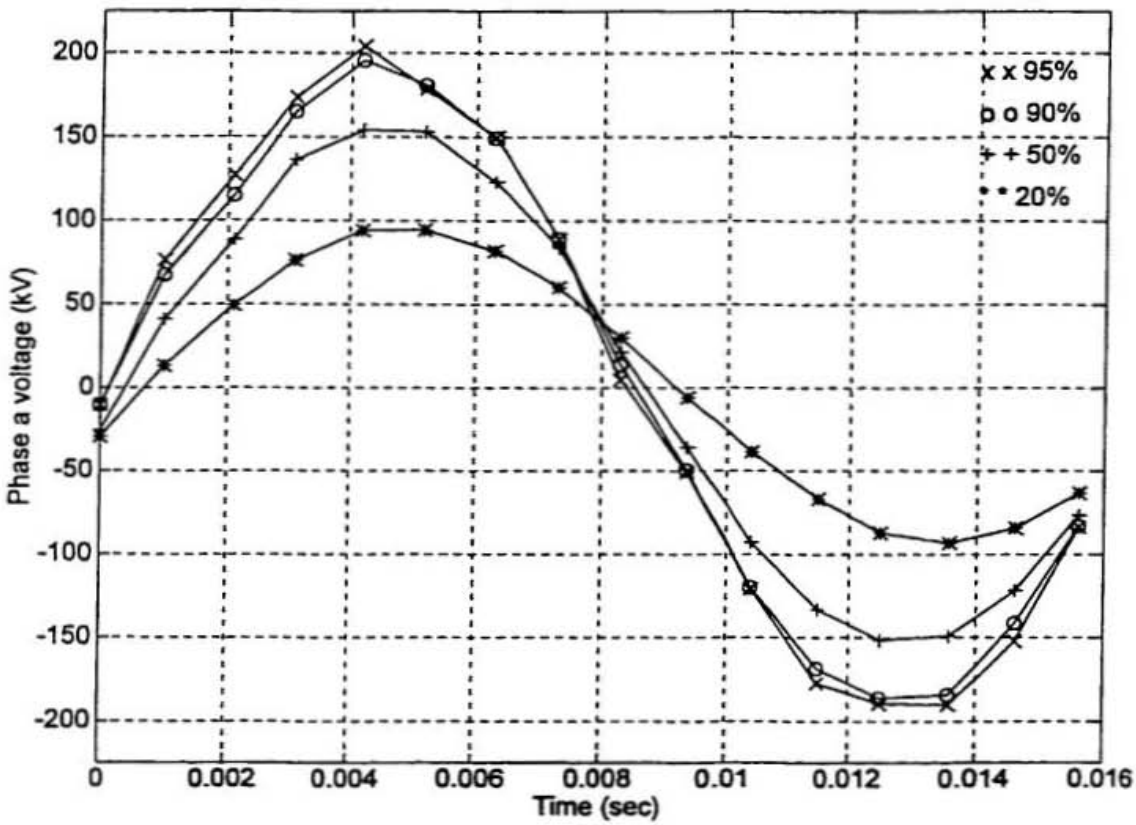

Figure 5.2: Filtered post-fault voltage at phase *a* for the single-line-to-ground fault occurring at 20%, 50%, 90% and 95% of the line.

($\varphi = 90°$, $R_f = 10\ \Omega$)

As a first step in any pattern classification technique, feature extraction is used to reduce the dimension of the raw data and extract useful information in a concise form [32]. For the ANN considered here, this process leads to a considerable reduction in size of the network, thereby significantly improving the performance and speed of the training process [35]. The technique adopted here for feature extraction is the one based on time domain frequency decomposition of voltage and current waveforms using Fast Fourier Transform (FFT). A one-cycle window is employed for this purpose. The work presented here has two main parts based on the input data of the one-cycle window. In the first part of the work on the proposed ANN based algorithm, this one cycle window consists of purely the post-fault voltage and current signals. It is found that inputs given in this way results in shorter training times. The trip decision is obtained after a cycle but the results obtained are encouraging. This prompted the author to investigate the possibility of reducing the response time. To achieve this, in the second part of the work, half-cycle pre-fault and half-cycle post-fault information of the voltage and current signals are used as the inputs.

5.2.1 Simulation Procedure to Obtain Frequency Components

The sample power system model as shown in Fig. 5.3 is simulated using EMTP to obtain the voltage and current data [23]. The data is generated for the following fault locations, instant of fault occurrence (fault inception angle) and fault resistance.

- Distance of fault (5, 10, 15, 20, 25, 30, 35, 40, 45, 50, 55, 60, 65, 70, 75, 80, 85, 87, 89, 90, 91, 93, 95% of the line length)

- Fault resistance (R_f = 0, 10 Ω for single-line-to-ground fault, R_f = 10, 50 Ω for three-phase fault)
- Fault inception angle (0°, 90°, 180°, 270°)

A total of 184 cases are simulated for single-line-to-ground fault and for three-phase fault, to train and test the ANN based on one-cycle post-fault information. For the ANN based algorithm using half-cycle pre-fault and post-fault information, a total of 344 fault cases are simulated. Different fault inception angles are selected, as in a practical situation, a fault can occur at any point of time.

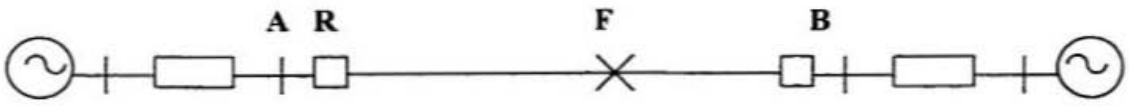

Figure 5.3: Single line diagram of the power system model

(Voltage at substation **A** = 1.02 p.u, Voltage at substation **B** = 0.97 p.u)

(Length of the line = 160 miles, Rating of the line = 345 kV)

In the simulations presented here, the frequency components of one cycle post-fault voltage and current signals are obtained using FFT. Since a sampling rate of 960 Hz has been used, the frequency components up to the eighth harmonic (480 Hz) are used. The frequency components are normalized with respect to the 60 Hz component. The normalized values of the frequency components are used as inputs by the ANN algorithm, to give the appropriate relaying decision. The frequency spectrum of the input current and voltage meet the sampling theorem which states that the sampling frequency should be at least twice the highest frequency in the spectrum. The highest frequency is thus 480 Hz in

the presented work. In the hardware implementation of this concept, a low pass filter with a cut off frequency lower than 480 Hz must be included.

5.2.2 Frequency Spectrum Using Post-fault Information

The frequency spectrum of the phase *a* voltage and current for a single-line-to-ground fault occurring at 20% and 75% of the line from substation **A** (Fig. 5.3) are shown in Fig. 5.4 and Fig. 5.5 respectively. The frequency spectrum is obtained using one-cycle of post-fault voltage and current signals. The Total Harmonic Distortion (THD) indicates that there is an unique relationship between the frequency spectrum of the voltage and current and the fault location. The THD is a measure of closeness between a waveform and its fundamental component [36]. The THD in the voltage waveform is defined as

$$THD_v = \frac{\sqrt{\sum_{n=1}^{8} v^2(f_n)}}{v_{fundamental}} * 100\% \qquad (5.1)$$

with v representing the voltage, f_1 representing the dc component, f_2 the second harmonic and so on. Similarly, the THD in the current waveform is defined as

$$THD_i = \frac{\sqrt{\sum_{n=1}^{8} i^2(f_n)}}{i_{fundamental}} * 100\% \qquad (5.2)$$

with i representing the current. The THD for some of the fault cases is indicated in Table 5.1. The THD in voltage and current is found to decrease with increase in the fault location from the generating end, as seen from Table 5.1.

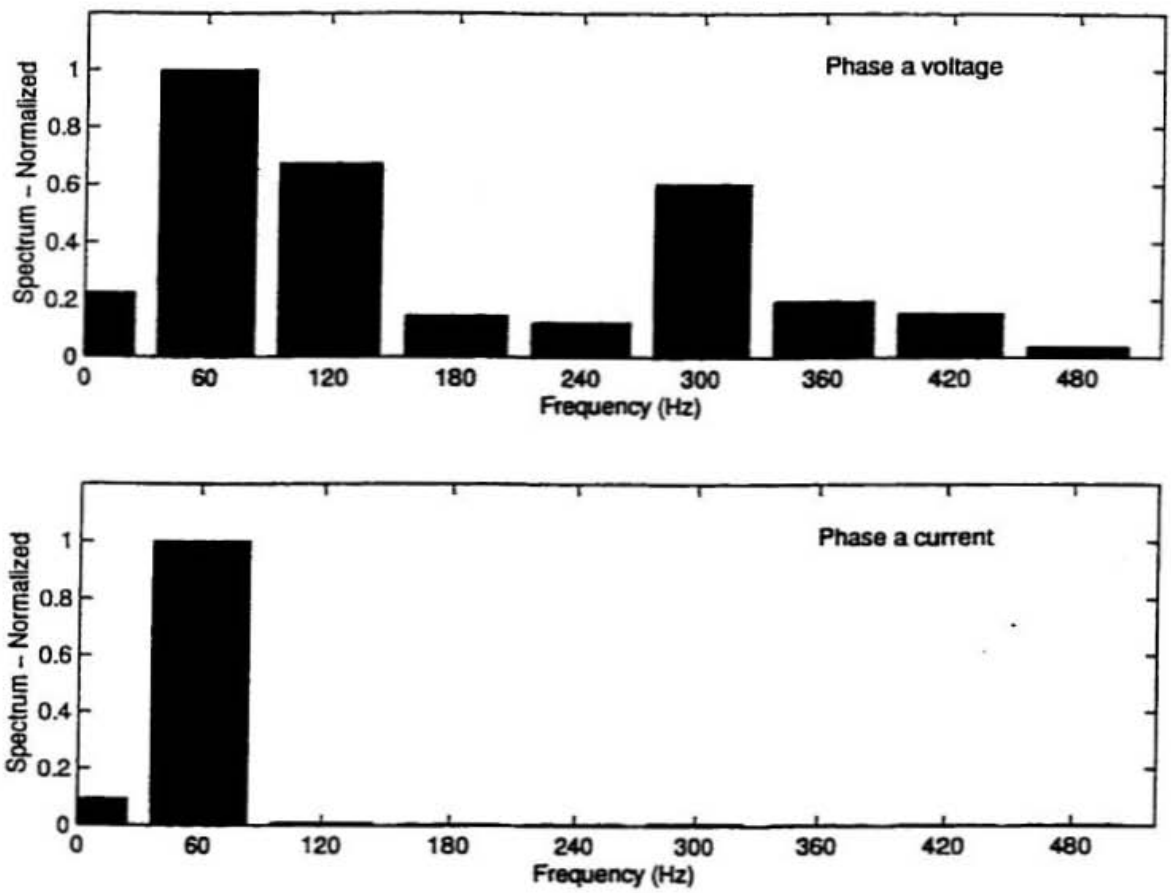

Figure 5.4: Frequency spectrum of phase *a* voltage and current for single-line-to-ground fault at 20% of the line

(One-cycle of post-fault, $\varphi = 0°$, $R_f = 10\ \Omega$)

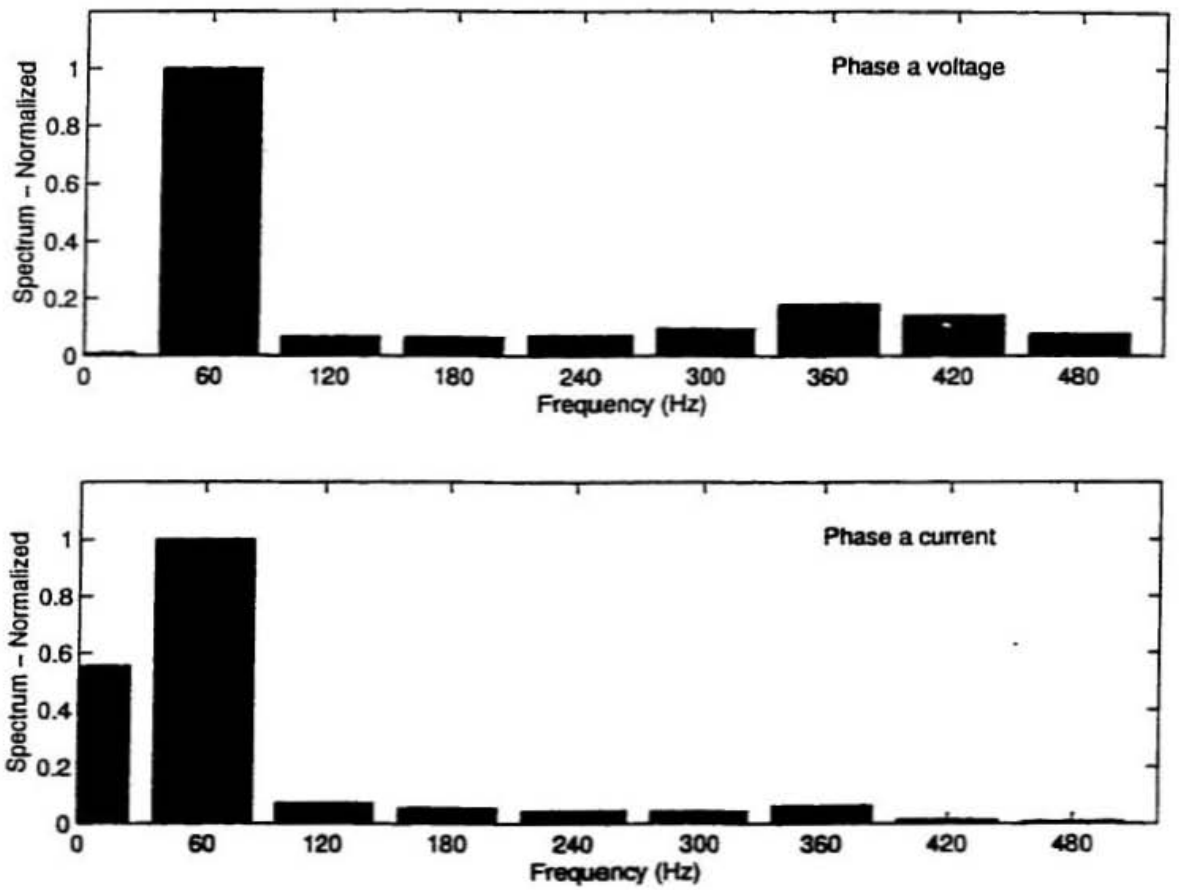

Figure 5.5: Frequency spectrum of phase *a* voltage and current for single-line-to-ground fault at 75% of the line

(One-cycle of post-fault, $\varphi = 0°$, $R_f = 10\ \Omega$)

Table 5.1: THD for single-line-to-ground faults using one-cycle of post-fault data

Fault location (%)	THD_v (%)	THD_i (%)
15	51.6458	93.8510
20	42.8878	90.2335
40	36.7637	76.2179
50	33.7611	70.6993
75	28.2200	56.9498

The study indicates that the frequency components of voltages and currents provide good information for the neural network to learn about the fault conditions. The ANN design is based on mapping the data of frequency spectrum to the relay decision for fault location.

Similar conclusions are drawn for the frequency spectrum of the voltages and currents for three-phase faults. Fig. 5.6(a) and Fig 5.6(b) respectively illustrates the frequency spectrum of the voltage and current of all the three phases, for a three-phase fault occurring at 20% of the transmission line. The frequency spectrum of the voltages and currents for a three-phase fault occurring at 60% of the line from substation **A** is shown in Fig. 5.7(a) and Fig. 5.7(b) respectively. Though a three-phase fault is symmetrical, the frequency spectrum reveals that the harmonic components for the voltages and currents in the three phases are quite different. For a three-phase fault, the frequency components of voltage and current in all the three phases should be used as the inputs to the neural network.

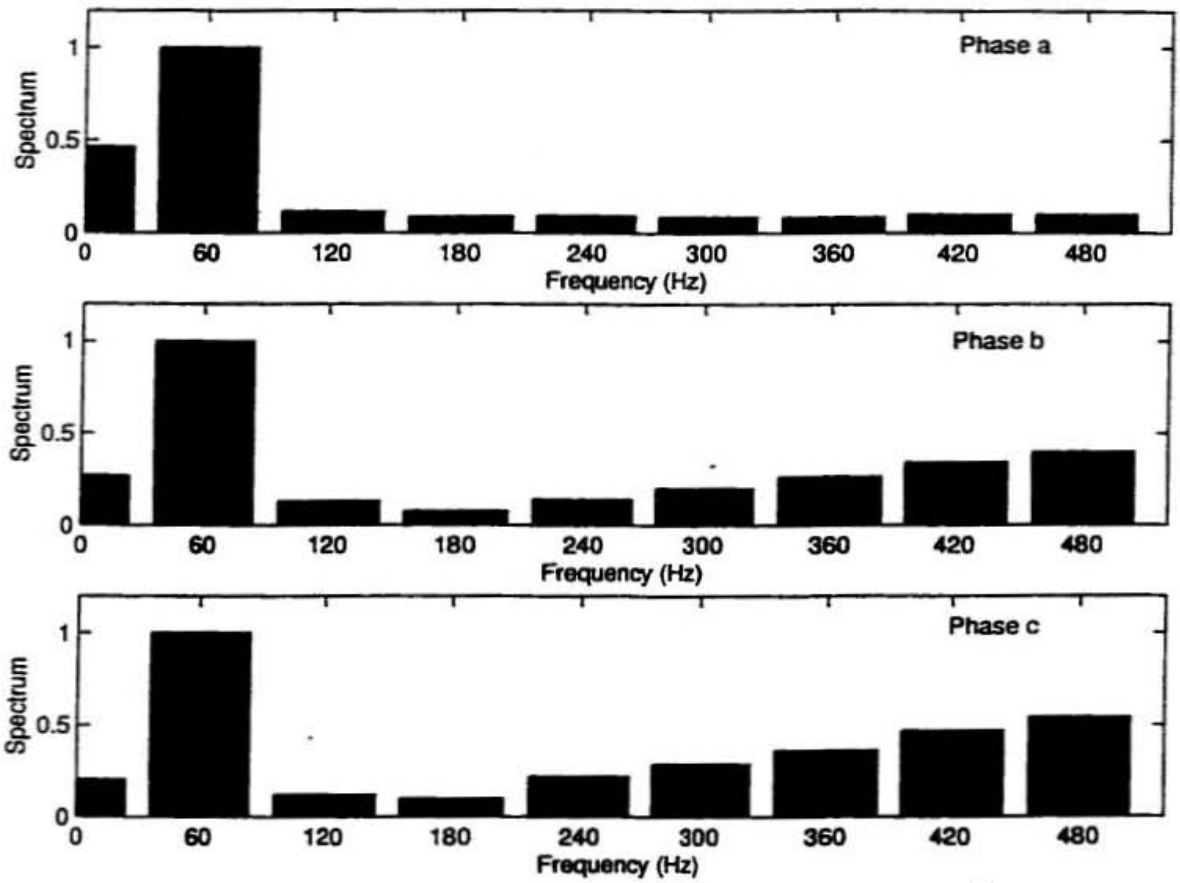

Figure 5.6(a): Frequency spectrum of phase voltages for a three-phase fault

at 20% of the line

(One-cycle of post-fault, $\varphi = 0°$, $R_f = 10\ \Omega$)

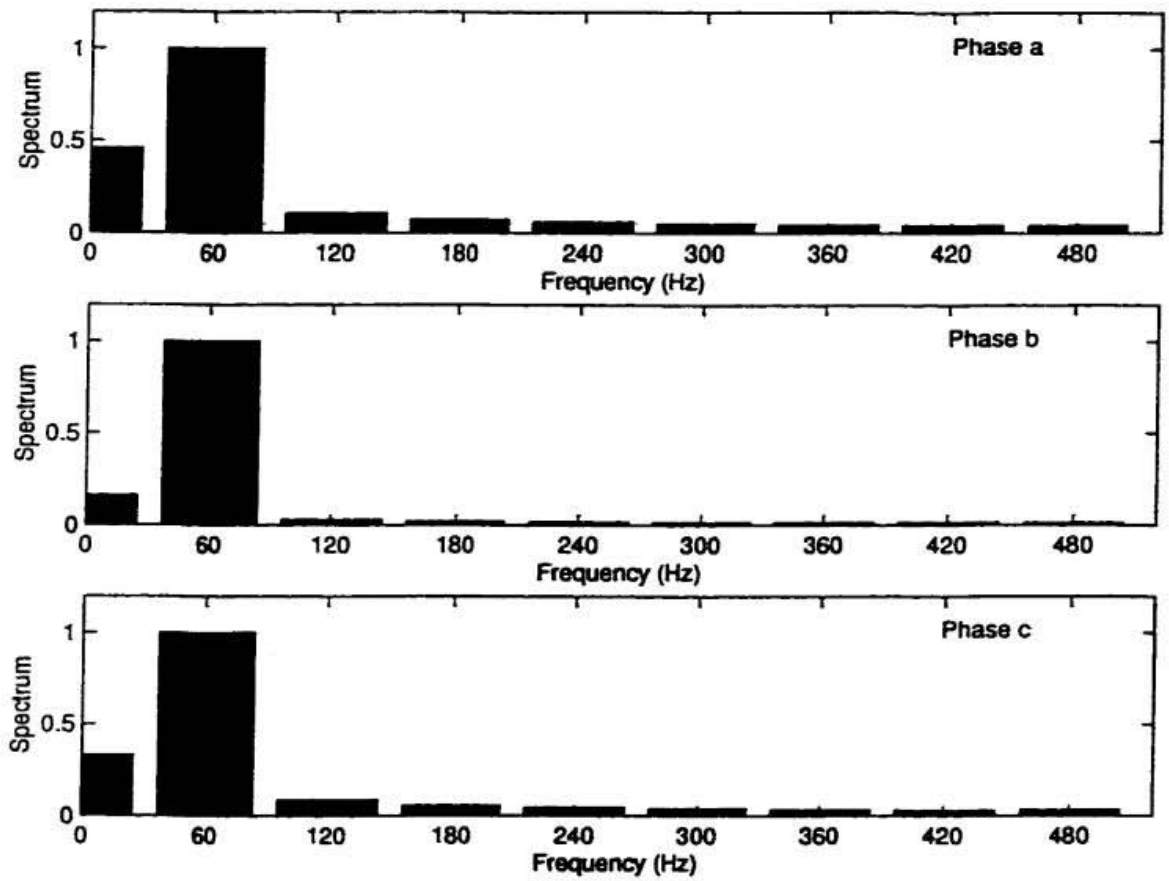

Figure 5.6(b): Frequency spectrum of phase currents for a three-phase fault

at 20% of the line

(One-cycle of post-fault, $\varphi = 0°$, $R_f = 10\ \Omega$)

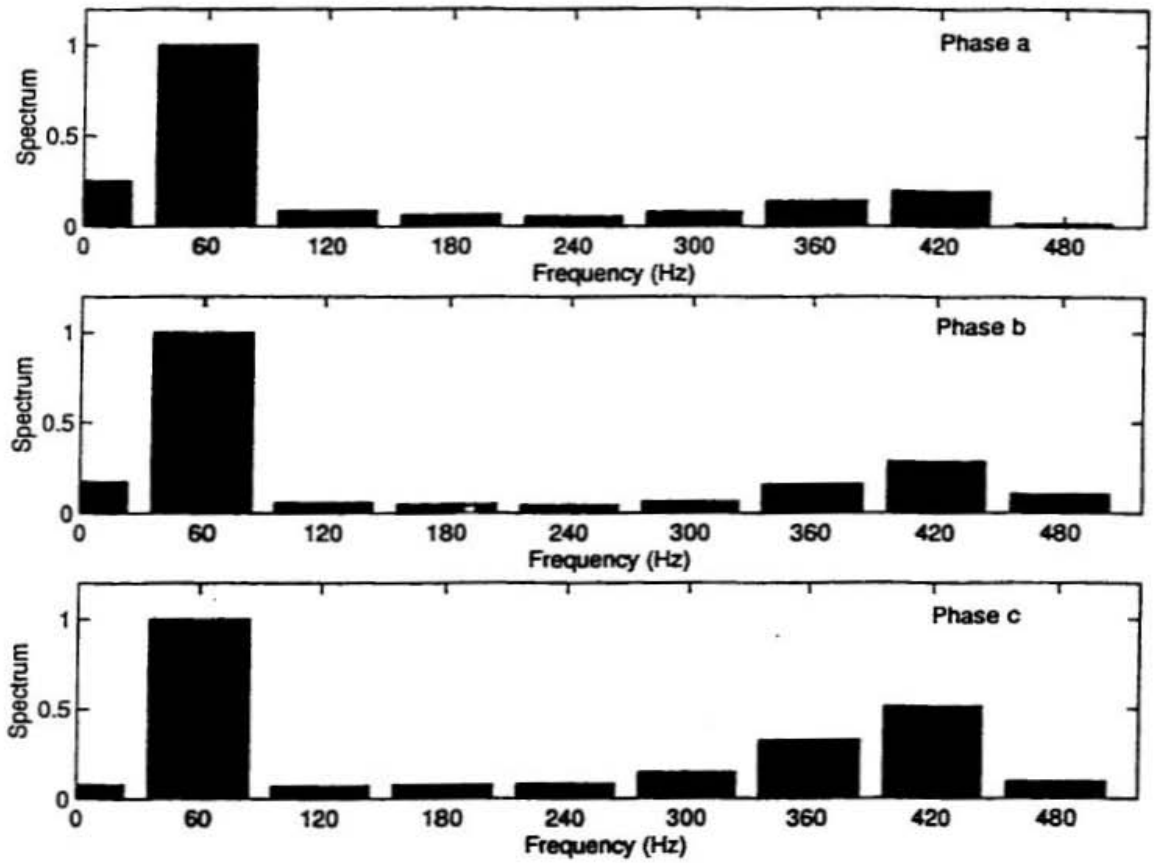

Figure 5.7(a): Frequency spectrum of phase voltages for a three-phase fault

at 60% of the line

(One-cycle of post-fault, $\varphi = 0°$, $R_f = 10\ \Omega$)

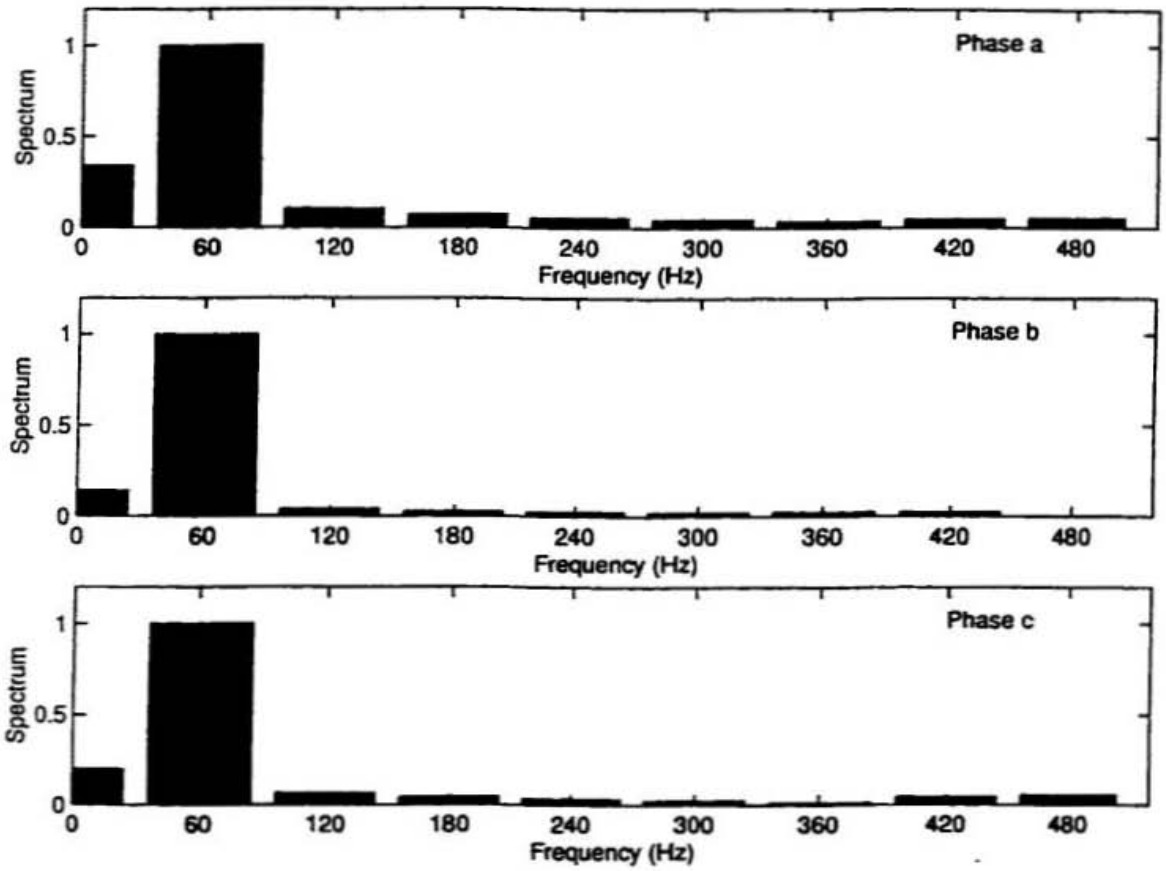

Figure 5.7(b): Frequency spectrum of phase currents for a three-phase fault

at 60% of the line

(One-cycle of post-fault, $\varphi = 0°$, $R_f = 10\ \Omega$)

The THD for the phase *a* voltage and phase *a* current for some of the fault cases is represented in Table 5.2. The THD in the voltage and current is found to decrease with increasing fault location from the substation **A**.

Table 5.2: THD for three-phase faults using one-cycle of post-fault data

Fault location (%)	THD_v (%)	THD_i (%)
5	56.5090	51.5090
20	53.0610	48.9555
40	40.4395	43.8008
50	39.0470	40.9711
60	37.6993	37.5972

An obvious question arises as regards to the exact selection of one-cycle of post-fault data. Many algorithms are available which can indicate an abnormal behaviour when a fault occurs. These algorithms indicate the possible occurrence of a fault. At the occurrence of a fault, the voltage decreases and the current increases (Fig. 3.4). A simple algorithm can be implemented using a sliding window to obtain the FFT of the signal. The initial values of the frequency components will have a low value. The frequency components will have a larger value when one cycle of post-fault data is selected. A threshold can be selected, so that the values above this threshold contain the frequency components corresponding to one-cycle of post-fault data. It is assumed that such an algorithm will be used prior to the ANN algorithm. At the instant of a possible fault occurrence, the algorithm selects one-cycle of the data that represents the data pertaining to pure fault.

5.2.3 Frequency Spectrum Using Pre-fault and Post-fault Information

Using only post-fault frequency components of the voltage and current signals the trip decision can be obtained only after a cycle. To improve the speed of the protective relay, a one-cycle window consisting of half-cycle pre-fault and half-cycle post-fault information is used as the inputs. At this stage it should be mentioned that a suitable logic should be developed that will exactly use half-cycles of pre-fault and post-fault information as the inputs to the ANN. This work is carried out under the assumption that such a suitable logic is available.

When there is no fault, only the fundamental frequency component is present and the selection logic should reject those cases. At the inception of the fault, the voltage and current signals are distorted. The FFT of the initial samples of voltage and current have small magnitudes. A threshold should be selected, such that when the FFT of voltage and current signals reaches the half-cycle condition, those values are taken as the inputs to the ANN. This could be one of the possible methods to design the logic for selecting the frequency components of half-cycle pre-fault and half-cycle post-fault data to be used as inputs to the neural network.

Fig. 5.8 and Fig. 5.9 represent the frequency spectrum of the phase *a* voltage and current for a single-line-to-ground fault occurring at 20% and 85% of the transmission line from substation **A** of Fig. 5.3. Table 5.3 represents the THD for some of the fault cases. The THD indicates a unique relationship between the frequency components and the fault location. The THD decreases with increasing fault location from substation **A**.

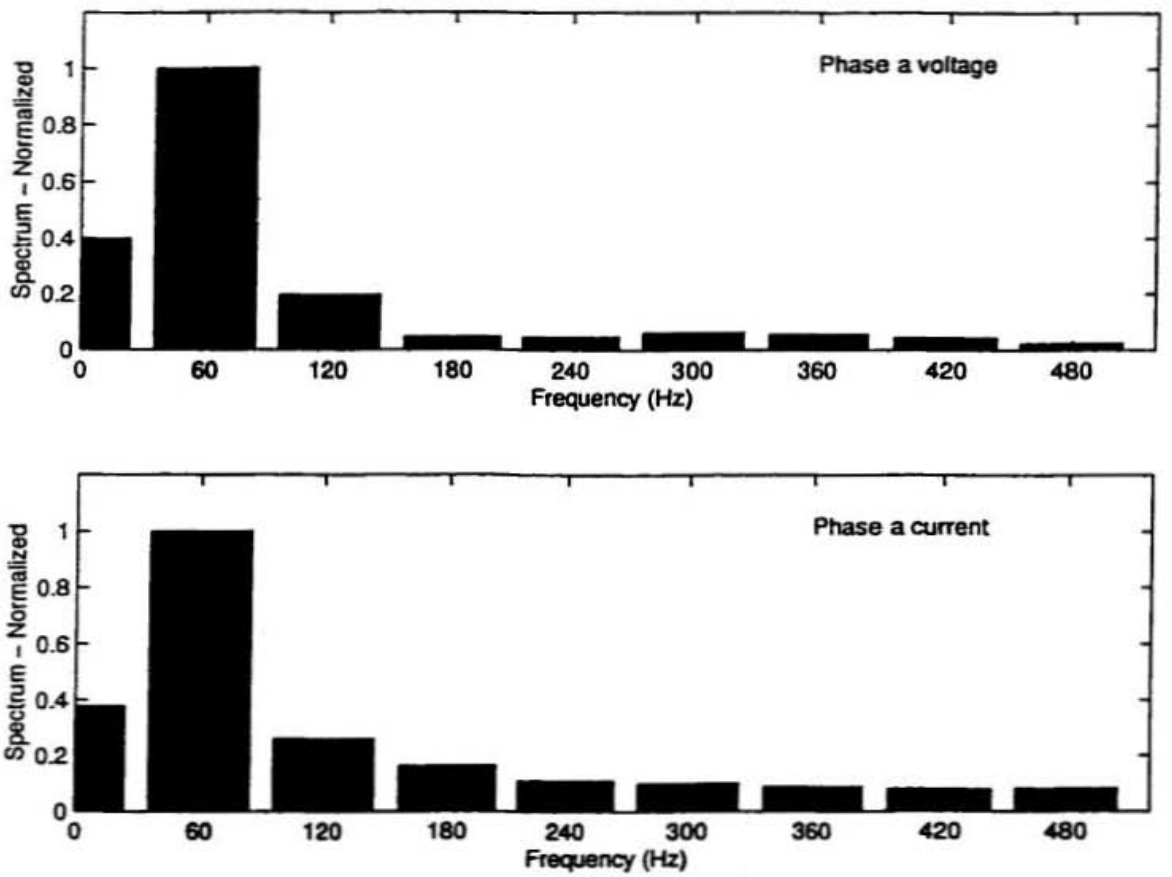

Figure 5.8: Frequency spectrum of phase *a* voltage and current for single-line-to-ground fault at 20% of the line

(Half-cycle of pre-fault and post-fault, $\varphi = 0°$, $R_f = 10\ \Omega$)

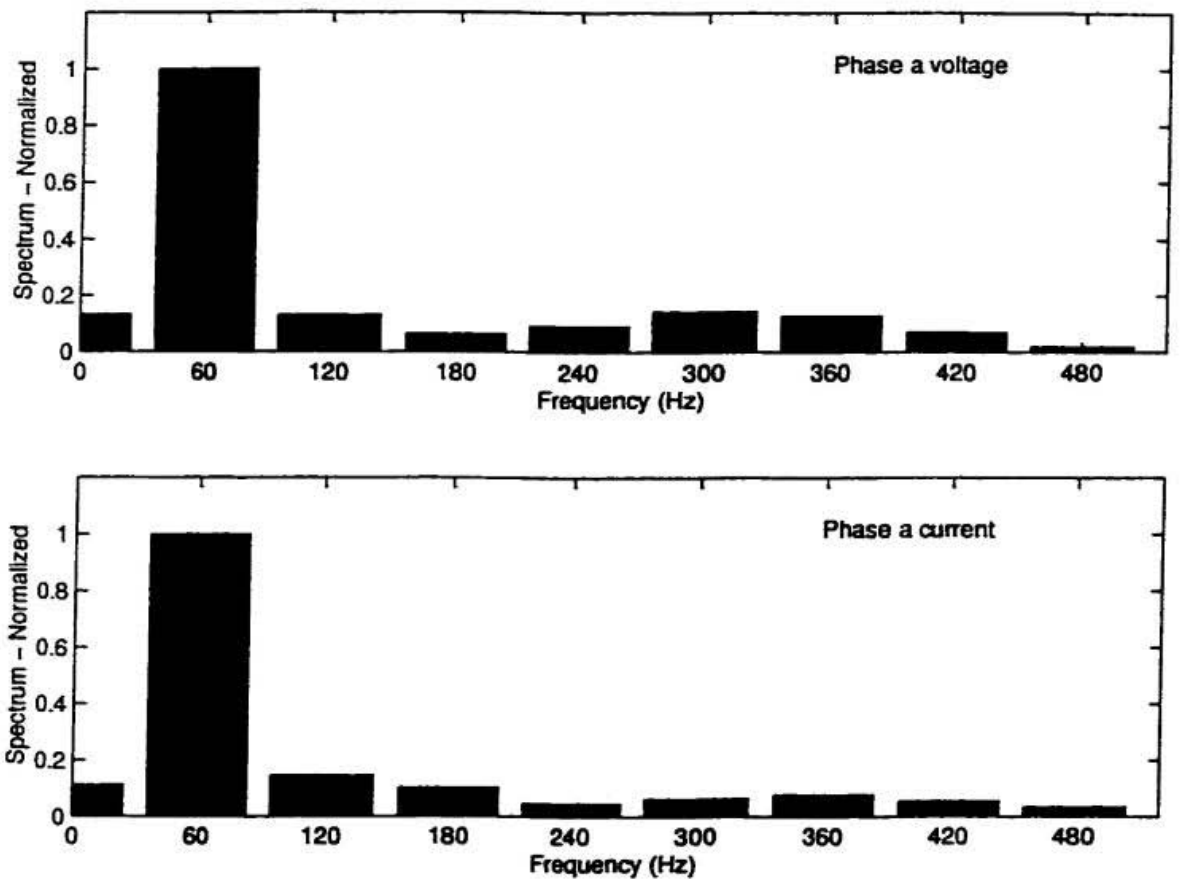

Figure 5.9: Frequency spectrum of phase *a* voltage and current for single-line-to-ground fault at 85% of the line

(Half-cycle of pre-fault and post-fault, $\varphi = 0°$, $R_f = 10\ \Omega$)

Table 5.3: THD for single-line-to-ground faults using half-cycle of pre-fault and post-fault data

Fault location (%)	THD_v (%)	THD_i (%)
15	54.7077	56.8875
20	45.8847	53.0572
40	41.3847	40.4175
50	33.2791	35.8135
85	30.0624	24.8446

The frequency spectrum of the voltage and current for a three-phase fault occurring at 20% of the line are illustrated in Fig. 5.10(a) and Fig. 5.10(b) respectively. Fig. 5.10(a) and Fig. 5.10(b) are obtained with a fault resistance R_f of 10 Ω and the fault inception angle φ being 0°. Fig. 5.11(a) and Fig. 5.11(b) represent the frequency spectrum of voltages and currents for a three-phase fault occurring at a fault distance of 90% of the line, with R_f of 10 Ω and φ of 0°.

The THD for phase *a* voltage and current for some of the fault cases is indicated in Table 5.4. As seen from Table 5.4, the THD in the voltage and current is found to decrease with increasing fault location, from substation **A**.

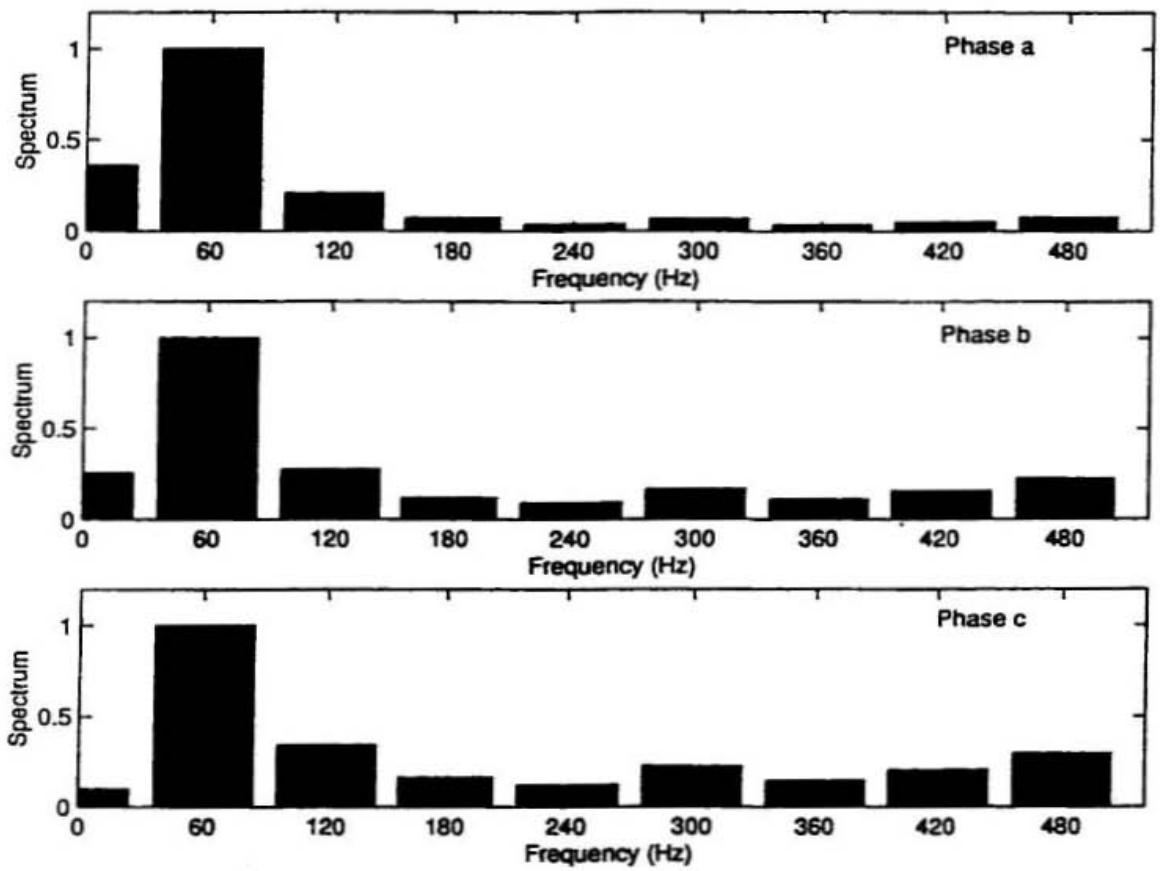

Figure 5.10(a): Frequency spectrum of phase voltages for a three-phase fault at 20% of the line

(Half-cycle of pre-fault and post-fault, $\varphi = 0°$, $R_f = 10\ \Omega$)

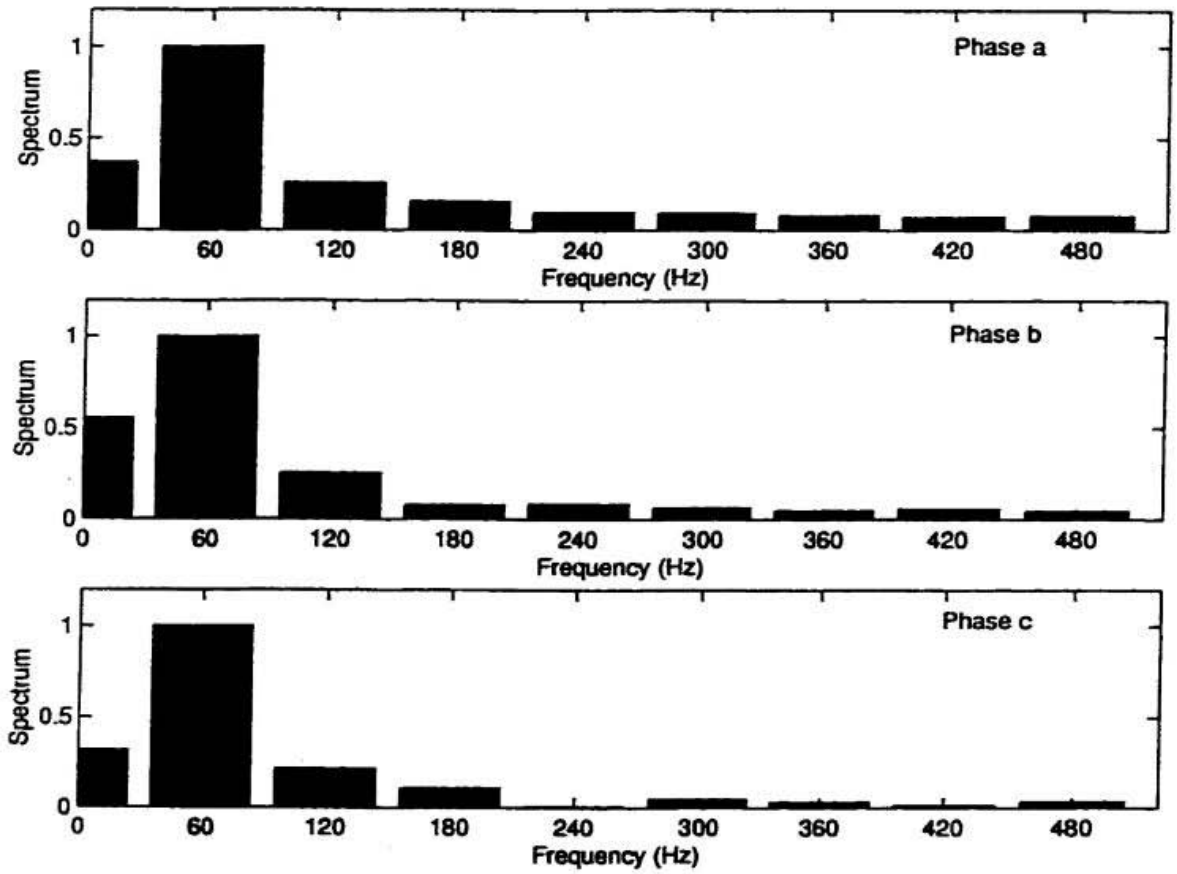

Figure 5.10(b): Frequency spectrum of phase currents for a three-phase fault at 20% of the line

(Half-cycle of pre-fault and post-fault, $\varphi = 0°$, $R_f = 10\ \Omega$)

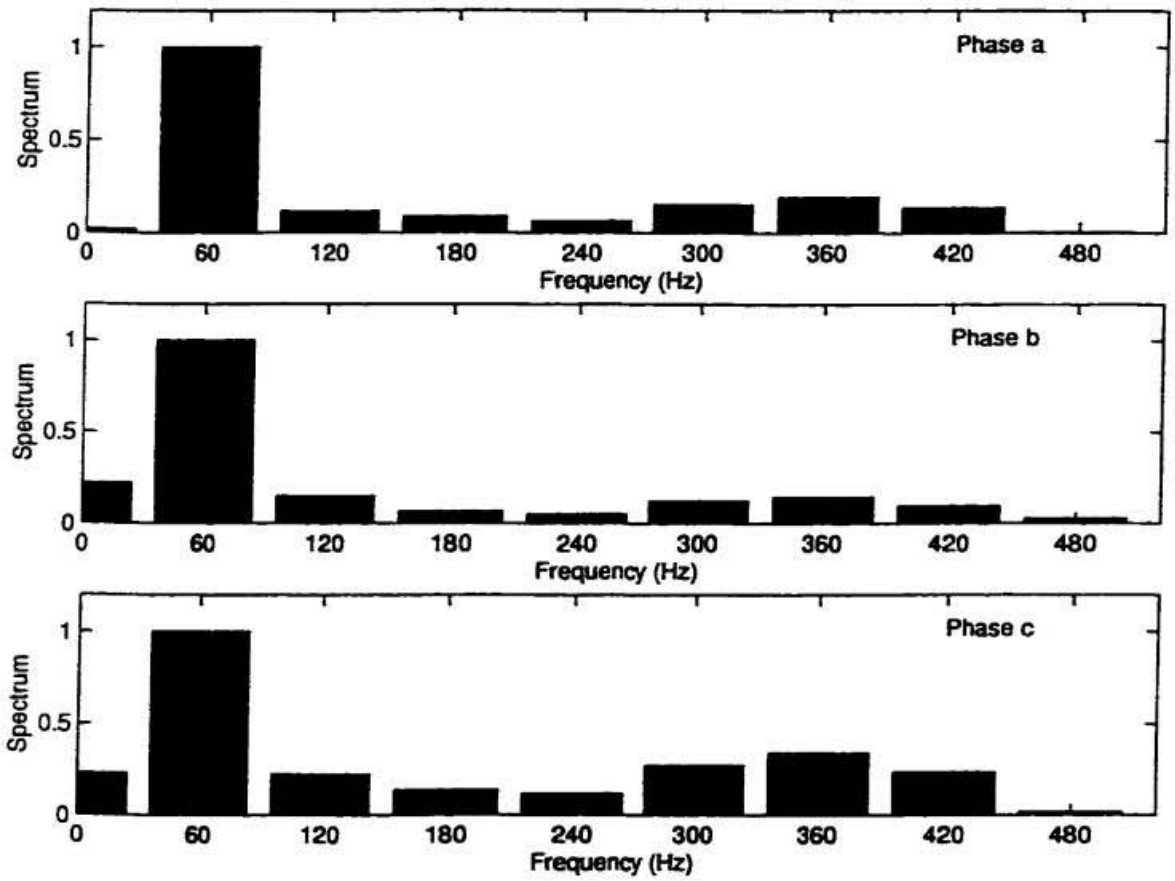

Figure 5.11(a): Frequency spectrum of phase voltages for three-phase fault at 90% of the line

(Half-cycle of pre-fault and post-fault, $\varphi = 0°$, $R_f = 10\ \Omega$)

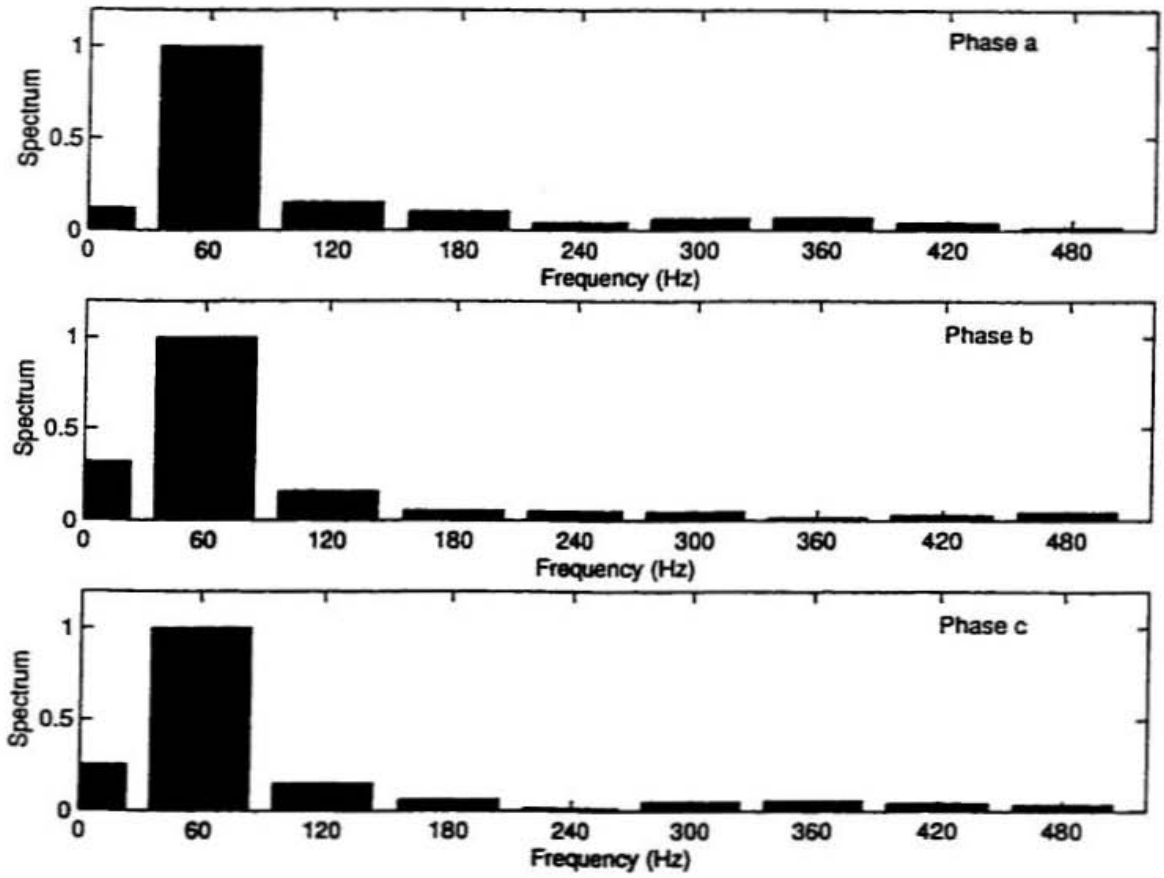

Figure 5.11(b): Frequency spectrum of phase currents for three-phase fault

at 90% of the line

(Half-cycle of pre-fault and post-fault, $\varphi = 0°$, $R_f = 10\ \Omega$)

Table 5.4: THD for three-phase faults using half-cycle of pre-fault and post-fault data

Fault location (%)	THD_v (%)	THD_i (%)
5	52.5295	58.4573
20	44.2288	51.2110
30	42.1474	46.7250
65	35.5611	32.6927
90	31.9178	24.4897

5.3 Artificial Neural Network Design

The block diagram of the proposed scheme for transmission line relaying is shown in Fig. 5.12. The required sampled values of voltage and current, representing the faults are obtained. In a power system environment, the data acquisition system provides sampled values of voltage and current signal from the power system. This data is fed to the FFT filter to obtain the frequency components of voltage and current signals. The ANN uses the frequency components as the inputs, for fault indication (distance protection) and fault location. It is assumed that signals are filtered to satisfy the sampling theorem.

A feedforward neural network is used in the work. The proposed ANN is trained using the backpropagation algorithm, which is an iterative gradient descent approach that minimizes the mean square error between the actual output of the neural network and the target output. The MATLAB Neural Network Toolbox is used for training the networks [27]. The function '*trainlm*' explained in chapter 4 is used, which converges in lesser time as well as in few epochs compared to the training function '*trainbpx*' of the neural

network toolbox. Though the training function '*trainlm*' requires significant memory, with today's technology this is unlikely to be a drawback.

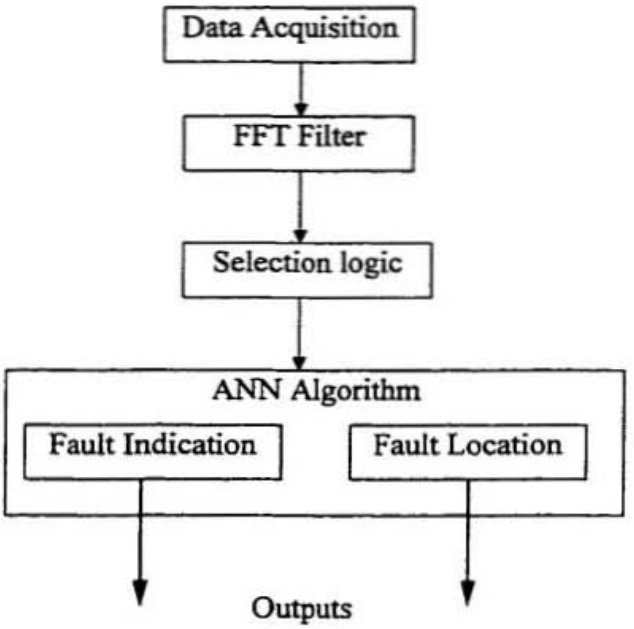

Figure 5.12: Block diagram of the proposed scheme

For each fault case considered, two neural networks are designed, one to indicate the fault and the other for the precise location of fault [35]. The general design structure is quite similar for the cases considered. Any neural network should have inputs and corresponding target output for training purposes. As indicated earlier, the frequency components of the voltage and current are the inputs to the ANN. The error goal is kept below 0.001% for all the cases. The learning rate is the same for all cases considered. For fault indication purpose, the output is either 0.9 or 0.1 indicating respectively whether the fault is inside the zone of protection or outside it. In practice, there will be small fluctuations in the ANN output and hence the values 0.9 and 0.1 are chosen as threshold

values. For fault location purpose, the output indicates the per unit (p. u) distance of the line length. A detailed explanation of the network inputs and outputs for the individual cases are explained in the following sections.

The neural network has to be trained for all possible conditions so as to generalize properly. Among the 184 cases of varying fault location, fault resistance and instant of fault occurrence, 130 cases are used to train the network and the rest of the cases are used for testing. This is for the case when only post-fault frequency components are used as inputs. It is found that for the case when the frequency components of half-cycle pre-fault and half-cycle post-fault voltage and current data are used as the inputs, few cases are needed to train the network. The details of this will be presented in chapter 6.

5.3.1 ANN Relay for Single-line-to-ground Faults

For the case of single-line-to-ground fault, it is found that only the voltage of the faulted phase and all three phase current information are able to classify faults [37]. All the harmonic components are normalized to the fundamental and the fundamental is not included as an input. During training process contradicting targets will be given as output to the fundamental component if it had been included. For example, for the case of fault indication, the fundamental component having unity value, would have a target output as 0.9 for faults occurring inside the trip region and the same fundamental component would have a target output of 0.1 for faults occurring outside the trip region.

The number of inputs for the single-line-to-ground fault is thus 32, namely:

$v_a(f_1)$, $v_a(f_2)$, $v_a(f_3)$, ... $v_a(f_8)$

$i_a(f_1)$, $i_a(f_2)$, $i_a(f_3)$, ... $i_a(f_8)$

$i_b(f_1)$, $i_b(f_2)$, $i_b(f_3)$, ... $i_b(f_8)$

$i_c(f_1)$, $i_c(f_2)$, $i_c(f_3)$, ... $i_c(f_8)$

f_1, f_2, f_3, ...f_8 indicate the frequency components, with f_1 representing the dc component, f_2 the second harmonic and so on.

For the fault indication case, the target outputs are 0.9 or 0.1 depending on whether the fault is inside the protection zone or outside it. The target output is selected as the per unit distance for the case of fault location. The relay should send a trip signal for faults located within the protection zone.

The number of hidden layers and the neurons are selected by extensive experimentation. The process of choosing the optimal structure of the network is iterative and the approach adopted in the work is as follows. A single hidden layer is chosen first. The number of neurons is gradually increased. Each time, the network is trained and then tested with the 54 patterns not seen before. If the network is able to identify the test patterns accurately, the structure is taken as the optimum one, otherwise two hidden layers are selected and the process is repeated. This process of trial and error can be termed as '*fine tuning*' of the neural network. It is suggested in [27] that adding more layers gives the network more degrees of freedom to learn, thus resulting in a greater potential at solving the problem. The MATLAB Neural Network Toolbox can support only two hidden layers.

For the ANN methodology to indicate the faults, using one-cycle of post-fault information, 3 neurons in the first hidden layer and 2 neurons in the second hidden layer

are selected. For fault location purposes, the first hidden layer has 4 neurons and the second hidden layer has 2 neurons. All the hidden neurons have log-sigmoidal transfer function to limit the output between 0 and 1.

ANN based relay for single-line-to-ground fault indication using half-cycle pre-fault and post-fault data has 4 neurons in the first hidden layer and 2 neurons in the second hidden layer. The network for fault location has 5 neurons in the first hidden layer and 3 neurons in the second hidden layer. The details of the inputs, number of neurons in the hidden layers and the output for the proposed ANN using one-cycle post-fault information and half-cycle pre-fault and post-fault information are summarized in Table 5.5 and Table 5.6 respectively.

Table 5.5: Structure of the ANN using one-cycle of post-fault data

Type	Inputs	Number of neurons in hidden layers		Output
		Layer 1	Layer 2	
Single-line-to-ground fault indication	32	3	2	1
Single-line-to-ground fault location	32	4	2	1
Three-phase fault indication	48	3	2	1
Three-phase fault location	48	5	3	1

Table 5.6: Structure of the ANN using half-cycle pre-fault and post-fault data

Type	Inputs	Number of neurons in hidden layers		Output
		Layer 1	Layer 2	
Single-line-to-ground fault indication	32	4	2	1
Single-line-to-ground fault location	32	5	3	1
Three-phase fault indication	48	3	3	1
Three-phase fault location	48	5	4	1

5.3.2 ANN Relay for Three-phase Faults

All the three-phase currents as well as the voltages are chosen as the inputs to train the algorithm for a three-phase fault. Thus for the case of a three-phase fault 48 inputs *i.e.* each sensing point having 8 frequency components are selected for the ANN algorithm to identify and locate the fault. The main difference in the network structure for the case of a three-fault and the single-line-to-ground faults is in the number of inputs. The inputs to the ANN algorithm for three-phase fault indication and fault location are as follows:

$v_a(f_1)$, $v_a(f_2)$, $v_a(f_3)$, ... $v_a(f_8)$

$v_b(f_1)$, $v_b(f_2)$, $v_b(f_3)$, ... $v_b(f_8)$

$v_c(f_1)$, $v_c(f_2)$, $v_c(f_3)$, ... $v_c(f_8)$

$i_a(f_1)$, $i_a(f_2)$, $i_a(f_3)$, ... $i_a(f_8)$

$i_b(f_1)$, $i_b(f_2)$, $i_b(f_3)$, ... $i_b(f_8)$

$i_c(f_1)$, $i_c(f_2)$, $i_c(f_3)$, ... $i_c(f_8)$

f_1, f_2, f_3, ... f_8 indicate the frequency components, with f_1 representing the dc component, f_2 the second harmonic and so on.

Regarding the outputs for fault indication and fault location, it remains the same as in the case of the algorithm for single-line-to-ground fault. The simulation results obtained will be presented in chapter 6.

Table 5.5 summarizes the network architecture for the fault cases using one-cycle post-fault data. The number of neurons used for three-phase fault indication are similar to that of the single-line-to-ground fault indication. For three-phase fault location purposes, 5 neurons in the first hidden layer and 3 neurons in the second hidden layer are chosen. When half-cycle of pre-fault and post-fault data is used, the network architecture slightly changes, as indicated in Table 5.6. In this case, the neural network used for three-phase fault indication has 3 neurons each in the hidden layers. For fault location purposes, 5 neurons are present in the first hidden layer and 4 neurons in the second hidden layer.

5.4 Summary

The frequency components of voltages and currents are found to be distinct for different faults. The frequency components can be used as pattern recognition by the ANN. Neural networks have been designed to map the relationship between frequency components and the information associated with the fault. The simulation procedure used to obtain these frequency components is explained. The main difference in the ANN based fault indication and fault location algorithm is the target outputs. In the former case, the target outputs are either 0.9 or 0.1 depending upon whether the fault is inside or outside the protection zone, whereas in the latter case, the target output is the per unit distance. The two ANN based algorithms have been designed for single-line-to-ground fault and three-phase faults.

In the initial part of the work, the frequency components of voltages and currents corresponding to one-cycle of post-fault are used as the inputs to the ANN based algorithms. Even though the FFT is taken over one complete cycle after the inception of fault, the voltage and current signals are found to have different patterns at different fault inception angles. ANN is basically a pattern recognizer and hence it is necessary to include the cases of different fault inception angles in the training/testing set. To obtain a better response in terms of speed, it is proposed to use half-cycle pre-fault and half-cycle post-fault data as the inputs for the ANN based algorithm. The same ANN can be used for indicating (or locating) faults under different fault conditions, such as change in the fault location, fault resistance and the fault inception angle. The simulation results for the two cases are presented in chapter 6.

Chapter 6

Simulation Results

6.1 Introduction

Motivated by the fact that Artificial Neural Networks (ANN) can be used as an alternative computational concept to the conventional approach in transmission line relaying, a novel feedforward network for fault indication as well as for fault location purposes has been proposed. The proposed neural network is trained by a set of input/output patterns using backpropagation learning algorithm. Chapter 5 presented the structure of the proposed ANN.

This chapter presents the simulation results using the proposed ANN algorithm. The study is divided into two main parts. The first part presents the results of the ANN-based algorithm using post-fault information only. The second part of the work deals with the ANN-based algorithm using both pre-fault and post-fault information. The proposed neural network is designed using the MATLAB Neural Network Toolbox. A typical learning process of the network in converging to the specified error goal is shown in Fig.

6.1. As seen from Fig. 6.1, the network is able to learn quickly. In Fig. 6.1, every epoch is an iteration in which the input is mapped to the output and the error is calculated. With increasing epochs, the error decreases and when the specified error goal is reached, the weights and biases of that epoch are stored. The trained ANN stores these weights and biases. The simulations are done on a 'DEC Alpha' WorkStation.

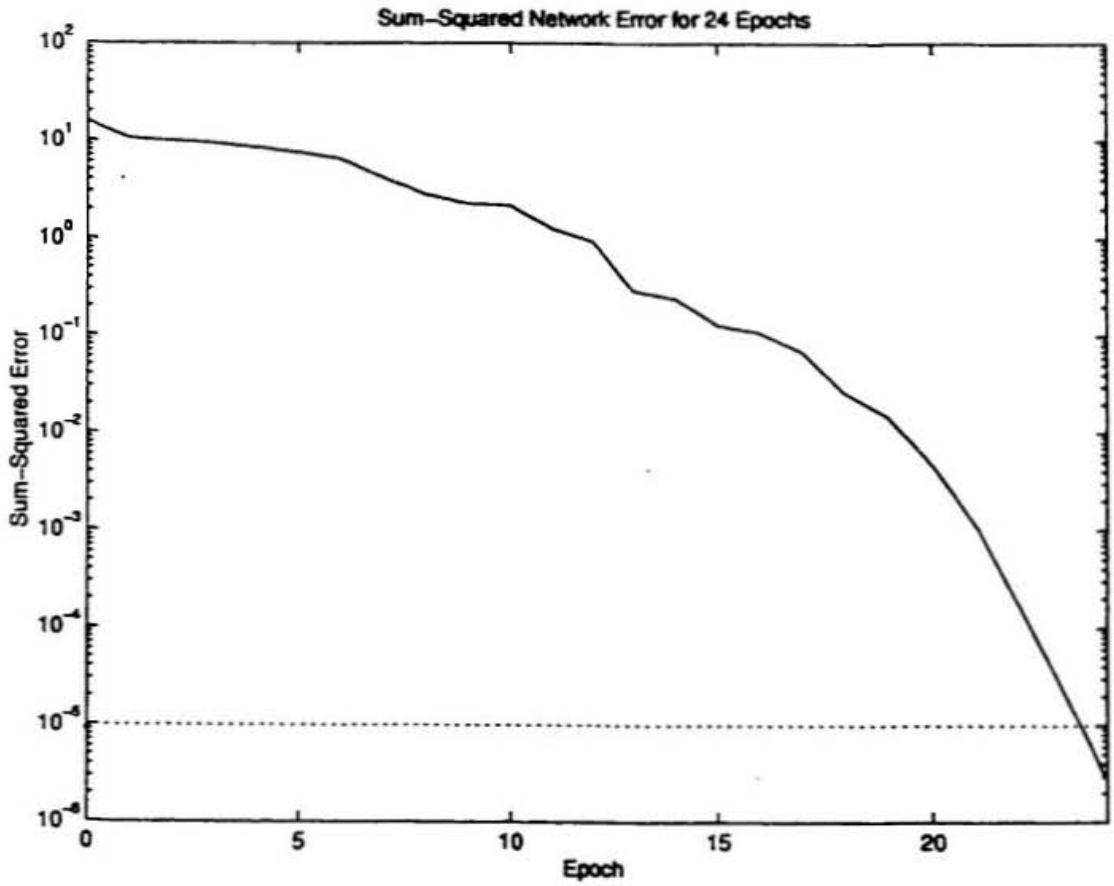

Figure 6.1: Learning process of the neural network

The simulation results obtained for fault indication and fault location for a single-line-to-ground fault and a three-phase fault are presented in this chapter. A comparison of the proposed ANN-based algorithm with a few existing ANN-based algorithms and also with the Fourier algorithm is provided. All these simulations are done off-line. A possible on-line implementation using the proposed algorithm is suggested.

6.2 ANN-based Algorithm Using Post-fault Information

All weights and biases of the neural network are initially set to random values. The input values and the desired output values are specified to the network. Then the network is used to calculate the actual output by the backpropagation method. In the training process, the ANN based algorithm does not explicitly use the voltage and current information as the basis of the decision making. It learns from experience gained during the training and recognizes the hidden relationship that exists in the patterns observed during the learning phase. In the first part of the research, one-cycle of post-fault data is considered [35]. In practice, a transient fault detector would start the one-cycle data window after the fault inception [15]. The training patterns are chosen randomly. The training process is repeated until the sum square of error (SSE) between the actual output and the desired output reaches the specified error goal of 0.001%.

For the case of the algorithm using one-cycle of post-fault information as the inputs, the network is trained with 130 patterns and tested with 54 patterns that the network has not seen earlier. But these 54 test patterns have the same fault distance, fault

resistance and angle of fault occurrence as that of the training patterns. The objective is to obtain a network that is able to give correct results for the patterns not seen before. In practical situations, there is every possibility that the network will experience different conditions. Hence, in the next part of the research, which uses half-cycle pre-fault and half-cycle post-fault information, additional testing patterns that are different from the training patterns are presented to the network.

6.2.1 Single-line-to-ground Fault Indication

There are 32 inputs to the neural network for the purpose of fault indication in a single-line-to-ground fault condition. The details of the ANN structure are given in Table 5.5. A two hidden layer network was found to be accurate in performance. There are 3 neurons in the first layer and in the second layer, 2 neurons are selected. The hidden layer units have the *log-sigmoidal* transfer function. The output is taken as 0.9 if the fault is within the trip zone, else it is taken as 0.1.

It is found that for the case when the fault resistance is 0 Ω and the distance of fault is near the sending end of the power system, the DC component has the maximum value. As discussed in Chapter 5, all the harmonic components are normalized to the fundamental and hence cases where the DC component has the maximum value are not considered in the training as well as in the testing set. These cases are found in the single-line-to-ground fault cases.

The training time for this neural network is 180 seconds and the network reached

the error goal in 24 epochs. The training process is represented in Fig. 6.1. 54 fault patterns that are different from the training set are used for testing. The network is able to identify 96% of the tested cases correctly [35]. The incorrect answers are mostly confined to the boundary region. The results obtained are shown in Fig. 6.2. The output of 0.9 given by the neural network indicates that the fault has occurred within the protection zone, and 0.1 represents fault occurring outside zone 1. The ANN correctly identifies the faults occurring in the trip/no trip region in the presence of a fault resistance of 10 Ω. The ANN does not suffer from the overreach condition that occurs in the Fourier algorithm based relay.

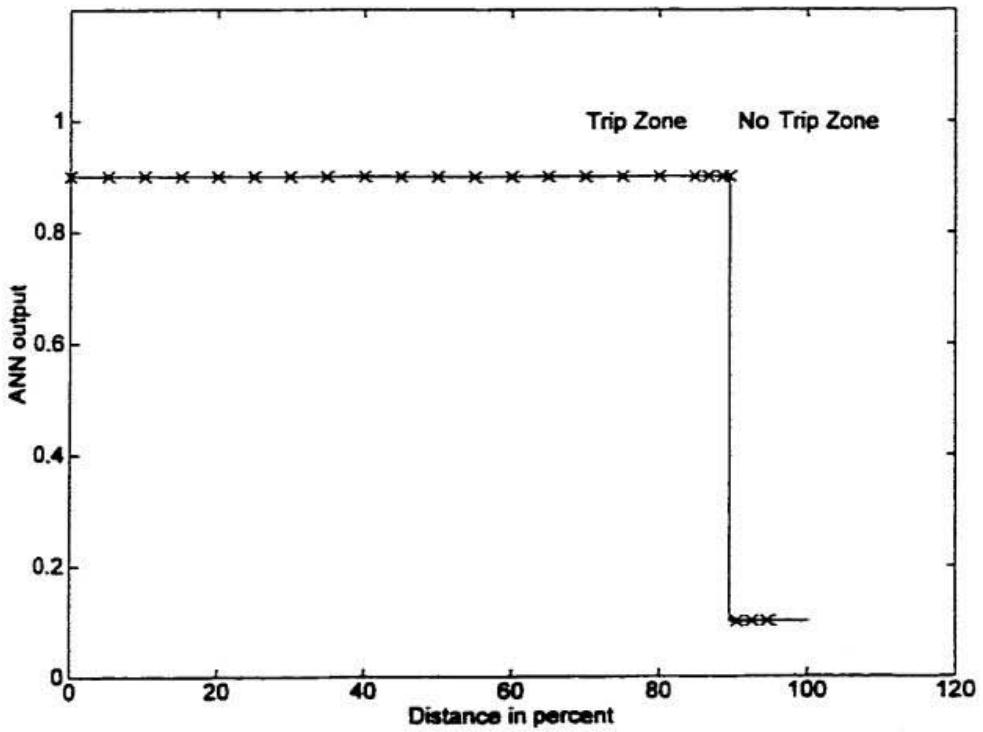

Figure 6.2. Response of ANN algorithm for fault indication using one-cycle post-fault information

Table 6.1 provides a comparison of the proposed feedforward network with a few feedforward networks available in the literature. As seen from Table 6.1, the proposed structure has a smaller size compared to the other neural networks. However, the number of inputs required for the proposed network is 32, compared to 5-8 inputs required by the other networks. The number of training patterns needed for the proposed network to learn is comparatively reduced. Also the training time of the proposed network is found to be significantly less. For on-line implementation, the run-time is an important measure. From Table 6.1, it can be seen that the proposed method features a slower run-time compared to two other methods. The limitation of the proposed method is the slow run-time, which is beyond the scope of the thesis to be investigated.

The response of the network for different loading conditions is not considered in the present study. But including the training patterns for different loading conditions is not expected to affect the overall performance of the neural network.

Table 6.1: Comparison of different neural networks for single-line-to-ground fault indication using one-cycle of post-fault information

Neural Network	Proposed	Ref. [8]	Ref. [12]	Ref. [11]
Structure	32-3-2-1	6-6-2-1	5-6-1	8-20-4-1
Inputs	Frequency components of voltage and current	Magnitude of voltage and current	Measured apparent impedance	Real and imaginary values of voltage and current
No. of training patterns	130	1144	512	Not documented
Training time (minutes)	3	120	Not documented	> 12000

6.2.2 Single-line-to-ground Fault Location

The number of inputs for performing the task of fault location remains the same as in the earlier case. The only difference is in the output. The output in this case is taken as the per unit (p. u.) distance of the transmission line. Even for the case of locating the points of single-line-to-ground fault, it is found that a network with 2 hidden layers gives good performance. The first hidden layer has 4 log-sigmoidal neurons and the second layer has 2 log-sigmoidal neurons, as indicated in Table 5.5.

The network reaches the error goal in 10 minutes and this convergence is achieved in 196 epochs. When tested with 54 cases not seen earlier, it is able to correctly locate the fault for about 92% of the testing data. It is to be noted that although the ANN locates the fault accurately, there are small fluctuations in the ANN output and in practice this cannot be avoided. The error in locating the exact fault can be expressed as a percentage of the length of the transmission line and is given by equation (6.1). The maximum error in locating the exact fault is found to be less than ± 2.5%.

$$\%\,Error = \frac{actual\ \ location - desired\ \ location}{length\ \ of\ \ the\ \ line} * 100 \qquad (6.1)$$

The proposed network employs only 32 inputs and is found to be an accurate fault locator. The protection zone is chosen to be 90% of the line, and the results given by the ANN algorithm have been found to be reliable. The results are found to be accurate even at the boundary location. The results for some of the tested cases are shown in Fig. 6.3.

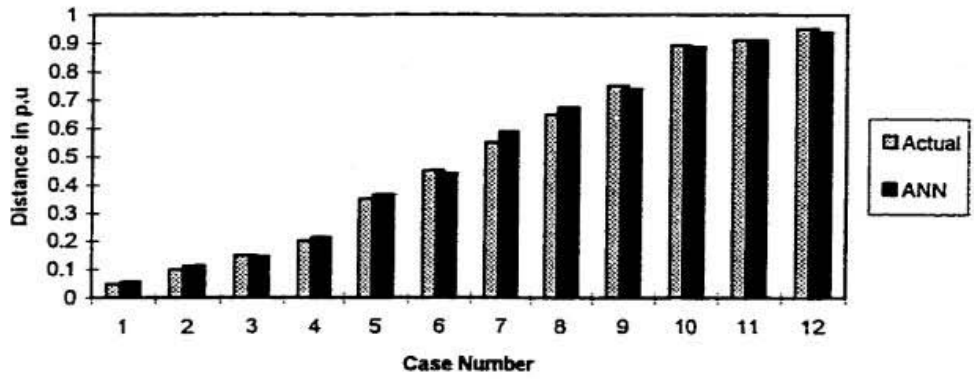

Figure 6.3: Response of the ANN algorithm for single-line-to-ground fault location using one-cycle of post-fault information

6.2.3 Three-phase Fault Indication

For three-phase fault indication, a neural network with 3 neurons in the first hidden layer and 2 neurons in the second hidden layer was found to give a reliable trip/no trip decision. The structure of the network is similar to the one used for identifying faults in a single-line-to-ground fault case, except for the increased number of inputs. The structure of the neural network for three-phase fault indication is 48-3-2-1. The selection of the hidden layers is done by trial and error experimentation with different configurations. The network reaches the error goal in 184 epochs and 180 seconds of training time.

The network tests correctly for 98% of the cases, which is not seen by the ANN before. The results are similar to those shown in Fig. 6.2, and are found to be accurate for

different fault conditions.

The basic structure of the neural network remains the same for both fault indication and fault location purposes. Since the network has to perform different tasks of either giving a trip/no trip decision or point of fault, the optimum neural network has been selected for the two different ANNs.

6.2.4 Three-phase Fault Location

The difference in the case of the ANN for three-phase fault location algorithm is the number of hidden neurons. The first hidden layer has 5 neurons and the second hidden layer has 3 neurons. The output of the neuron is the per unit distance of the fault from the relay location. The network reaches the error goal in 218 epochs and the training time is 15 minutes. The test results for few test cases are shown in Fig. 6.4. The results show that the ANN output accurately locates the fault. The percentage of correct answers is 89% (maximum error being ±2.5%). The ANN output is termed incorrect if the maximum error is greater than ±2.5%. For the incorrect answers, the maximum output is found to be less than ±5%. The correct percentage of the tested cases is slightly less compared to that for the single-line-to-ground fault location case.

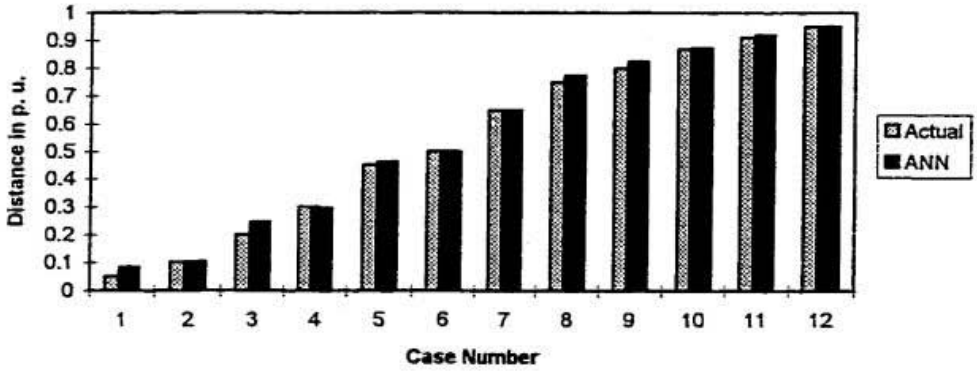

Figure 6.4: Response of the ANN algorithm for three-phase fault location using one-cycle of post-fault information

Table 6.2 presents a summary of the convergence time, number of epochs used and accuracy of the designed neural networks. There is every possibility that the four ANNs indicated in Table 6.2 might not test accurately when tested with data, which are entirely different from the training patterns. But the ANNs based on the one-cycle post-fault information have demonstrated the ability to train in a short time, and give the decision of trip/no trip and locate the fault in about a cycle after the fault inception. The research results at this stage form the basis for the next phase of the ANN design.

Table 6.2 Structure and performance of the ANN using one-cycle of post-fault data

Type of fault	Number of training cases	Number of testing cases	Number of inputs	Number of neurons		Training time (minutes)	Number of epochs	Accuracy of Test
				Layer 1	Layer 2			
Line-to-ground fault indication	130	54	32	3	2	3	24	96%
Line-to-ground fault location	130	54	32	4	2	10	196	92%
Three-phase fault indication	130	54	48	3	2	3	184	98%
Three-phase fault location	130	54	48	5	3	15	218	89%

6.3 ANN-based Algorithm Using Pre-fault and Post-fault Information

Using only post-fault information of voltage and current frequency components as the inputs to the neural network provided good results, but the decision is obtained after one-cycle of fault inception. In order to improve the speed of the relaying decision, half-cycle pre-fault and half-cycle post-fault information of voltage and current frequency components are taken as the inputs to the ANN. This method can provide a relaying decision in about half-cycle after fault occurrence. As observed from the frequency spectrums of voltage and current signals, half-cycle pre-fault and post-fault data contain sufficient information regarding the fault.

In addition to the 184 fault cases used earlier in the training and testing of the ANN based on one-cycle post-fault information, another 160 fault cases are simulated for testing the network. These 160 test patterns are simulated for faults with different fault location, fault inception angle and fault resistance compared to that of the training patterns. Also, for the case when half-cycle pre-fault and post-fault information are used, the DC component is found to be less than the fundamental component and hence all the 344 fault cases generated are used either in the training set or the testing set. Out of these 344 test cases, about 100 cases are used in the training set for fault indication purposes and the rest are used in testing the ANN. For fault location purposes, more fault cases are needed in the training set and the details are explained in the sections to follow.

Table 6.3 represents the combinations of different system conditions for which the

fault data are generated, to be used in the ANN algorithm for fault indication and fault location purposes. For example, a single-line-ground fault is simulated with a fault resistance of 5 Ω, with fault location at 80% of the line from the substation **A** (Fig. 5.3) and the fault inception angle of 0°. Similarly, faults for other combinations are simulated.

Table 6.3: Combinations for which fault data is simulated

Fault resistance R_f (Ω)	Location of fault (%)	Fault inception angle
0, 10	81, 83	0°, 45°, 90°, 180°, 270°
5 (Line-to-ground) 25 (Three-phase fault)	80, 81, 85, 90, 95	0°, 45°, 90°, 180°, 270°
10	5, 10, 15, 20, 25, 30, 35, 40, 45, 50, 55, 60, 65, 70, 75, 80, 85, 87, 89, 90, 91, 93, 95	28°, 40°, 45°, 95°
0 (Line-to-ground) 50 (Three-phase fault)	5, 10, 15, 20, 25, 30, 35, 40, 45, 50, 55, 60, 65, 70, 75, 80, 85, 87, 89, 90, 91, 93, 95	28°, 40°, 45°, 95°

6.3.1 Single-line-to-ground Fault Indication

Fine tuning procedure is adopted to design the neural network. Only 100 cases are found to be sufficient to train the proposed network for single-line-to-ground fault indication. These 100 cases included the patterns for faults occurring at different fault location, with a fault resistance of 0 Ω and/or 10 Ω, and the fault inception angle φ of 0°, 90°, 180° and/or 270°. The testing is first done only with the 84 test cases having the same fault distance, fault resistance and the fault angle as that of the training patterns. The

fine tuning method, as explained in chapter 5, results in a two hidden layer network with 4 neurons in the first hidden layer and 2 neurons in the second hidden layer to give the best result. The convergence to the error goal is obtained in 5 minutes and in 146 epochs.

In order to make the ANN more generalized in nature the ANN algorithm is presented with 160 fault data that has entirely different patterns from the training data, as explained in the previous section. The neural network never saw these patterns, and its task is to classify new patterns based solely on the previous experience *i.e.*, using the information learned during the training. The ANN is found to test accurately 97% of the different fault patterns. The correct testing indicates that the ANN has generalized and not just memorized the patterns. The trip decision in this case is obtained in just half-a-cycle after the fault inception. This is clearly an advantage over the same algorithm when one-cycle of post-fault information is considered. The response of the ANN algorithm for the single-line-to-ground fault indication purposes is shown in Fig. 6.5.

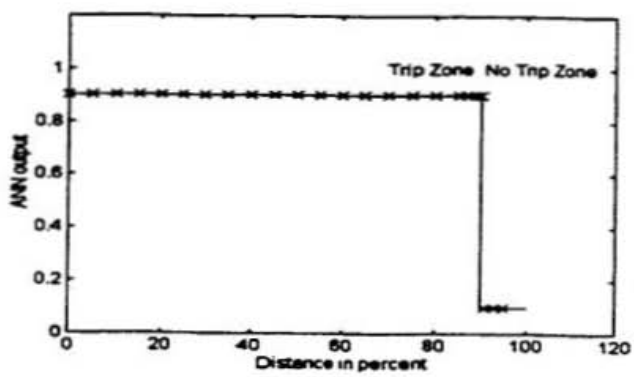

Figure 6.5: Response of the algorithm for single-line-to-ground fault indication using half-cycle pre-fault and post-fault information

The ANN does not suffer from the reach accuracy that was present in the Fourier algorithm. The Fourier algorithm was not able to classify the fault occurring at 95% of the line and with a fault resistance of 10 Ω as being outside the protection zone (Fig. 3.6), whereas the ANN based algorithm has successfully recognized it (Fig. 6.5). While training the neural network, 85 of the 100 cases represented the faults lying inside the trip region and the remaining 15 cases represented the faults lying outside the trip region. Even though the training patterns are not symmetrically distributed between the trip and no trip region, the network is able to learn all the cases well. The first zone of protection can be safely set to 90% of the transmission line.

6.3.2 Single-line-to-ground Fault Location

With the *fine tuning* procedure, the network structure of 32-5-3-1 is found to be accurate for the single-line-to-ground fault location case. In this case, 125 training cases are found to be sufficient for the network to learn the patterns. These 125 training patterns included the cases for faults occurring at different fault location, with a fault resistance of 0 Ω and/or 10 Ω, and the fault inception angle φ of 0°, 45°, 90°, 180° and/or 270°. To converge to the error goal, 242 epochs are needed for the chosen network structure and this is achieved in 37 minutes of real time. The algorithm locates 92% of the faults accurately when presented with the 84 test patterns that are similar to the testing patterns. When tested with different test data, the neural network identifies 84% of the cases accurately. When presented with test data of faults occurring at a different fault resistance

of 5 Ω, the network is able to accurately identify the location of the fault, as illustrated in Fig. 6.6. The decision of the ANN algorithm is obtained in half a cycle after fault inception.

Figure 6.7 illustrates the response of the network in the presence of different fault distances not used earlier. The results show that the ANN algorithm accurately locates the faults. The results are shown for faults occurring at 81% and 83% of the transmission line, with the fault resistance of 0 Ω.

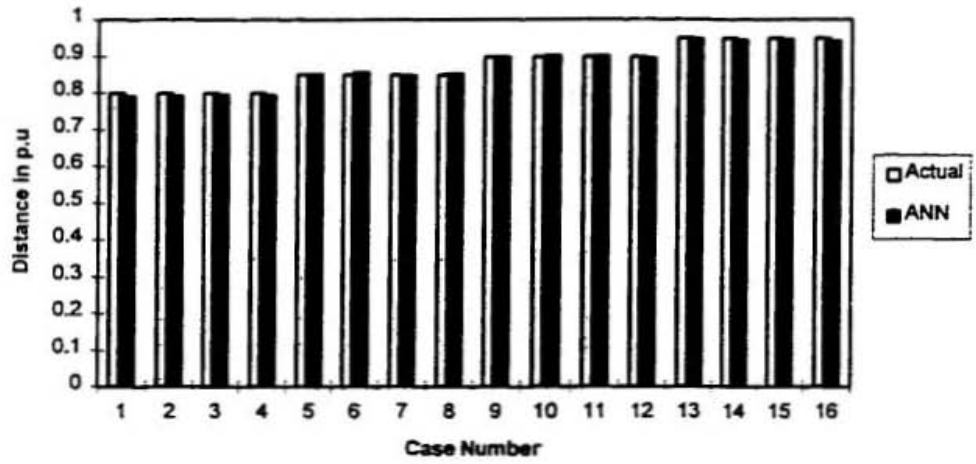

Figure 6.6: Response of the ANN algorithm for single-line-to-ground fault location in the presence of a 5 Ω fault resistance

(Distance of fault = 80%, 85%, 90% and 95%, φ = 0°, 90°, 180° and 270°)

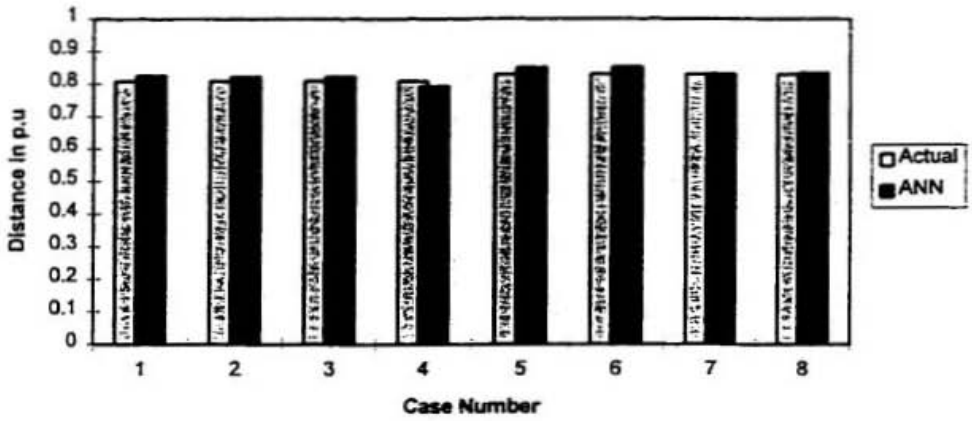

Figure 6.7: Response of the ANN algorithm for single-line-to-ground fault location

(Distance of fault = 81% and 83%, $\varphi = 0°$, 90°, 180° and 270°, $R_f = 0\ \Omega$)

The network is tested with cases of faults occurring at the fault inception angle φ of 28°, 40° and 95°, not seen by the ANN before. These test patterns are entirely different from the training patterns. Figure 6.8 illustrates the results for few cases, for faults with φ of 95°. As seen from Fig. 6.8, the network is able to identify the faults accurately. The same is found to be true for the fault angle of 28° and 40°.

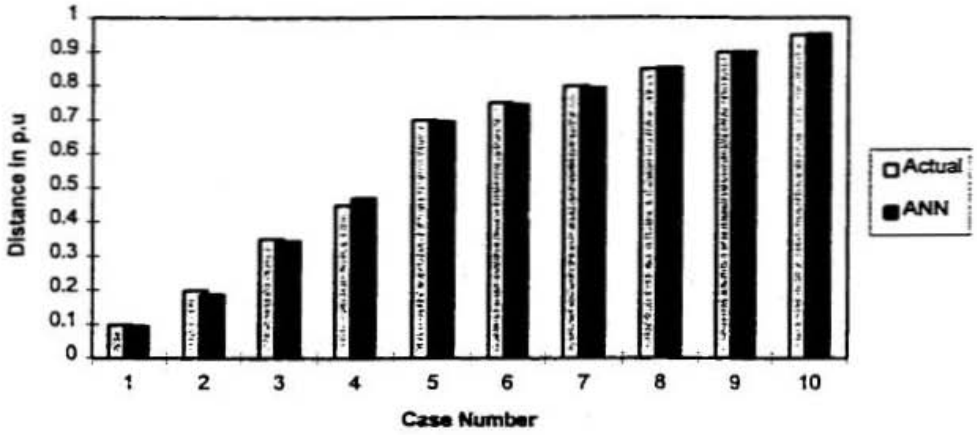

Figure 6.8: Response of the ANN algorithm for single-line-to-ground fault location in the presence of fault inception angle of 95°

During training of the neural network for fault location, patterns with fault inception angle of 0°, 45°, 90°, 180° and 270° are presented. The ANN output in this case is the per-unit distance of fault and since the distances are chosen to be about 1% apart in few cases, more training patterns representing all possible cases of fault should be included to train the network properly. For the case of fault indication, patterns with fault inception angle of 0°, 90°, 180° and 270° are sufficient. The network output in this case has to be either 0.1 or 0.9 and the distinction between these fault patterns is easily obtained by the ANN algorithm.

The research is undertaken for only one loading condition. A neural network should be trained for all possible conditions to be able to generalize properly. To obtain a more accurate fault locator, it is important to include more training patterns representing

all possible cases of fault. Since the learning rate of the network is fast, including more training patterns will not pose difficulty in re-training of the network.

6.3.3 Three-phase Fault Indication

For the three-phase fault indication, 100 cases are considered for training and 84 cases for *fine tuning* the network. The 100 training cases represent the faults occurring at various fault locations, with fault resistance of 10 Ω and 50 Ω and the fault inception angles at 0°, 90°, 180° and 270°. A network structure of 48-3-3-1 is able to classify the faults in the region of trip/no trip for the case of three-phase faults using half-cycle pre-fault and post-fault information. The network converged to the error goal in about 42 epochs and 3 minutes.

As in the case of single-line-to-ground fault indication, 160 fault patterns that have different fault resistance, fault distance and fault angles are tested. The response of the ANN output for few cases is illustrated in Fig. 6.9. The network is able to identify 97% of the 160 test cases presented to it. The incorrect answers are mostly in the boundary region. It is to be noted that the testing patterns are different from the training patterns. Also, as indicated earlier, there are small fluctuations in the ANN output. For practical applications, small threshold levels have to be built onto the ANN algorithm in order to minimize the degree of uncertainty [8, 32]. In this application, for most of the cases, the output is either 0.9 or 0.1 depending on the fault cases and the deviation from this value is observed only in few cases. In such a case, if the output falls in the interval 0-0.499, it is

classified into the no trip region and if it falls in the interval 0.5-1, it is classified into the trip region.

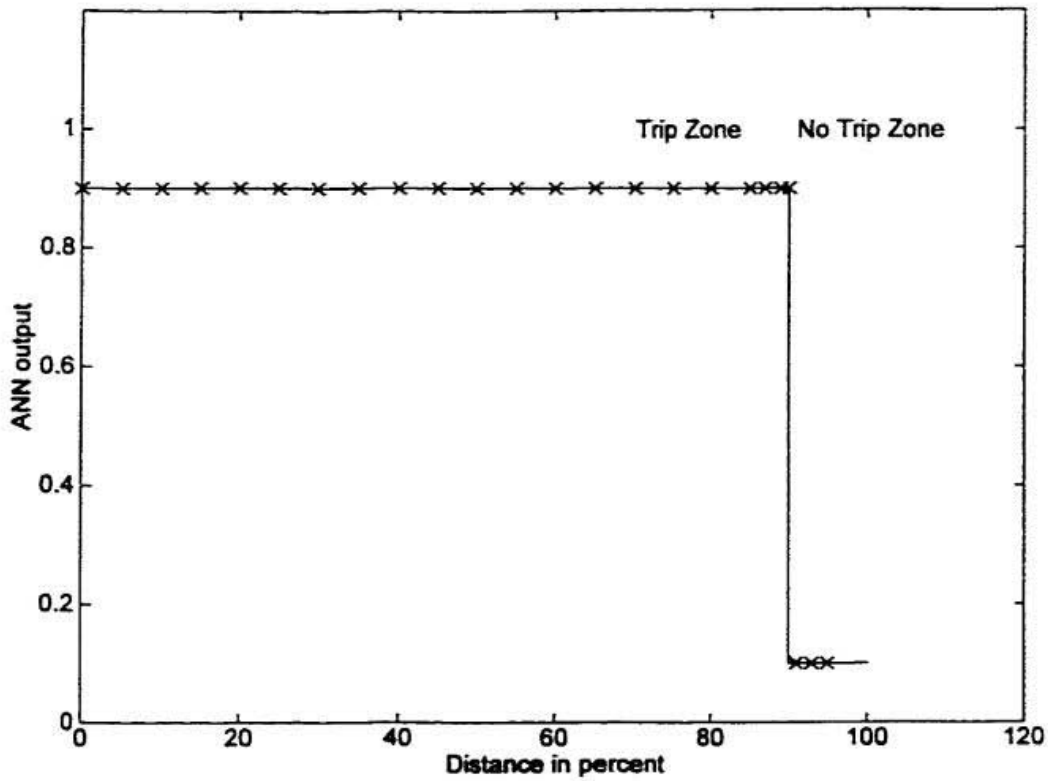

Figure 6.9: Response of the ANN algorithm for three-phase fault indication using half-cycle pre-fault and post-fault data

Similar to the case with single-line-to-ground fault indication, the neural network for three-phase fault indication is found to maintain the reach accuracy. Further, though the testing patterns using different fault distances are spaced by only about 2% apart, the network is able to classify it properly.

6.3.4 Three-phase Fault Location

For this case, 170 training patterns are needed for the network to learn the patterns. The training patterns represent the faults occurring at different fault locations, with the fault inception angle of 0°, 45°, 90°, 180° and 270°, the fault resistance being 10 Ω and 50 Ω. *Fine tuning* the network with 54 test patterns that are similar to the training patterns, a network structure of 48-5-4-1 is found to be accurate. The network trains in 76 epochs and the training time is 24 minutes.

Similar to the case of the single-line-to-ground fault, the response of the ANN algorithm for three-phase fault is accurate for faults occurring in the presence of different fault distances, fault resistance and different fault inception angles. 160 patterns are tested and the network is accurate for 85% of the cases. It is to be mentioned that further work can be carried out to improve the percentage of correct testing.

Figure 6.10 illustrates the response of the ANN for three-phase fault location in the presence of a fault resistance of 25 Ω. As seen from Fig. 6.10, the faults have been located accurately. It is to be noted that the ANN algorithm is tested for cases not seen by the ANN at any point of time, and these test cases are quite different from the training cases, as the fault resistance is entirely different. The ANN based algorithm is found to be an accurate fault locator in the presence of different fault distances, as indicated in Fig. 6.11. Taking into account that in some cases, the distances are spaced just by 1% apart, the ANN-based algorithm has been able to identify the faults accurately for the cases not seen before. Hence the neural network can be considered as accurate.

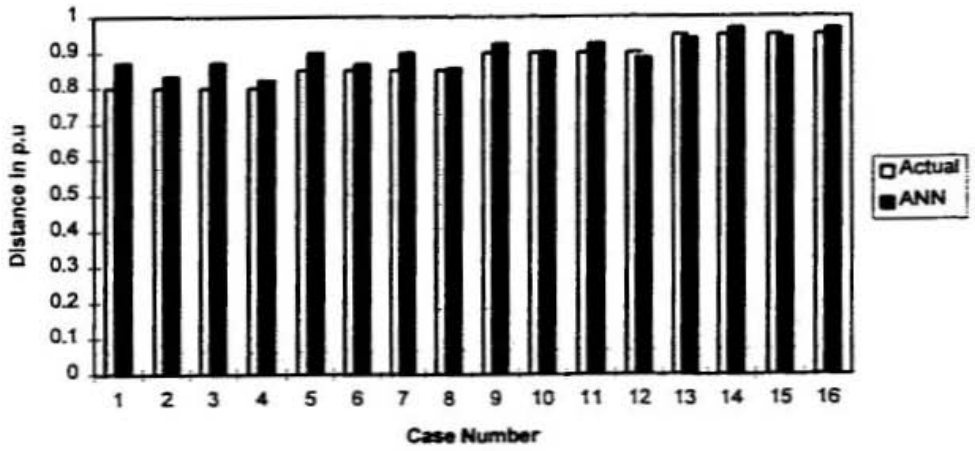

Figure 6.10: Response of the ANN algorithm for three-phase fault location in the presence of a 25 Ω fault resistance

(Distance of fault = 80%, 85%, 90% and 95%, φ = 0°, 90°, 180° and 270°)

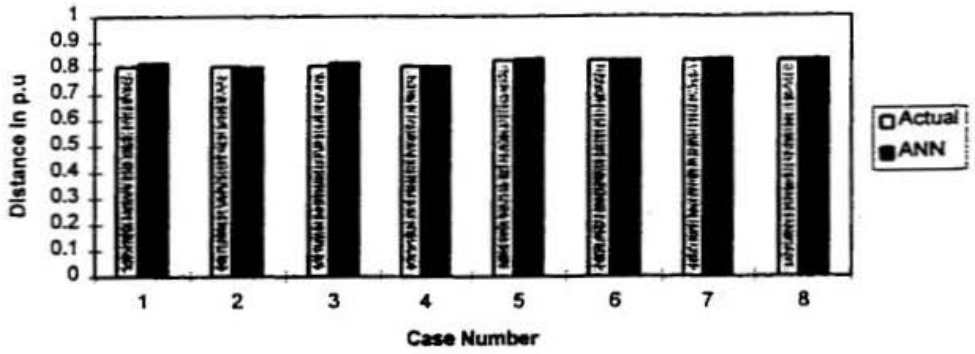

Figure 6.11: Response of the ANN algorithm for three-phase fault location at different fault distances (81% and 83%) , R_f = 0 Ω

The behaviour of the ANN based algorithm for three-phase fault location, in the presence of different fault angles is found to be similar to the single-line-to-ground fault location case. The ANN output for some of the test cases when the fault inception angle is 95° are shown in Fig. 6.12. As seen from the results, the ANN based algorithm has located the faults accurately, even though the test patterns are different from the training patterns. Hence generalization of the algorithm has been achieved. The maximum error in locating the exact fault is less than ± 2.5% even for the testing patterns not seen by the network before. The percentage of correct testing is 85%. Similar to the testing for φ of 95°, the network is found to locate the faults accurately in the presence of different fault inception angle of 28° and 40°.

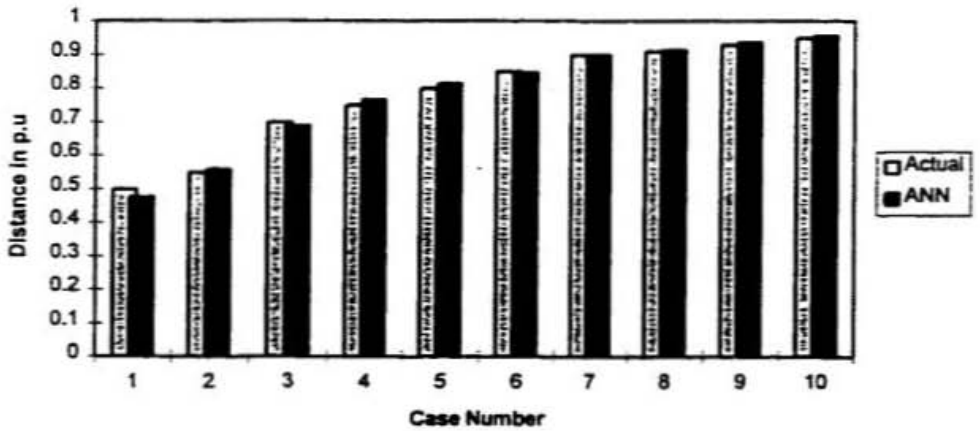

Figure 6.12: Response of the algorithm for three-phase fault location in the presence of fault inception angle of 95°

6.4 Performance Analysis of the ANN for Transmission Line Relaying

The optimum structure chosen for the ANN based algorithm (using half-cycle pre-fault and half-cycle post-fault data) for transmission line relaying in case of single-line-to-ground faults and three-phase faults is shown in Table 6.4. For the cases of single-line-to-ground fault indication and three-phase fault indication, the percentage of correct testing is found to be 97% and 96% respectively. For fault indication, it is found that only 100 cases are sufficient for training and the network is able to identify the faults lying in the trip/no trip region for cases that are different from the training patterns and not seen by the network before.

For fault location purposes, the percentage of correct testing is 84% in case of single-line-to-ground faults and 85% in case of three-phase fault. The response of the neural network for different loading conditions is not considered in the present work. The ANN should be trained with a wide range of data to obtain an accurate fault locator.

The proposed neural network is small in size, robust and accurate. The learning time is less in comparison with that of [8, 11, 12]. The maximum training time, in the case of single-line-to-ground fault location is 37 minutes. For on-line implementation, a shorter training time is definitely an advantage. The trip decision is obtained in about half-cycle after the fault inception. The neural network tests accurately for faults occurring at different location, fault inception angle and fault resistance.

Table 6.4 Structure and performance of the ANN using half-cycle pre-fault and half-cycle post-fault data

Type of fault	Number of training cases	Number of test cases different from training cases	Number of inputs	Number of neurons		Training time (minutes)	Number of epochs	Accuracy of Test
				Layer 1	Layer 2			
Line-to-ground fault indication	100	160	32	4	2	5	146	97%
Line-to-ground fault location	125	160	32	5	3	37	242	84%
Three-phase fault indication	100	160	48	3	3	3	42	96%
Three-phase fault location	170	160	48	5	4	24	76	85%

6.4.1 Comparative Analysis

With the proposed scheme, the trip decision is obtained in about half-cycle after fault inception, in comparison with the trip decision obtained after one-cycle in [9] and [15]. Also, the proposed method has a small network size and is able to learn the patterns in a short interval.

This research has shown that an ANN-based method for transmission line relaying has the potential to provide more accurate results compared to the Fourier algorithm. The reach accuracy of the Fourier algorithm based distance relay is affected by the different fault conditions. This problem has been overcome in the proposed ANN method for the distance protection of transmission lines. The time taken for the trip decision in case of full-cycle Fourier algorithm is found to be approximately 1½ cycle after the fault inception. The ANN based algorithm arrives at a decision in half-cycle after the fault inception.

It is seen that the ANN method based on one-cycle of post-fault information and on half-cycle of pre-fault and post-fault information are both reliable. The main difference in these algorithms is the time taken to give a decision. In the former case, the trip decision is obtained after one cycle of fault inception, whereas in the latter, the decision is obtained in just half a cycle after the fault inception. Both algorithms are found to be reliable in all the cases considered, *i.e.*, single-line-to-ground fault indication, single-line-to-ground fault location, three-phase fault indication as well as three-phase fault location. The ANN method using half-cycle pre-fault and post-fault information needs lesser

number of training sets compared to the one using only post-fault information. From Table 6.2 and 6.4, it is seen that the number of neurons are only slightly different and hence the training time and number of epochs needed are different for the algorithms based on post-fault information only and based on using both pre-fault and post-fault information. But this difference is due to the design process adopted in modifying the structure so as to obtain a good network.

This study has shown that an ANN based algorithm using half-cycle pre-fault and half-cycle post-fault information gives a better performance in terms of speed as well as accuracy compared to the one based on the post-fault information only. The results presented in Table 6.4 are for the test cases that are different from the training cases and are not seen by the ANN before.

6.4.2 Advantages of the Proposed ANN Scheme

Some of the advantages of the proposed ANN based algorithm are:

- The trip decision is obtained in half-cycle after fault inception
- The results obtained are reliable and accurate
- The neural network employed is small in size
- The proposed neural network has fast learning capability
- Fault indication and fault location are achieved simultaneously
- The proposed algorithm is able to give an accurate decision in the presence of fault resistance and thus not suffer from the reach accuracy

- The performance of the ANN is not affected by the changes in the fault conditions such as different fault resistance, fault inception angle and fault location

These advantages are true both in the case of single-line-to-ground fault case as well as in the three-phase fault case.

6.4.3 Limitations of the Proposed ANN Scheme

The design process is basically a trial and error method [33, 38]. This is one area in which research work is yet to be undertaken for a proper method to be adopted for designing the neural network. The study did not consider the different loading conditions of the power system. This may be one of the reasons why the proposed neural network gave incorrect answers for some of the test cases. A possible approach to overcome this problem is to include more data to train the network.

6.5 Proposed Scheme for On-line Implementation

The performance of the trained neural network shows promise and has the potential for implementation in a digital relay for transmission line protection. The work was done off-line, using data generated by EMTP [23]. Figure 6.13 shows the complete block diagram for a possible on-line implementation of the ANN based relay. One end of the transmission line is connected to the generating station through a high voltage bus and the other end is connected to the remote power system. The voltage and current signals are taken from the transmission line by the voltage transformers and the current

transformers respectively and passed on to the anti-aliasing filters that have a low cut-off frequency. The anti-aliasing filter should behave as a low pass filter with a cut-off frequency lower than 480 Hz. The data at the required sampling rate is obtained and passed on to the Fast Fourier Transform (FFT) filter. The frequency components of the voltage and current signals are obtained for consecutive samples, till the selection logic identifies that there is sufficient information regarding the fault, *i.e.*, the selection logic chooses patterns containing half-cycle pre-fault and half-cycle post-fault information.

The results of this research are based on the assumption that the frequency components of half-cycle pre-fault and half-cycle post-fault voltage and current signals are available. However, in the real environment it is very difficult to exactly know the point of fault occurrence. But different methods can be investigated and included as a pre-processor for the proposed ANN based relay.

A one-cycle sliding window of voltage and current signals can be used. This will determine the frequency components of voltage and current signals using the FFT algorithm during each sampling interval. Before the occurrence of the fault, only the fundamental frequency component will be significant. After the fault occurs, the non-fundamental frequency components will also become non-negligible. As the data window moves, the frequency components will contain sufficient information concerning the fault.

The ANN trained using a fixed type of data window will not give accurate results when provided with frequency components information obtained from a different type of data window. If the time of fault occurrence is known, the data window that is specific to

the ANN can be used. Also, a sliding window of one cycle can still be used. In this case, the frequency components should be continuously stored. Once the possibility of a fault is known, the frequency components can be retrieved and given to the ANN.

Many ANN based fault classification algorithms are already available [9, 32, 39]. The purpose of the fault classification algorithm is to utilize the respective fault data in the proper ANN based algorithm for the fault indication and fault location. For the single-line-to-ground fault case, the present study considered the fault occurring at phase *a* of the transmission line, and hence the inputs used are the frequency components of the voltage at phase *a* and the current at all the three phases. For single-line-to-ground fault occurring at other phases, the corresponding phase voltage is to be selected to obtain the off-line weights and biases. In the on-line implementation, the fault classification algorithm would indicate the phase in which the fault has occurred in a single-line-to-ground fault.

The weights and biases obtained in the off-line process for fault indication and fault location purposes are stored in the microprocessor for the on-line application. The procedure to obtain off-line weights and biases involves three main tasks:

i. EMTP simulation → To obtain the fault data

ii. FFT computation → To obtain the frequency components of voltage and current signals

iii. Training of the ANN → To map the input-output pairs and thus obtain the weights and biases.

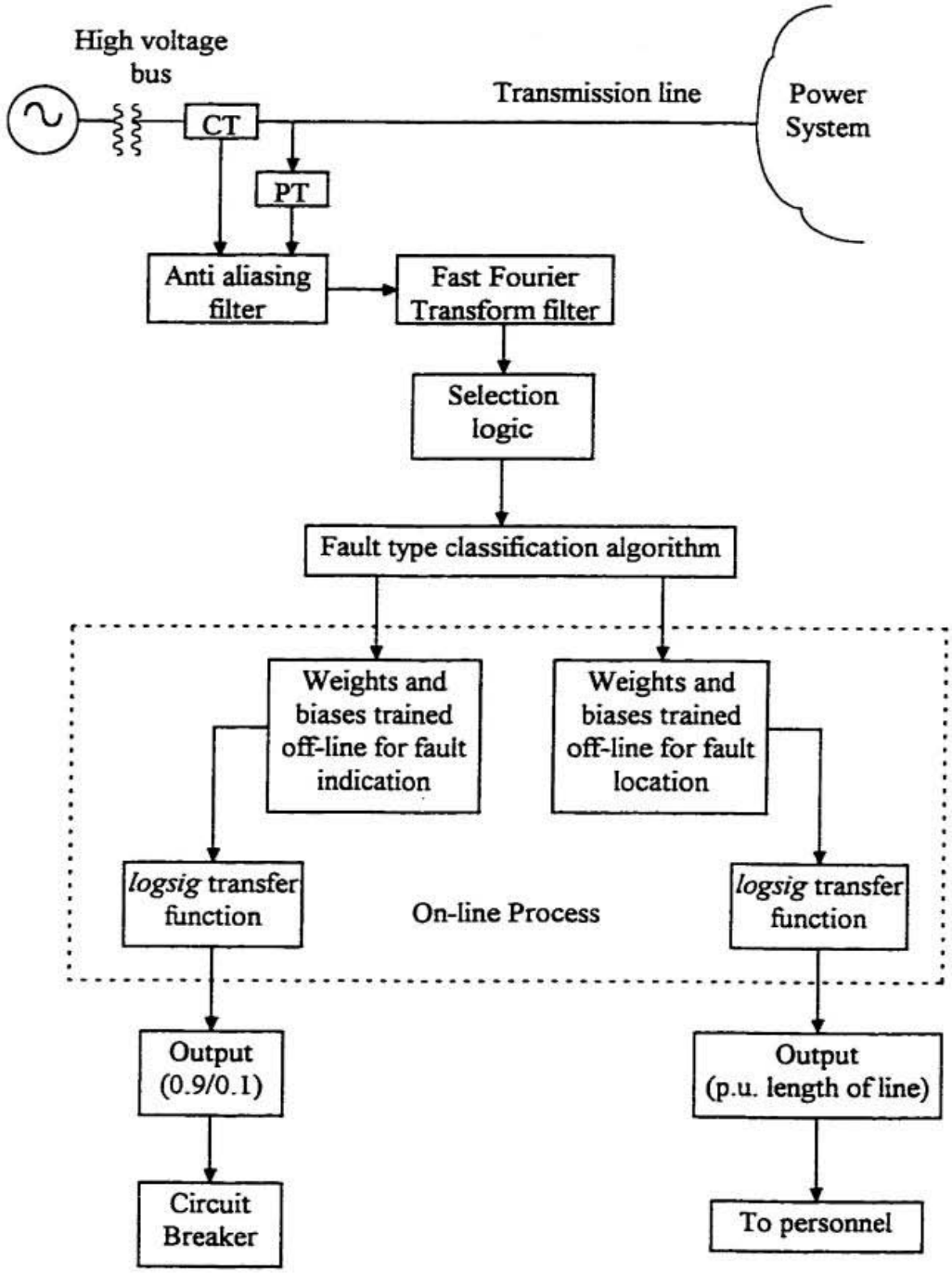

Figure 6.13: Block diagram for the on-line implementation using the proposed scheme

In the off-line training, the neural network learns and generalizes the different fault patterns. This learning is basically stored in the form of weights and biases that represents the mapping between the input-output patterns. In the on-line process, the neural network recognizes any fault pattern by comparing the inputs with this mapping and thus provides a corresponding output.

In the off-line training, the hidden layers have neurons with log-sigmoidal transfer function. The *logsig* transfer function is so chosen, as it limits the output to a continuous value between 0 and 1. The output needed for the proposed scheme is also within 0 and 1. For the on-line scheme, this *logsig* transfer function is implemented in the hardware.

For fault indication, the trip decision is obtained as either 0.9 or 0.1 and this is relayed to the circuit breaker. For fault location purposes, the exact location of fault is conveyed to the power system operator, so that the necessary maintenance can be undertaken. The decision in both the fault indication and fault location cases is arrived in about half a cycle after the fault inception.

Many transmission line fault locators indicate the location of the fault using the post-fault processing features of the digital relay. Using the ANNs proposed in this research, the location of the fault can be known as soon as the circuit breakers open the faulted line based on the trip signal received from the relay.

6.6 Summary

The concept of utilizing the frequency components of the voltage and current signals as inputs to the neural network has resulted in a neural network that is small in size, robust and accurate. The time taken to give a trip decision is around half a cycle after the fault inception. In comparison with the neural networks available in this area, the proposed neural network has the advantages of being small in size, accurate, faster learning rate as well as accurate relaying decision.

This chapter has presented in detail the simulation results obtained for the proposed ANN scheme for transmission line relaying. The algorithm based on the post-fault information is found to be accurate both in the case of fault indication and fault location purposes. The neural network employed is small in size and reliable. The trip decision is obtained after one-cycle of fault inception.

In order to improve the speed of the relay, half-cycle pre-fault and half-cycle post-fault information of the voltage and current frequency components are used as the inputs for the algorithm. In all the four cases considered, *i.e.*, single-line-to-ground fault indication, single-line-to-ground fault location, three-phase fault indication and three-phase fault location, the results are found to be accurate and reliable. The trip decision is given in about half a cycle after the inception of the fault.

In the cases considered, the basic structure of the neural network is similar, *i.e.*, each of them have two hidden layers. The number of epochs needed to converge to the error goal is quite less. One of the advantages of the proposed algorithm is that the

network learns fast, thus significantly reducing the training time.

For fault indication purposes, the network is able to identify all the fault cases and generalize well. The proposed neural network fault locator shows good performance with changes in fault resistance as well as in fault distance. In the presence of a fault resistance, it is seen that the neural network is able to identify the cases correctly, thus maintaining the reach accuracy of the relay.

A comparative study indicates that the neural network based on half-cycle pre-fault and post-fault information, shows better performance in comparison with the neural network based only on the post-fault information. A scheme is proposed for the on-line implementation of the proposed algorithm.

Chapter 7

Conclusions

7.1 Contributions of the Research

The rapid progress in electrical power technology has made it possible to construct economic and reliable power systems capable of satisfying the continuing growth in the demand for electrical energy. Power system protection plays a significant part and progress in the field of power system protection is a vital prerequisite for the efficient operation and continuing development of power supply systems as a whole. Fast and accurate location of faults in an electrical transmission line has become increasingly important, as transmission lines are a vital link between the generating system and the distributing system.

A protective relay responds to abnormal conditions in an electrical power system and controls the circuit breaker so as to isolate the faulty section of the system, with minimum interruption to service. With artificial intelligence becoming popular in the area of power systems, protective relays are experiencing improvements related to shorter decision time, as well as in being accurate. The research demonstrates the use of an

Artificial Neural Network (ANN) as a pattern recognizer for transmission line protective relaying.

An ANN relay for the transmission line protection has been proposed and simulated in the present research work. The feedforward neural network employed indicates whether a fault is within or outside the protection zone and also identifies the exact location of the fault. Data obtained from the EMTP is used to train and test the neural network. Faults at various locations in the transmission line, with different fault inception angle and fault resistance are simulated.

The proposed ANN relay utilizes the frequency components of voltage and current signals as the inputs. The frequency components are obtained by passing one cycle of fault data through a Fast Fourier Transform (FFT) filter. In the earlier part of the research, this one-cycle of data consisted of pure post-fault information. The results of the ANN of this case are found to be accurate. The next part of the research concentrated on improving the speed of the relaying decision. To achieve this objective, the one cycle of fault data consisted of half-cycle of pre-fault and half-cycle of post-fault information.

The sampling frequency is 960 Hz and the frequency components up to the eighth harmonic are found to be sufficient. A unique relationship is found between the fault and the frequency components of the voltage and current. The Total Harmonic Distortion (THD) in voltage and current decreases with increase in the fault location, from the generating end. The design of the ANN for transmission line protection can be essentially treated as a pattern recognition problem. The ANN identifies the patterns of the associated

voltage and current frequency components and gives a relaying decision. The proposed ANN uses the backpropagation algorithm.

Four neural networks are designed for the following cases: single-line-to-ground fault indication, single-line-to-ground fault location, three-phase fault indication and three-phase fault location. The single-line-to-ground fault at phase *a* is considered and the frequency components of voltage at phase *a* and frequency components of currents in all the three phases form the 32 inputs to the ANN. For the case of three-phase fault, the frequency components of all the phase voltages and currents are used, thus forming 48 inputs to the ANN. The output of the ANN for fault indication case is either 0.9 or 0.1 depending upon whether the fault is inside the protection zone or outside the protection zone. For fault location purposes, the ANN gives an output that indicates the per unit distance of the transmission line.

The neural network structure is found to be small in size. The existing ANNs in the concerned area of study are found to have long training times. Utilization of the frequency components of the voltages and currents resulted in the proposed neural network with fast learning capability. Shorter learning time is an advantage for the on-line implementation schemes.

The performance of the proposed ANN has shown promising results. The decision to give a trip/no trip signal as well as the exact location of fault is obtained simultaneously in about half a cycle of the fundamental frequency, after the fault inception. The results of the ANN output are found to be accurate under different fault conditions. In the presence of fault resistance, the network is able to maintain the reach

accuracy of the relay, which is set at 90% of the transmission line. Thus, with the use of the ANN relay, it is possible to extend the first zone reach of the relays, enhancing system security. The main advantage of the ANN relay in comparison with the conventional relay is the ability to maintain this reach accuracy. For the case of fault location, the maximum error is found to be within ± 2.5%. In practice, the exact location of fault will significantly reduce the span of the line length that would have to be inspected.

The existing work is mostly concentrated on the single-line-to-ground fault case. The present research has been carried out for both the single-line-to-ground fault case as well as the three-phase fault case. The results are found to be accurate in both the cases.

7.2 Suggestions for Future Work

The work reported in this thesis can be extended in the following areas:

- The design process for selecting the optimum neural network is through trial and error procedure. The methodology for the training sequence and selection of the optimal training conditions are issues of concern while designing the neural network. Further work can be carried out in this area to select the ANN based on certain fixed guidelines.
- Different ANN algorithms like Self Organizing Maps, Radial Basis Network and Learning Vector Quantization can be studied for suitability of application to transmission line protection. These algorithms are self-learning and have the potential to be competitive with conventional backpropagation algorithm. Radial Basis Networks lead to smaller ANNs.

- The research work is carried out only for one loading condition. The power system is prone to different loading conditions and hence to obtain a more accurate ANN relay for transmission line protection, more patterns that are representative of the various faults should be used in the training set.
- The results obtained by the proposed ANN scheme shows promise and has the potential for the on-line implementation in a digital relay. Further investigation can be carried out to improve the run-time of the proposed method.

References

1. W. A. Elmore, *Protective Relaying Theory and Applications*, ABB Power T&D Company Inc., 1994.
2. S. H. Horowitz and A. G. Phadke, *Power System Relaying*, John Wiley & Sons Inc., 1995.
3. S. H. Horowitz, *Protective Relaying for Power Systems II*, IEEE Press, 1992.
4. J. Lewis Blackburn, *Protective Relaying Principles and Applications*, Marcel Dekker Inc., 1987.
5. A. R. V. C. Warrington, *Protective Relays: Their Theory and Practice*, Volume 2, John Wiley & Sons, 1977.
6. A. G. Phadke and J. S. Thorp, *Computer Relaying for Power Systems*, Research Studies Press Ltd., 1988.
7. SEL - 321 Relay, Schweitzer Engineering Laboratories Inc., Pullman, WA 99163-5603.
8. D. V. Coury and D. C. Jorge, "Artificial Neural Network Approach to Distance Protection of Transmission Lines", IEEE Trans. on Power Delivery, Vol. 13, No. 1. Jan. 1998, pp. 102-108.
9. T. Dalstein, T. Friedrich, B. Kulicke and D. Sobajic, "Multi Neural Network Based Fault Area Estimation for High Speed Protective Relaying", IEEE Trans. on Power Delivery, Vol. 11, No. 2, April 1996, pp. 740-747.
10. S. Kang, K. Kim, K. Cho and J. Park, "High Speed Offset Free Distance Relaying Algorithm Using Multilayer Feedforward Neural Networks", Intelligent System Application to Power System (ISAP '96), Jan 28 - Feb. 2, 1996, Orlando, Florida, pp. 210-214.

11. S. Kang, S. Kim, K. Park, Y. Kang and J. Park, "A Digital Distance Relaying Algorithm Based on Artificial Neural Networks", Intelligent System Application to Power System (ISAP '97), July 6-10, 1997, Seoul, Korea, pp. 221-228.
12. W. Qi, G. W. Swift, P. G. McLaren and A. V. Castro, "An Artificial Neural Network Application to Distance Protection", Intelligent System Application to Power System (ISAP '96), Jan 28 - Feb. 2, 1996, Orlando, Florida, USA, pp. 284-288.
13. M. T. Sant and Y. G. Paithankar, "On Line Digital Fault Location For Overhead Transmission Lines", IEE Proc., 127, No. 11, Nov. 1979, pp. 1181-1185.
14. V. Cook, "Fundamental Aspects of Fault Location Algorithms Used in Distance Protection", IEE Proc., 133, Part C, No. 6, Sept. 1986, pp. 359-368.
15. D. Novosel, B. Bachmann, D. Hart, Y. Hu and M. M. Saha, "Algorithms for locating Faults on Series Compensated Lines Using Neural Network and Deterministic Methods", IEEE Trans. on Power Delivery, Vol. 11, No. 4, Oct. 1996, pp. 1728-1736.
16. M. M. Tawfik and M. M. Morcos, "ANN-Based Fault Locator Scheme used with Automatic Reclosing", 1997 North American Power Symposium, Oct. 13-14, 1997, Laramie, Wyoming, USA, pp. 319-324.
17. Y. G. Paithankar, *Transmission Network Protection: Theory and Practice*, Marcel Dekker Inc., 1998.
18. V. Cook, *Analysis of Distance Protection*, Research Studies Press, 1985.
19. F. H. J. Altuve, V. I. Diaz and M. E. Vazquez, "Fourier and Walsh Digital Filtering Algorithms for Distance Protection", IEEE Trans. on Power Systems, Vol. 11, No. 1, Feb. 1996, pp. 457-462.
20. D. D'Amore and A. Ferrero, "A simplified Algorithm for Digital Distance Protection based on Fourier Techniques", IEEE Trans. on Power Delivery, Vol. 4, No. 1, Jan. 1989, pp. 157-164.
21. IEEE Tutorial Course, "*Microprocessor Relays and Protection Systems*", 88EH0269-1-PWR, 1988.
22. S. Haykin, *Neural Networks: A Comprehensive Foundation*, IEEE Press, Macmillan College Publishing Company Inc., 1994.

23. F. L. Alvarado, R. H. Lasseter, W. F. Long, *Electromagnetic Transients Program (EMTP) Workbook*, EMTP Development Coordination Group, EPRI, Sept. 1986.

24. A. A. Girgis and R. G. Brown, "Modelling of Fault-Induced Noise Signals for Computer Relaying Applications", IEEE Trans. on Power Apparatus and Systems, Vol. PAS-102, No. 9, Sept. 1983, pp. 2834-2841.

25. MATLAB User's Guide, Version 5.0, The MathWorks Inc., USA, 1996.

26. B. Jeyasurya, "Accurate Distance Relaying with Error Compensation", Electric Machines and Power Systems, Vol. 25, No. 1, Jan. 1997, pp. 29-40.

27. Demuth and M. Beale, *Neural Network Toolbox: For use with MATLAB*, The Math Works Inc., 1994.

28. B. Kasztenny, "Artificial Neural Network Approach to Power System Protection", Intelligent System Application to Power System (ISAP '94), Montepllier, France, Sept. 1994.

29. K. K. Li, L. L. Lai and A. K. David, "Intelligent Digital Distance Relay", Intelligent System Application to Power System (ISAP '97), July 6-10, 1997, Seoul, Korea, pp. 279-283.

30. Y. H. Song, "Accurate Fault Location Scheme Based on Neural Networks Applied to EHV Transmission Systems", Proceedings of the International Conference on Power System Technology (ICPST '94), Beijing, China, pp. 1028-1031.

31. D. Zhou, K. Yasuda and R. Yokoyama, "Real Time Fault Location in Power System Combining Neocognitron and BP Neural Network", Proceedings of the International Conference on Power System Technology (ICPST '94), Beijing, China, pp. 1032-1036.

32. R. K. Aggarwal, M. Joorabian and Y. H. Song, "Fuzzy Neural Network Approach to Accurate Transmission Line Fault Location", Engineering Intelligent Systems, Vol. 4, 1997, pp. 251-258.

33. T. S. Sidhu, "Transmission Line Protection Using ANNs: Proposed Applications, Advantages and Roadblocks to Acceptance", Engineering Intelligent Systems, Vol. 4, 1997, pp. 213-220.

34. M. Kezunovic and I. Rikalo, "Detect and Classify Faults Using Neural Nets", IEEE Computer Applications in Power, Oct. 1996, pp. 42-47.

35. F. Zahra, B. Jeyasurya and J. E. Quaicoe, "Artificial Neural Network Based Transmission Line Protective Relaying", accepted for the 30th North American Power Symposium (NAPS98), Cleveland State University, Cleveland, Ohio, Oct. 18-20, 1998.

36. M. H. Rashid, *Power Electronics: Circuits, Devices and Applications*, Prentice-Hall Inc., 1993.

37. M. Sanaye-Pasand and O. P. Malik, "Performance of a Recurrent Neural Network-Based Power Transmission Line Fault Directional Module", Engineering Intelligent Systems, Vol. 4, 1997, pp. 221-228.

38. M. Kezunovic, "A Survey of Neural Net Applications to Protective Relaying and Fault Analysis", Engineering Intelligent Systems, Vol. 4, 1997, pp. 185-192.

39. Y. H. Song, Q. X. Xuan and A. T. Johns, "Comparison Studies of Five Neural Network Based Fault Classifiers for Complex Transmission Lines", Electric Power Systems Research, Vol. 43, No. 2, Nov. 1997, pp. 125-132.

Appendix-A

Transmission Line Parameters

A 345 kV, 160 mile transmission line is simulated using EMTP [23]. Figure A.1 represents the sample power system used in the simulation. AB represents the transmission line and **F** represents the fault. It is assumed that the relay **R** is located at substation A. On a 345 kV base, the voltage at the sending end of the line represented by **A** is 1.02 p.u and the voltage at the receiving end of the line represented by **B** is 0.97 p.u. The simulations are carried out for a loading condition of 520 MW and 245 MVAR at the receiving end.

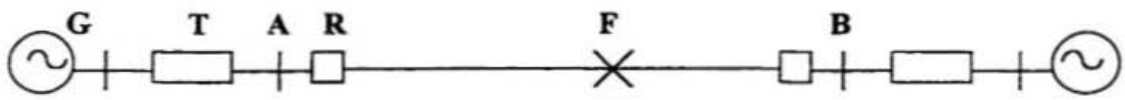

Figure A.1: Single line diagram of the sample power system

The line parameters of the transmission line are represented in Table A.1 [24]. R_0, L_0 and C_0 represent the zero sequence components of resistance, inductance and capacitance respectively. R_1, L_1 and C_1 represent the respective positive sequence components of resistance, inductance and capacitance. The negative sequence parameters (R_2, L_2 and C_2) are the same as the positive sequence parameters.

Table A.1: Line parameters of the transmission line

$R_0 = 0.461\ \Omega$/mile	$R_1 = R_2 = 0.0614\ \Omega$/mile
$L_0 = 5.9944$ mH/mile	$L_1 = L_2 = 1.7344$ mH/mile
$C_0 = 0.015\ \mu$F/mile	$C_1 = C_2 = 0.01856\ \mu$F/mile

The system frequency is 60 Hz.

Ratings of the generator **G**: 400 MVA, 15 kV, wye grounded

Ratings of the transformer **T**: 400 MVA, 15 kV/345 kV, wye grounded-wye grounded